Laser-Compton Gamma-ray Sources and the Emergence of Nuclear Photonics

CHILI 2013
Tel Aviv, Israel

Dr. C. P. J. Barty
Chief Technology Officer
National Ignition Facility & Photon Science Directorate
Lawrence Livermore National Laboratory
Livermore, California
December 4, 2013

This work performed under the auspices of the U.S. Department of Energy by Lawrence Livermore National Laboratory under Contract DE-AC52-07NA27344

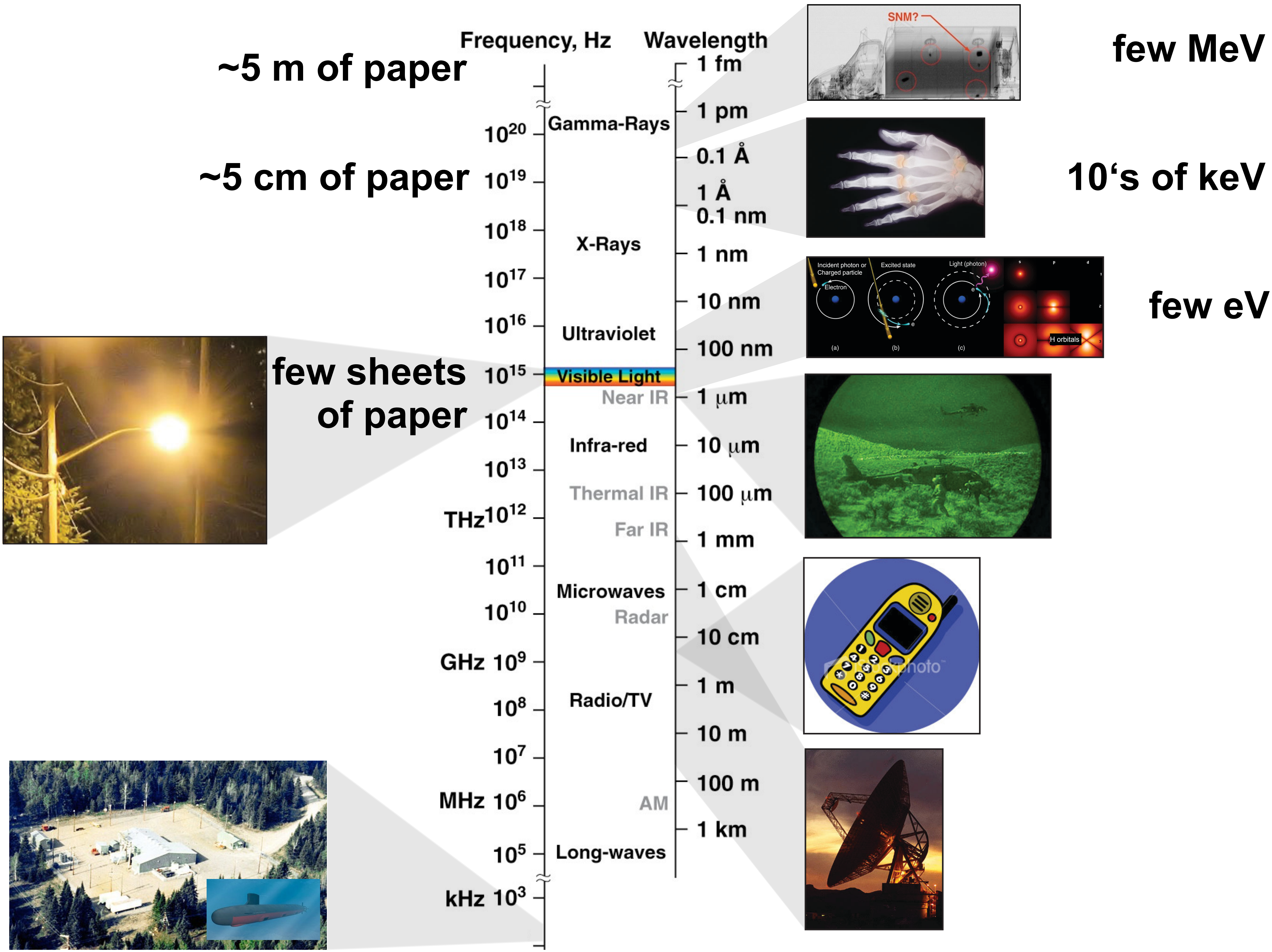

~5 m of paper
~5 cm of paper
few sheets of paper
Frequency, Hz
Wavelength
few MeV
10's of keV
few eV
SNM?
Gamma-Rays
X-Rays
Ultraviolet
Visible Light
Near IR
Infra-red
Thermal IR
Far IR
Microwaves
Radar
Radio/TV
AM
Long-waves
10^{20}
10^{19}
10^{18}
10^{17}
10^{16}
10^{15}
10^{14}
10^{13}
THz 10^{12}
10^{11}
10^{10}
GHz 10^{9}
10^{8}
10^{7}
MHz 10^{6}
10^{5}
kHz 10^{3}
1 fm
1 pm
0.1 Å
1 Å
0.1 nm
1 nm
10 nm
100 nm
1 µm
10 µm
100 µm
1 mm
1 cm
10 cm
1 m
10 m
100 m
1 km
Incident photon or Charged particle
Electron
Excited state
Light (photon)
(a)
(b)
(c)
H orbitals

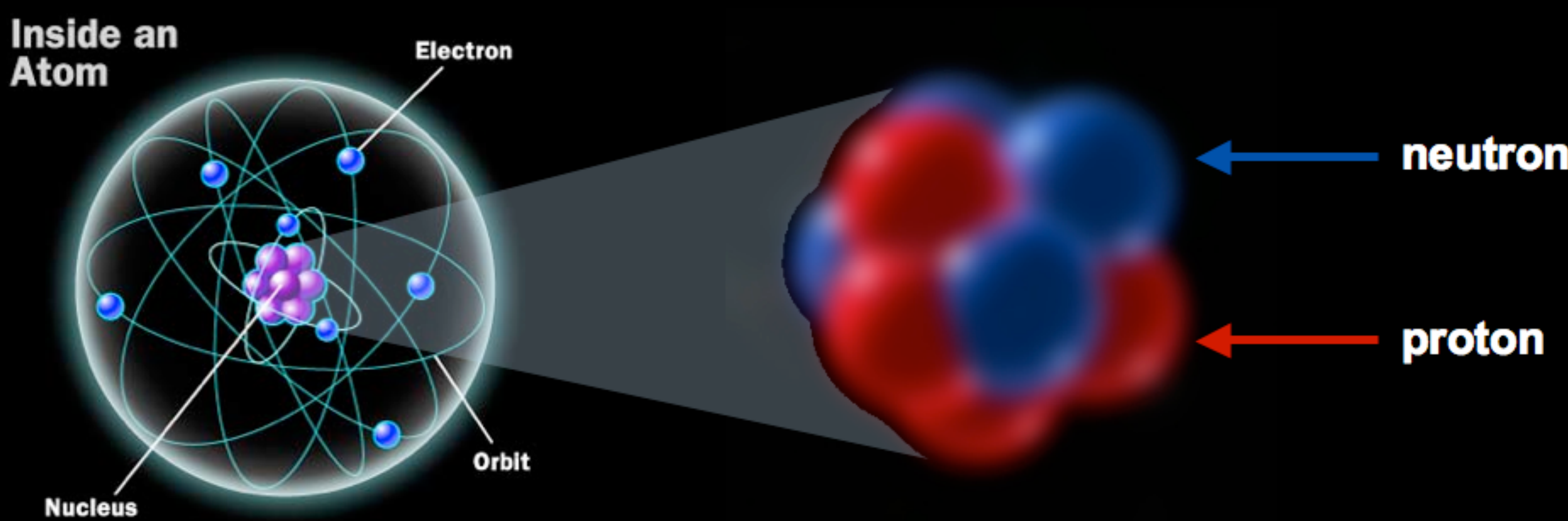
Inside an Atom
Electron
Orbit
Nucleus
neutron
proton

Gamma-ray absorption & radiation by the nucleus is an “isotope-specific” signature of the material

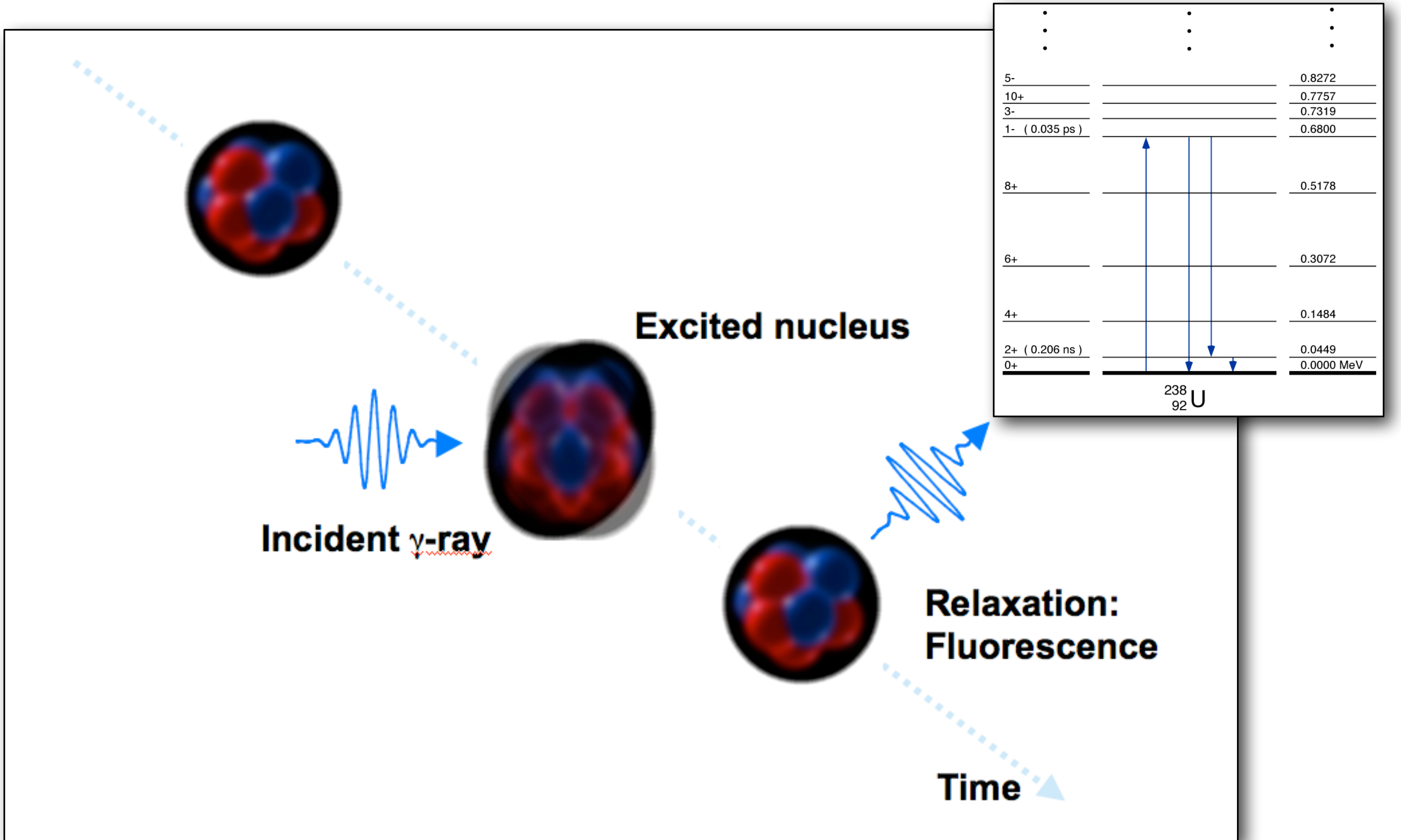

NRF energy is dependent upon the number of protons AND the number of neutrons in the nucleus and involves interactions with BOTH the strong & EM forces

Selective excitation of NRF is possible with narrow bandwidth gamma-rays ($\Delta E/E \sim 10^{-3}$)

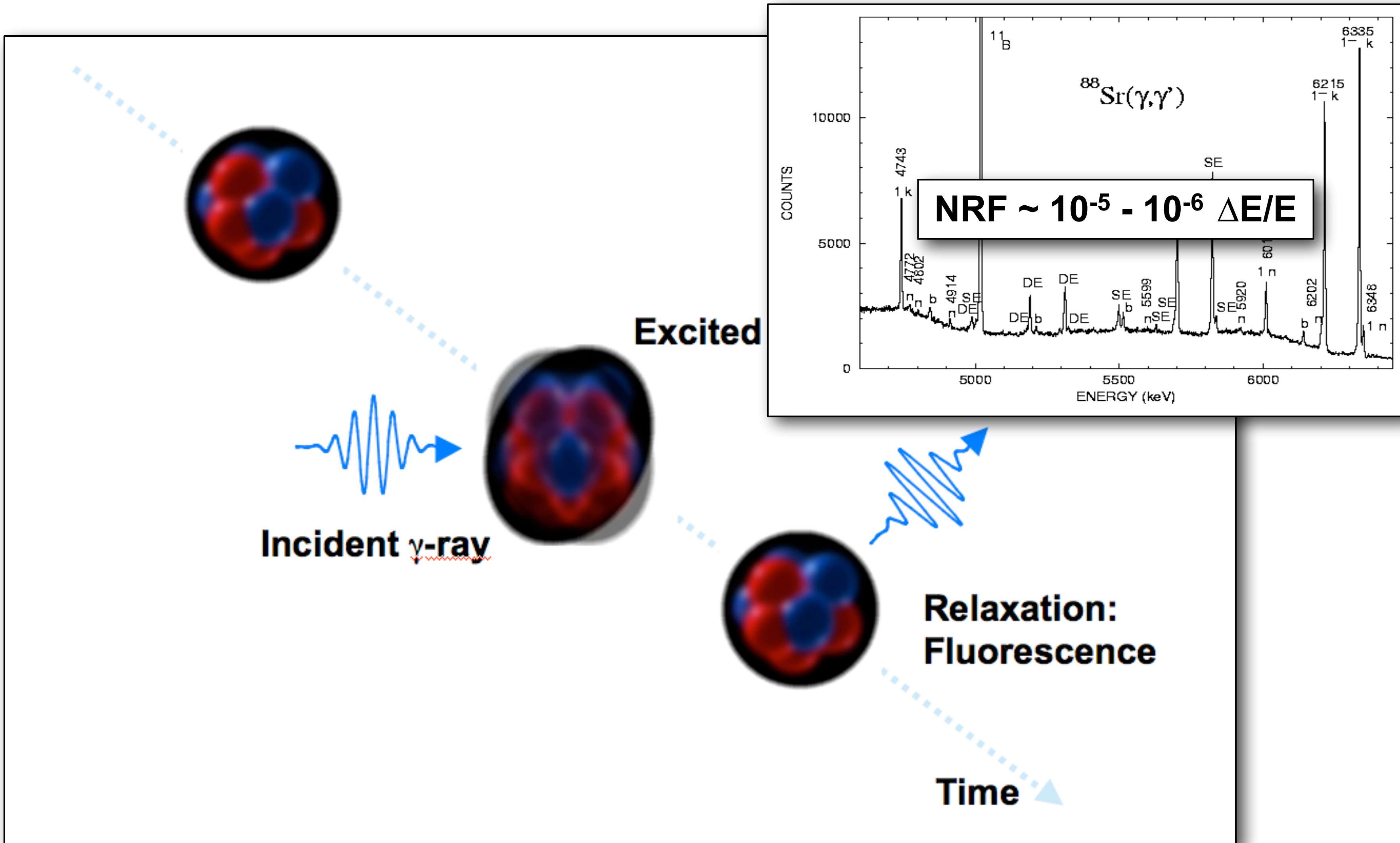

NRF energy is dependent upon the number of protons AND the number of neutrons in the nucleus and involves interactions with BOTH the strong & EM forces

NRF transitions are common and many have cross sections larger than the atomic background

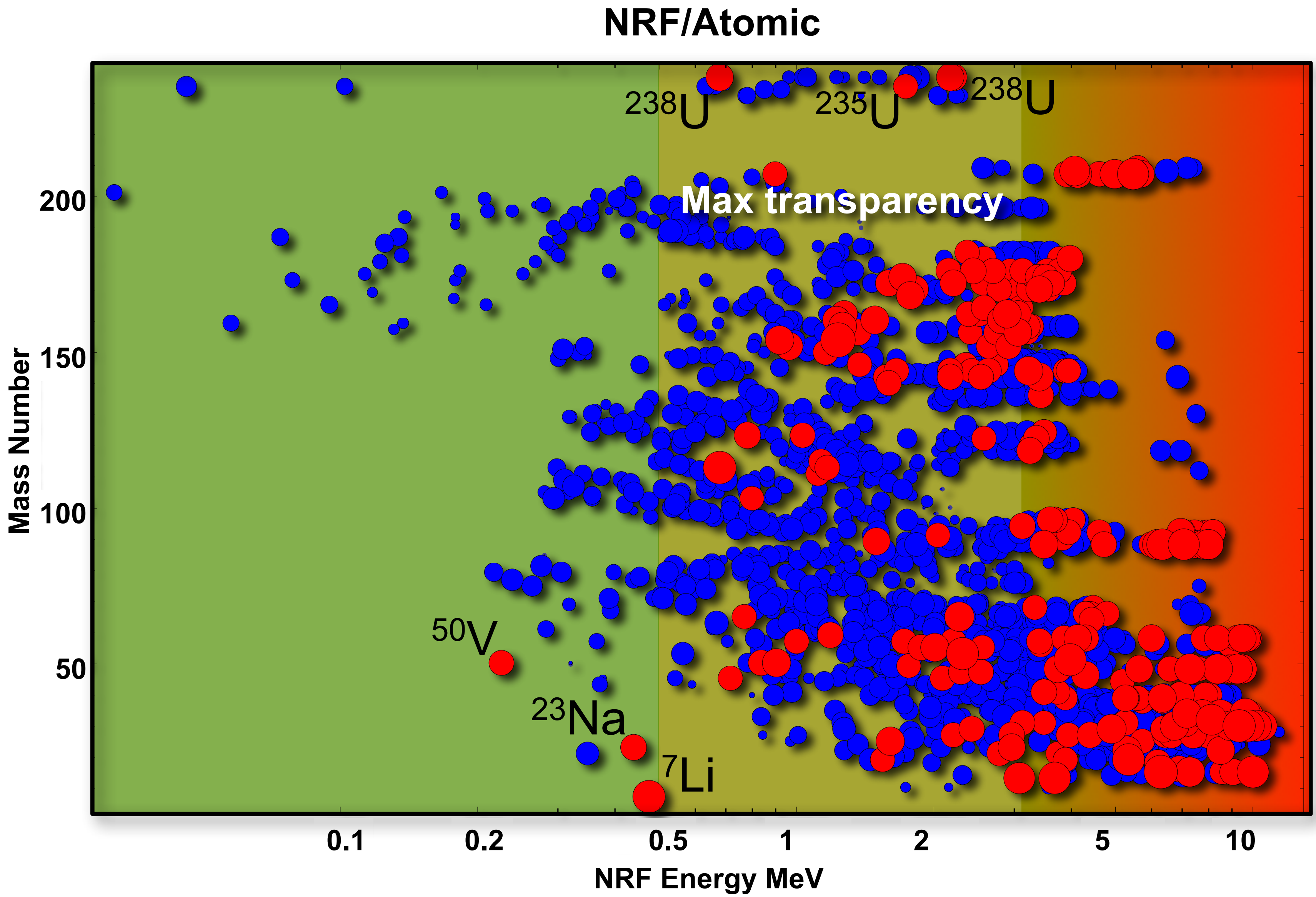

Gammas in the 1 MeV to 3 MeV range are both highly penetrating and non-activating

At higher gamma-ray energies (>5 MeV) photons can also split/fission the nucleus

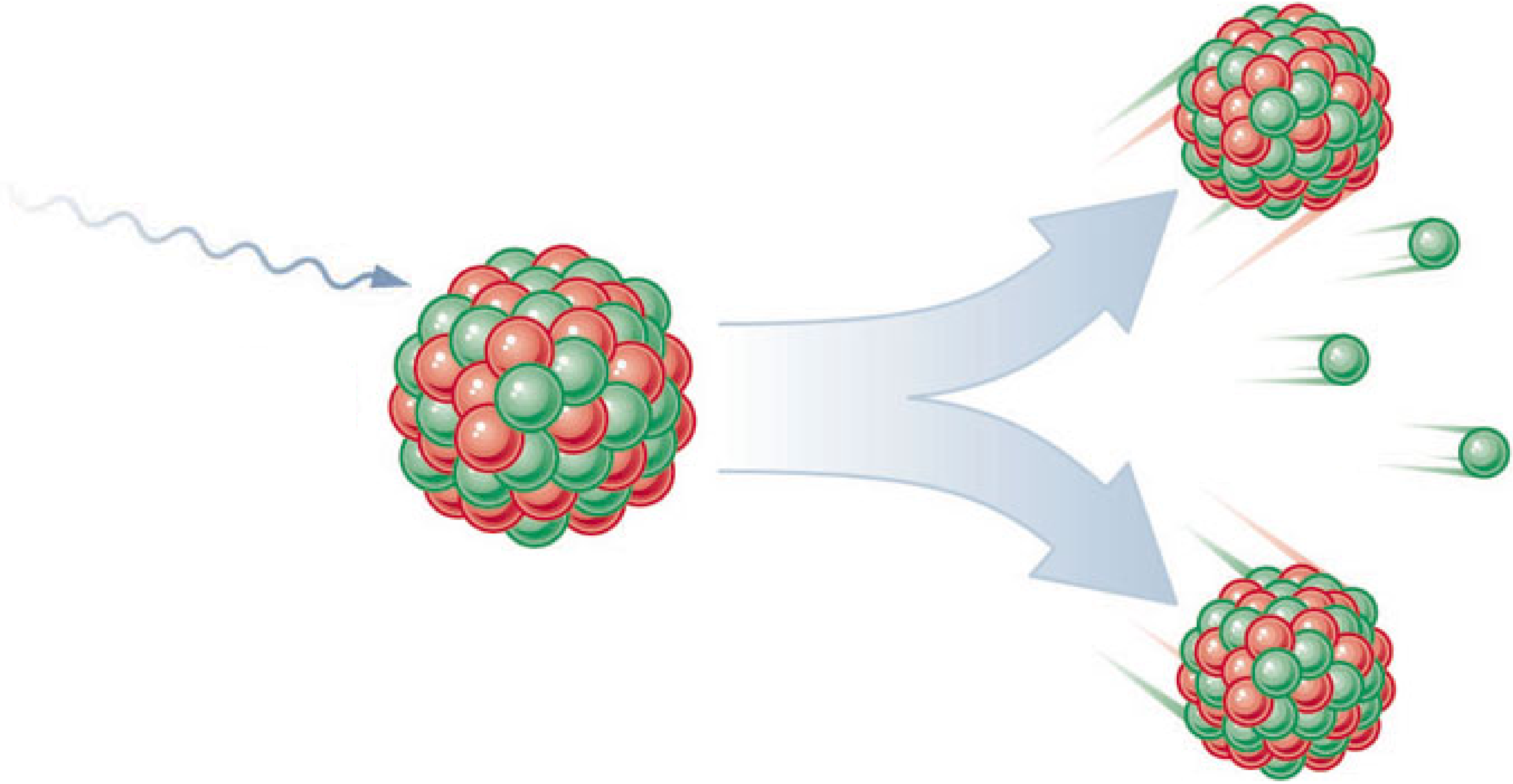

Laser Compton back scattering off of high energy electrons can produce tunable gamma-rays

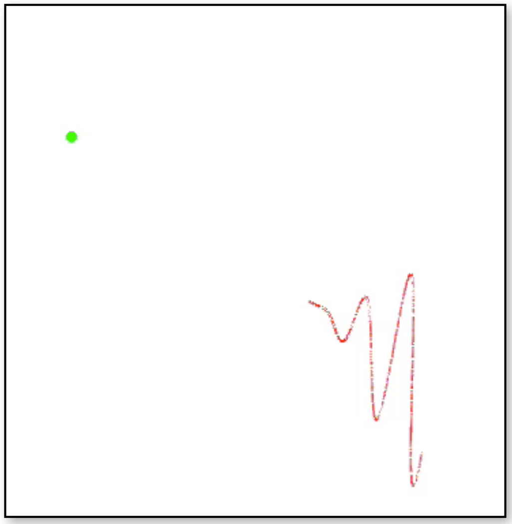

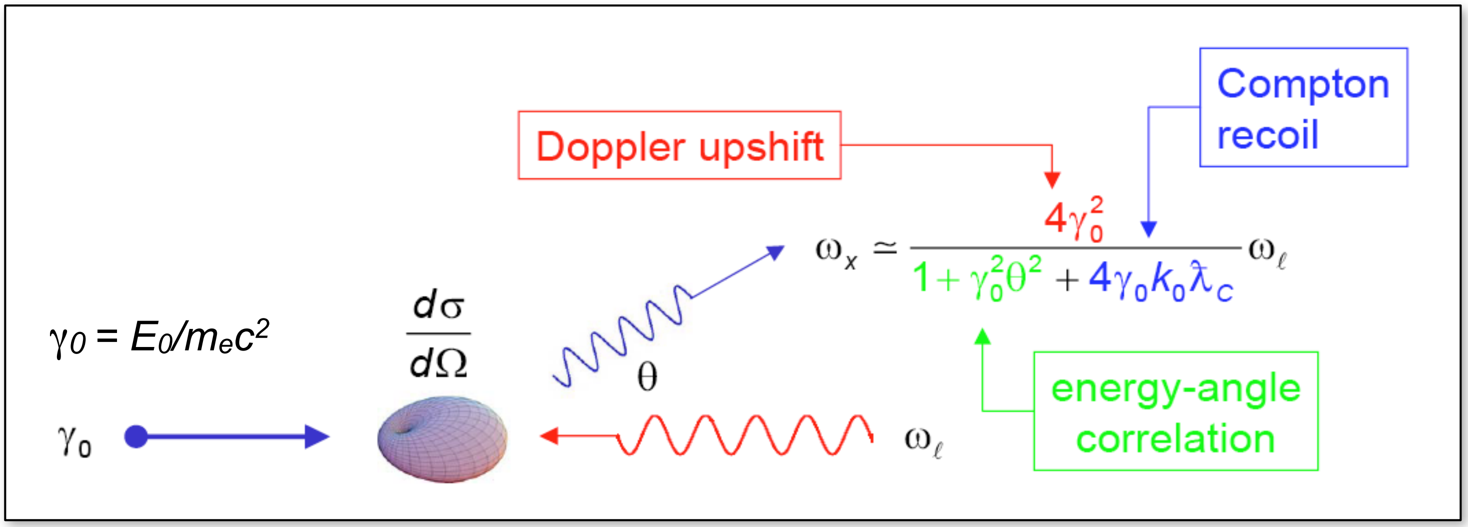

Energy-momentum conservation yields ~4γ^2 Doppler upshift

1965 First Light: 8 photons

PHYSICAL REVIEW VOLUME 138, NUMBER 6B 21 JUNE 1965

High-Energy Photons from Compton Scattering of Light on 6.0-GeV Electrons*

CARLO BEMPORAD†, RICHARD H. MILBURN, AND NOBUYUKI TANAKA
Department of Physics, Tufts University, Medford, Massachusetts

AND

MIRCEA FOTINO
Cambridge Electron Accelerator, Harvard University, Cambridge, Massachusetts

(Received 28 January 1965; revised manuscript received 1 March 1965)

Compton scattering of optical photons on 6.0-GeV electrons has been observed at the Cambridge Electron Accelerator. A giant-pulsed ruby-laser burst of 0.2 J, impinging upon a 2-mA circulating electron current, was observed to yield about 8 scattered photons per pulse. These photons acquire, through a twofold Doppler shift, energies of hundred of MeV, and are expected to retain to a high degree the polarization of the laser beam. The observed yield is compatible with predictions based upon the theory of Compton scattering.

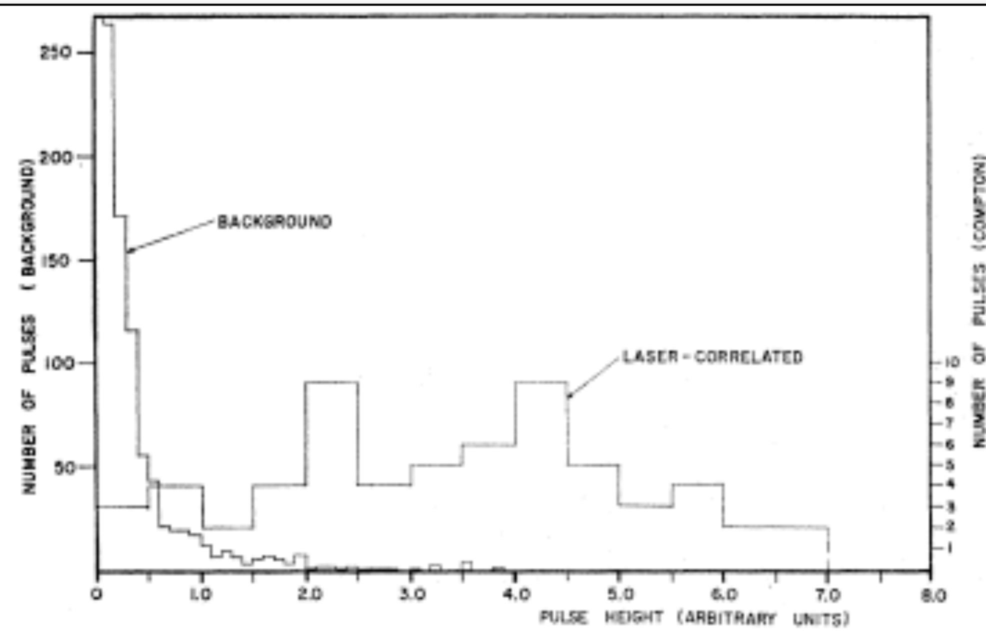

FIG. 6. Čerenkov-counter pulse-height distributions. Laser-correlated pulses are associated with second laser pulse. (2.3 units = 3 GeV).

The Thomson cross section for laser-electron scattering is very small: 6 X 10^{-25} cm^2

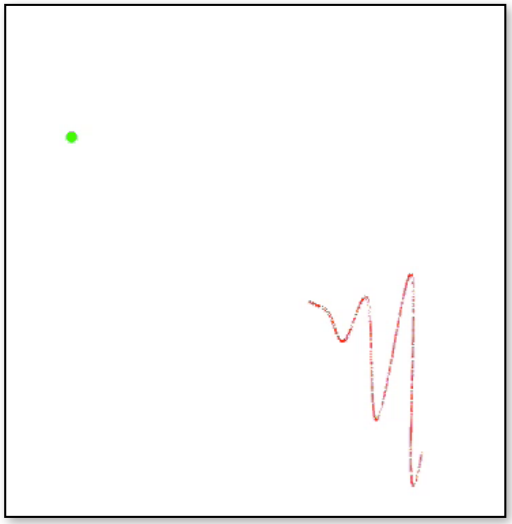

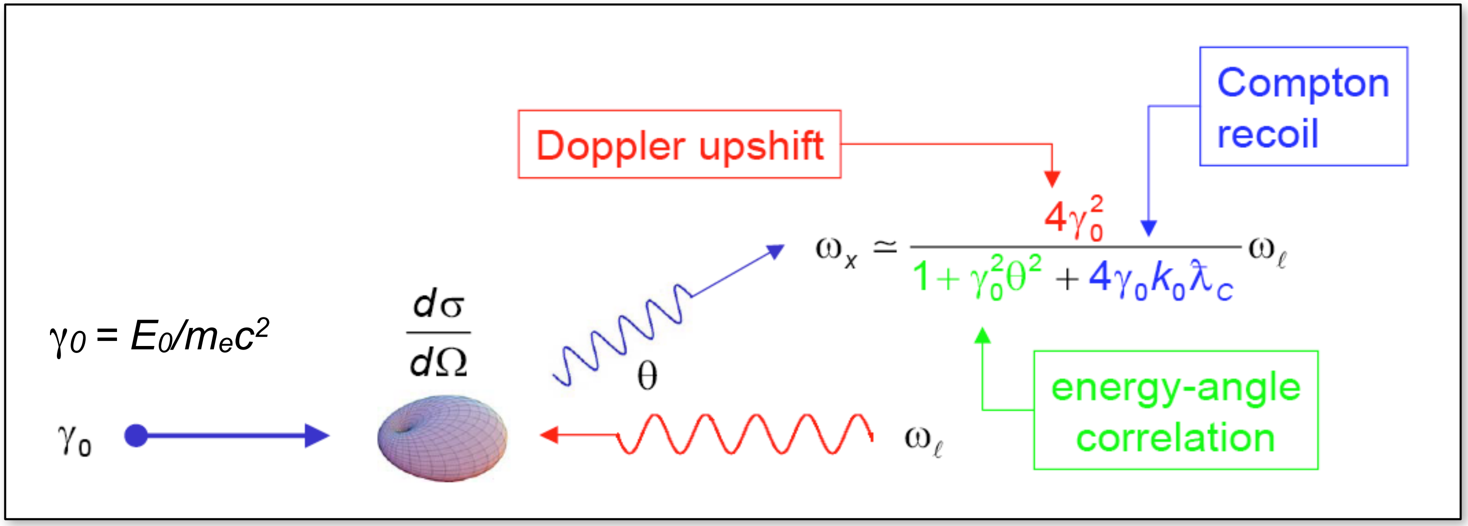

High photon and electron densities are required

High-flux, laser-Compton scattering arrangements aim to produce high photon & electron densities at a common focus

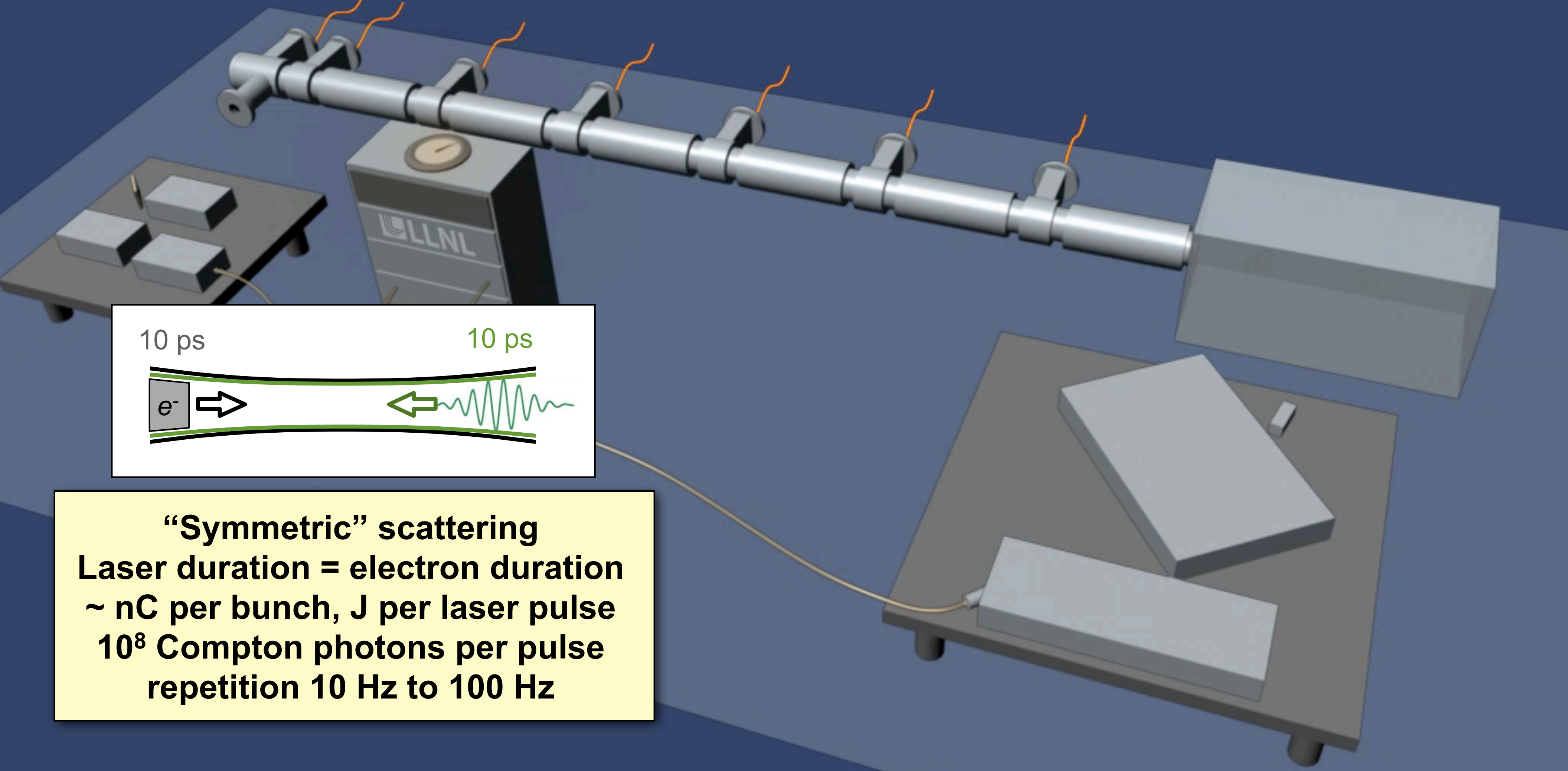

"Symmetric" scattering
Laser duration = electron duration
~ nC per bunch, J per laser pulse
10^8 Compton photons per pulse
repetition 10 Hz to 100 Hz

At 250 MeV, scattered radiation is Doppler upshifted by ~1,000,000x and is forwardly-directed in a narrow, polarized, tunable, laser-like, gamma beam

High-flux, laser-Compton scattering arrangements aim to produce high photon & electron densities at a common focus

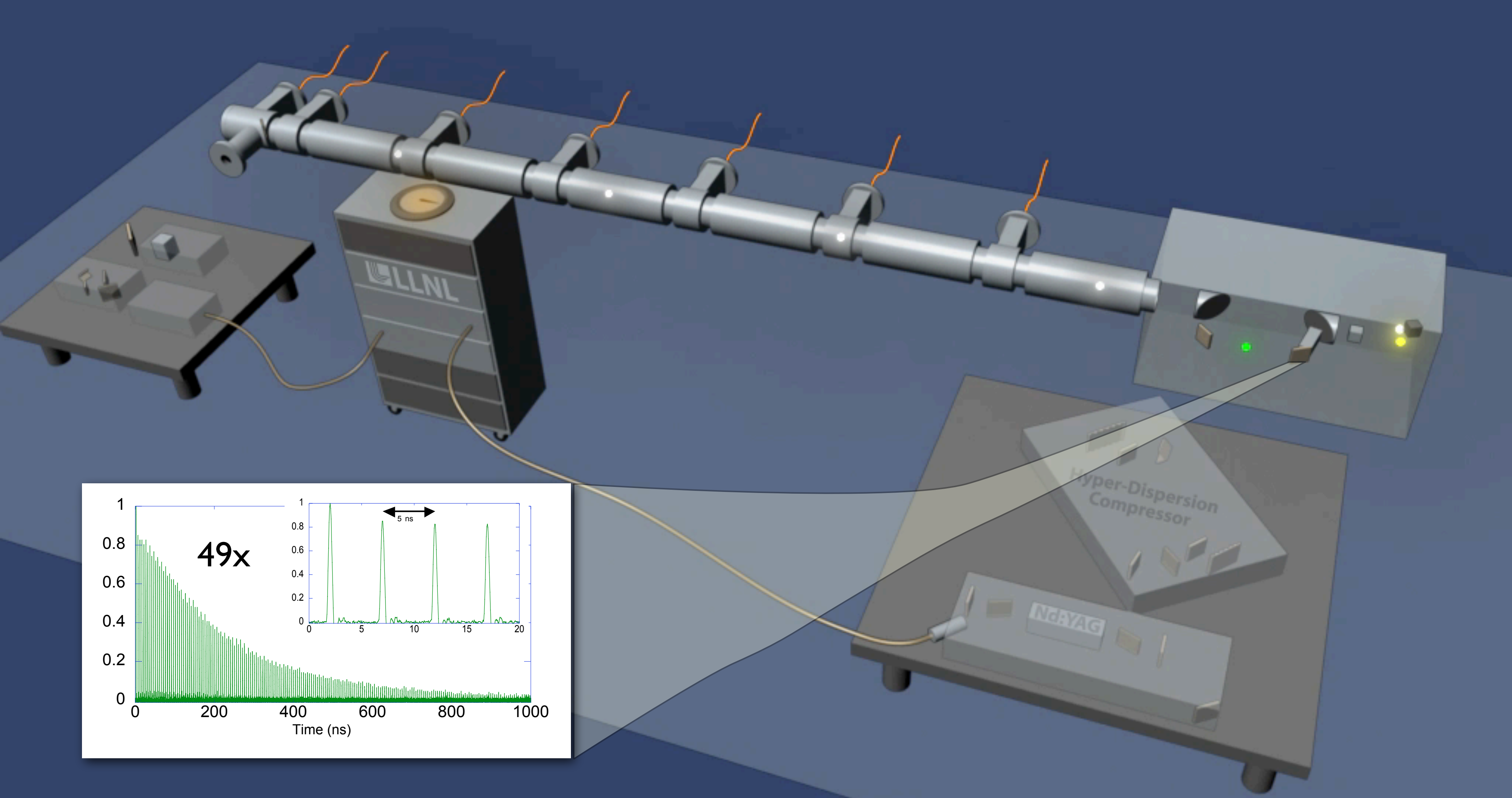

To first order no laser photons are used in laser-Compton scattering and the laser pulse may be reused to interact with subsequent electron bunches

Overall Compton scattering is broadband, but it is highly angle correlated and is 'narrowband' on axis

$$\Delta\Omega \approx \pi\left(\frac{1}{\gamma}\right)^2$$

few mrad

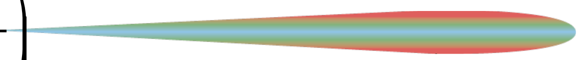

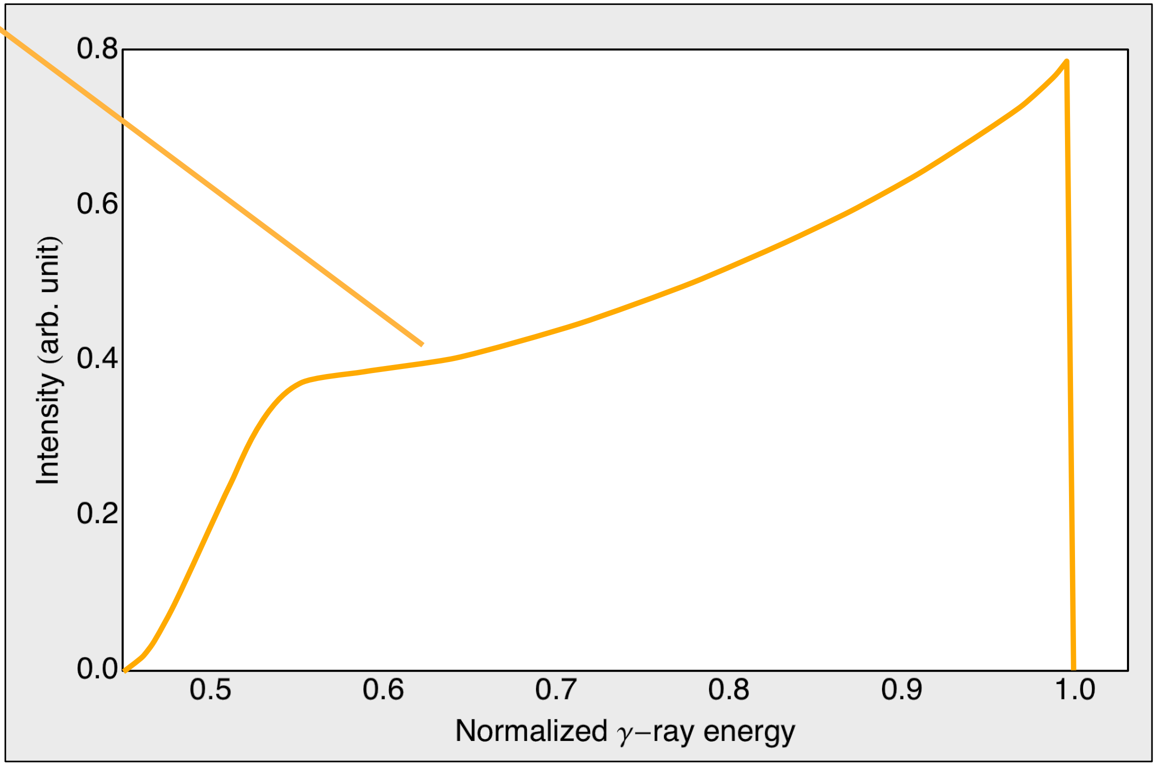

Overall Compton scattering is broadband, but it is highly angle correlated and is ‘narrowband’ on axis

$\Delta\Omega \; ; \; \pi\left(\frac{1}{\gamma}\right)^2$ 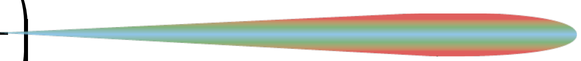

few mrad

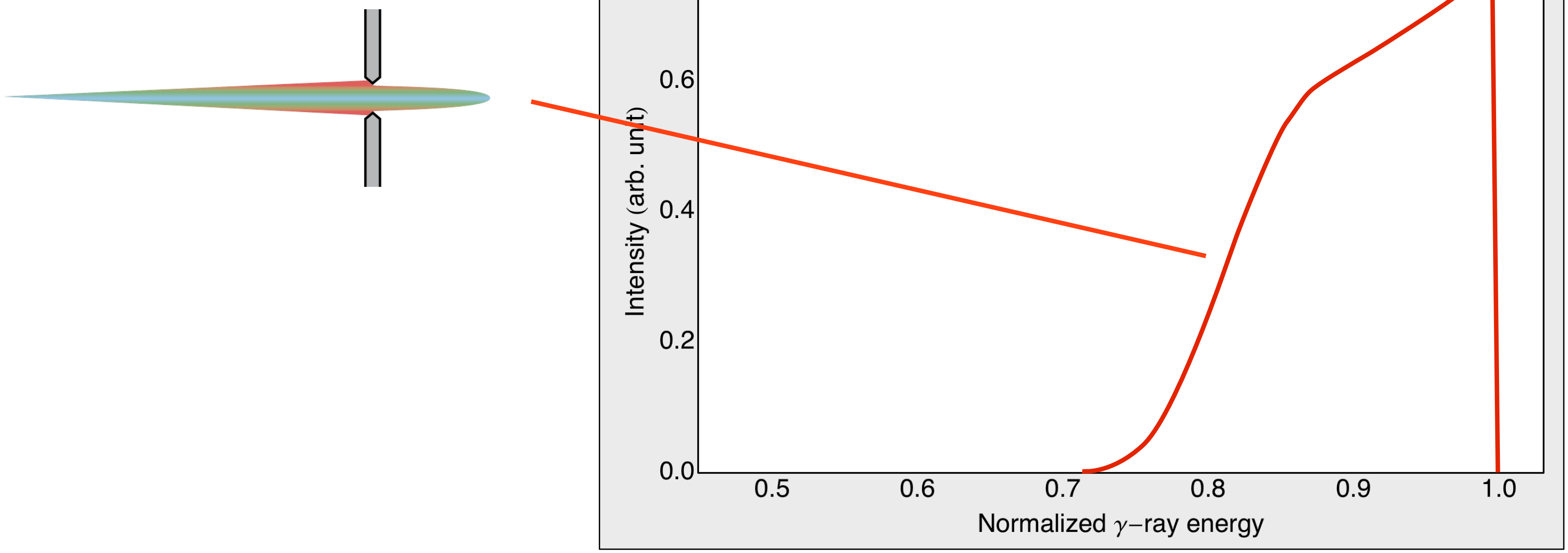

Overall Compton scattering is broadband, but it is highly angle correlated and is ‘narrowband’ on axis

$\Delta\Omega \; ; \; \pi\left(\frac{1}{\gamma}\right)^2$

few mrad

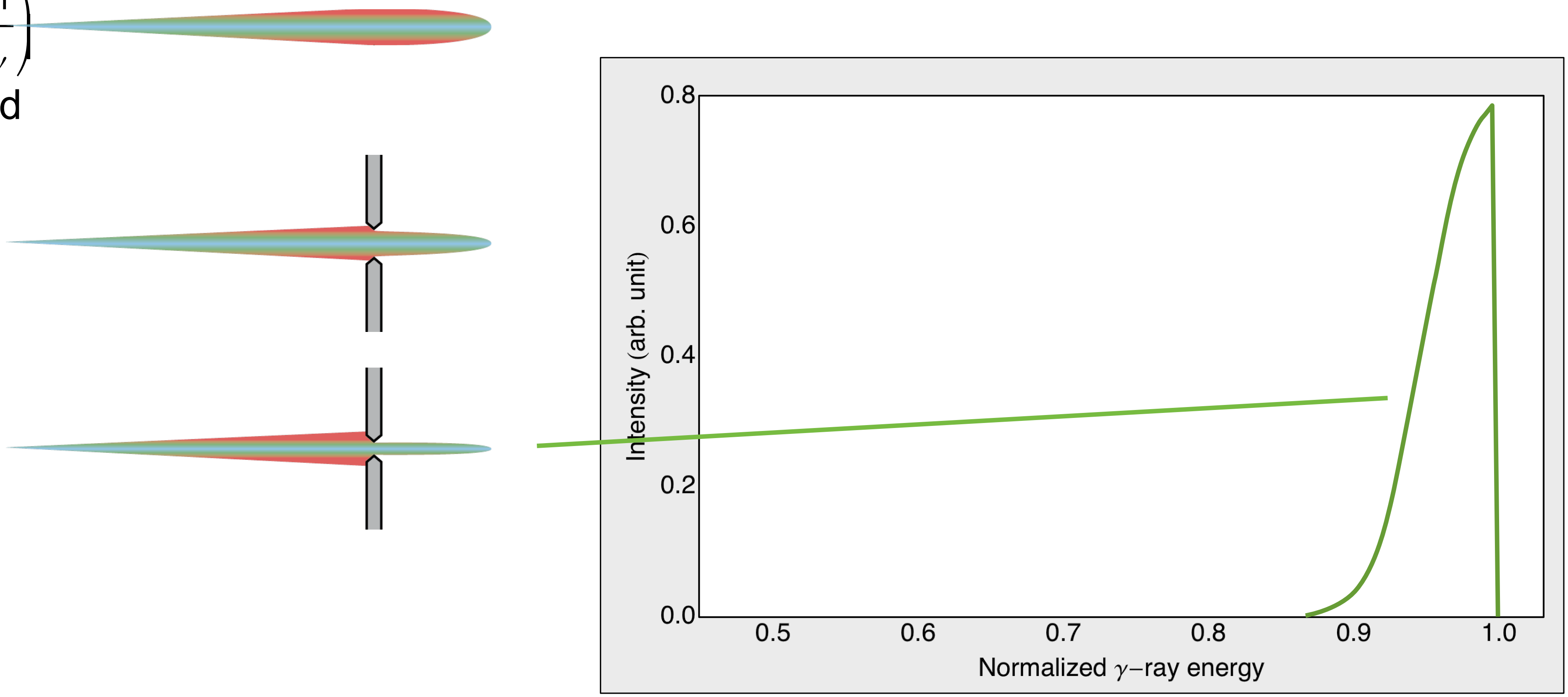

Overall Compton scattering is broadband, but it is highly angle correlated and is 'narrowband' on axis

$\Delta\Omega \sim \pi\left(\frac{1}{\gamma}\right)^2$

few mrad

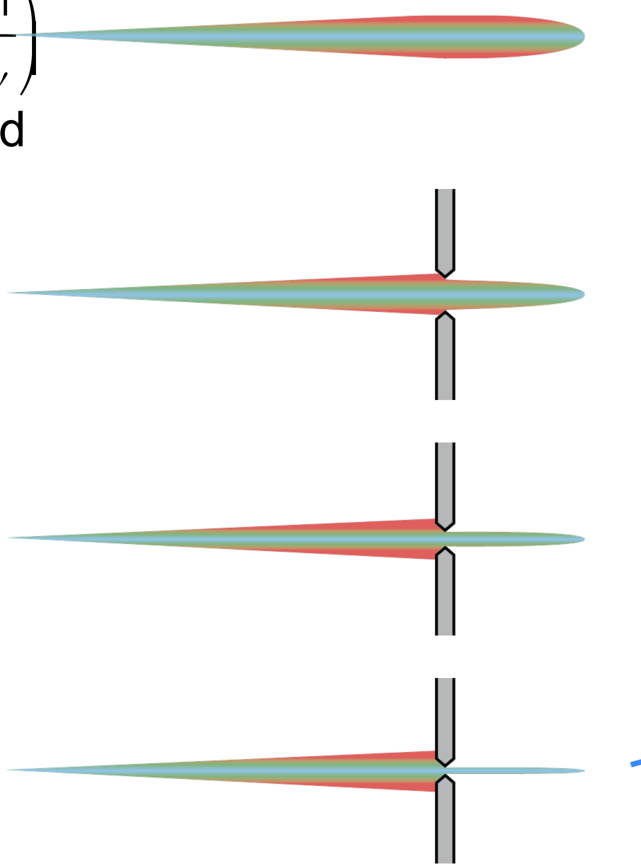

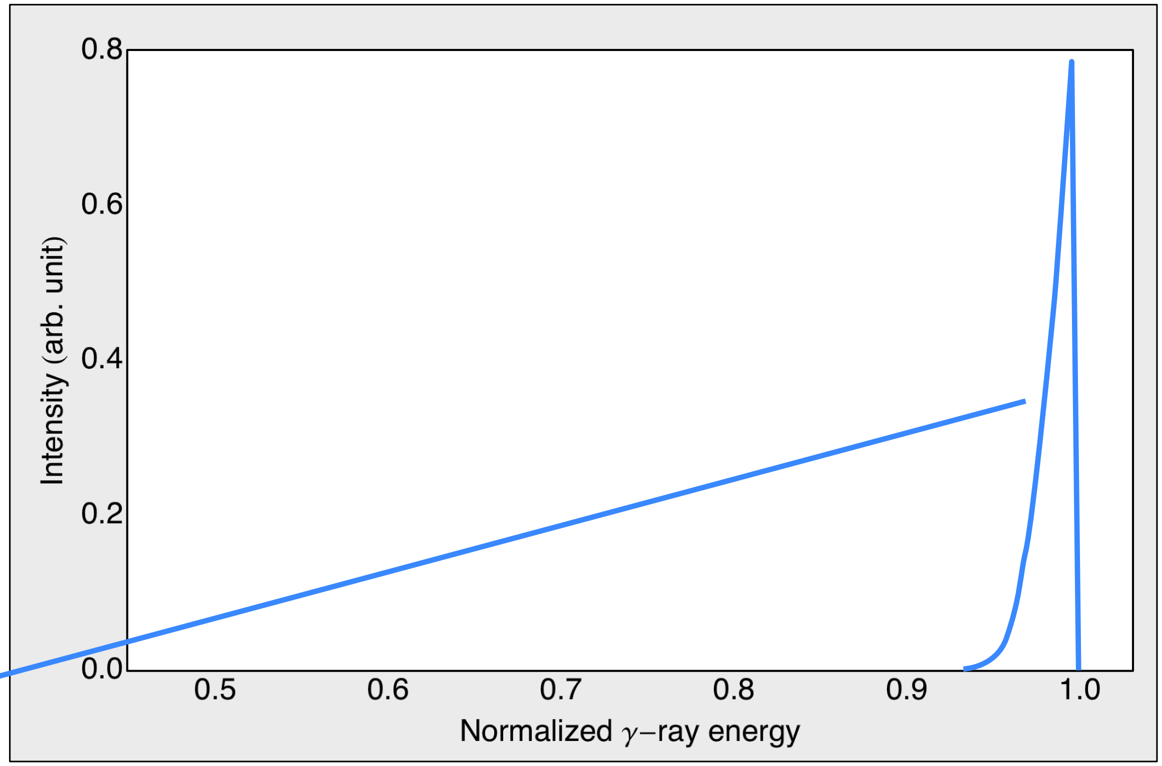

Overall Compton scattering is broadband, but it is highly angle correlated and is ‘narrowband’ on axis

$\Delta\Omega \; ; \; \pi\left(\frac{1}{\gamma}\right)^{2}$

few mrad

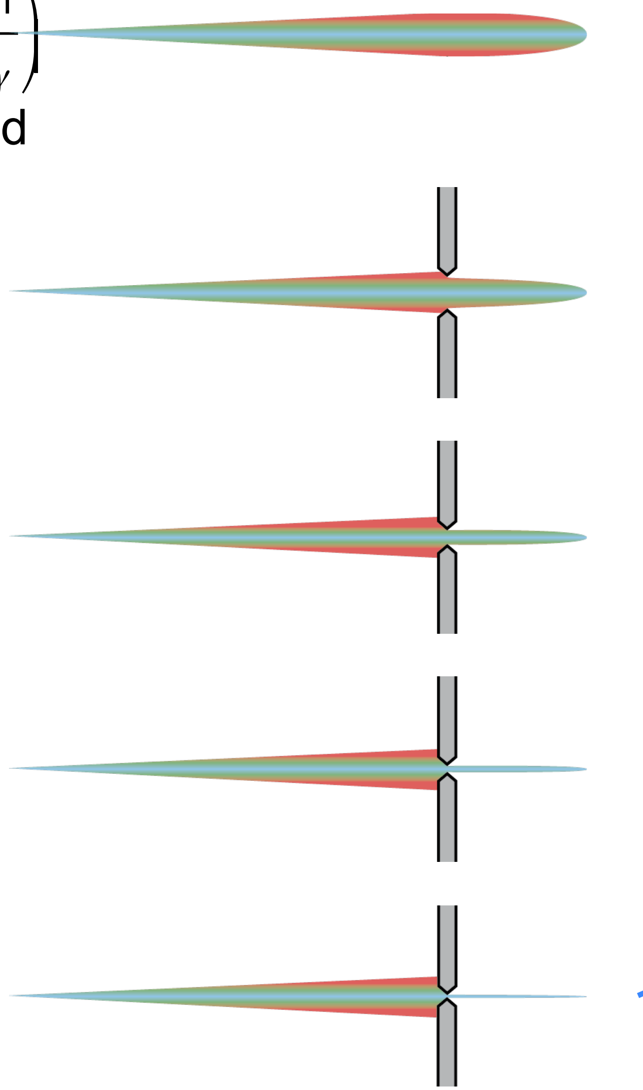

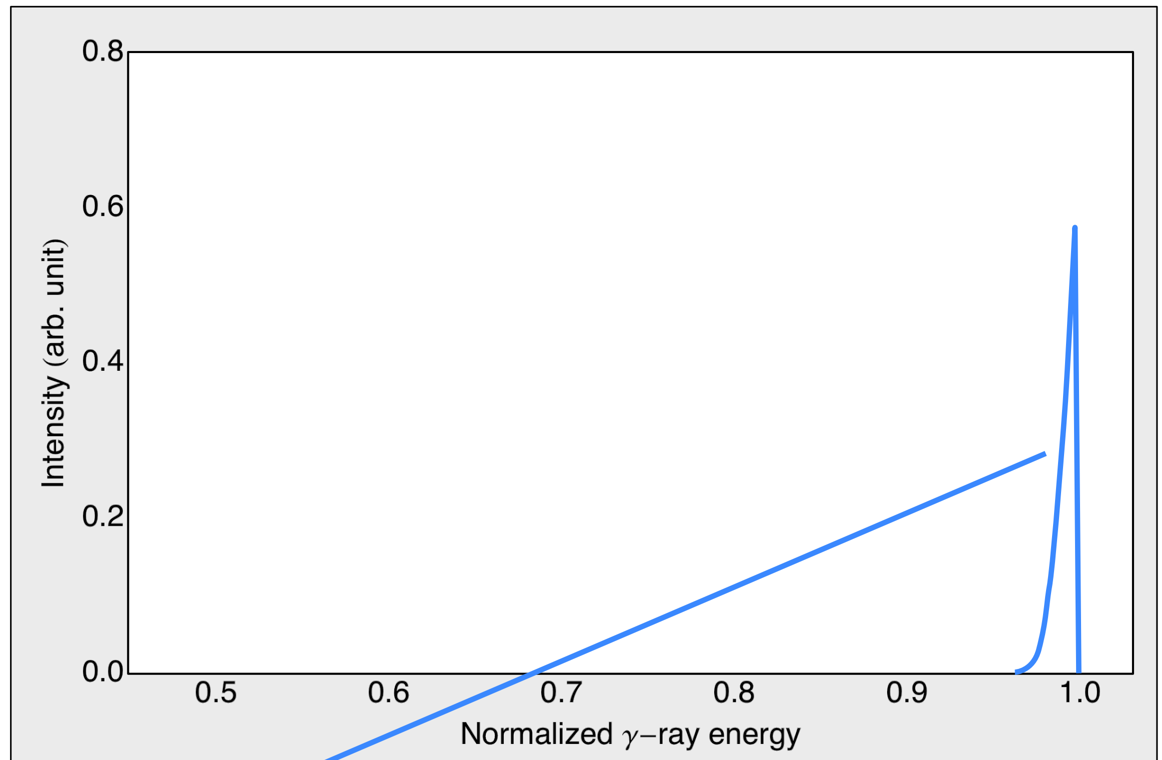

Overall Compton scattering is broadband, but it is highly angle correlated and is ‘narrowband’ on axis

$$\Delta\Omega \;;\; \pi\left(\frac{1}{\gamma}\right)^2$$

few mrad

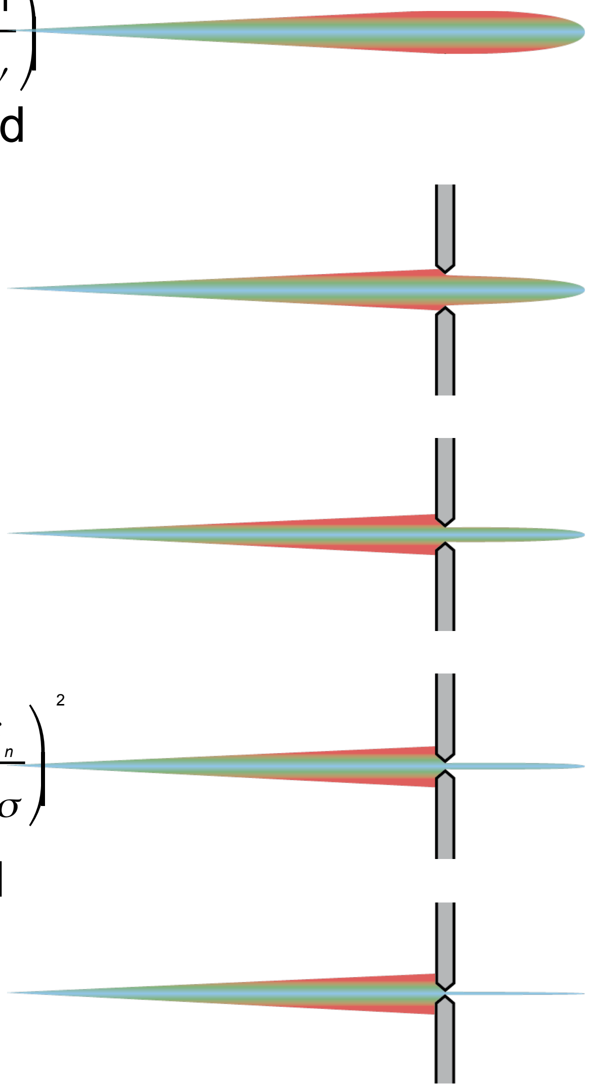

$$\Delta\Omega \;;\; \pi\left(\frac{\varepsilon_n}{\gamma\sigma}\right)^2$$

few μrad

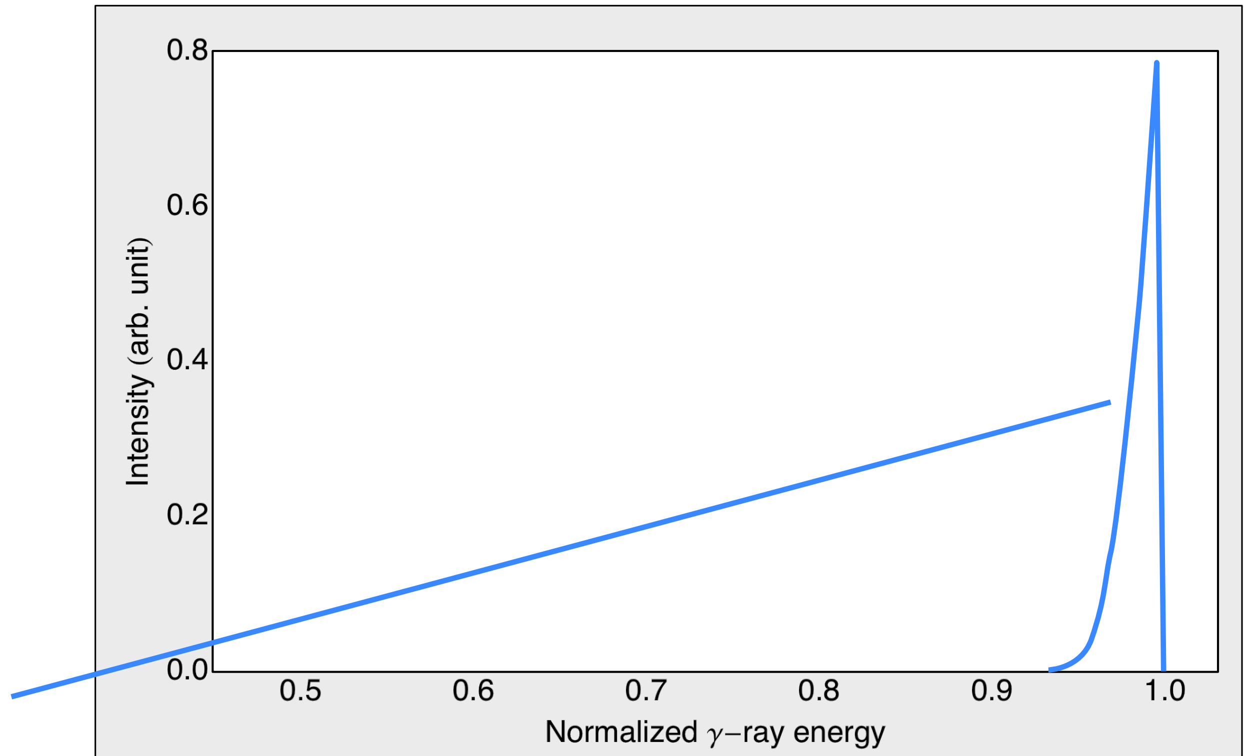

“<u>M</u>ono-<u>E</u>nergetic <u>Ga</u>mma-<u>rays</u>” - MEGa-rays

Many factors contribute to the minimum possible laser-Compton bandwidth that can be obtained

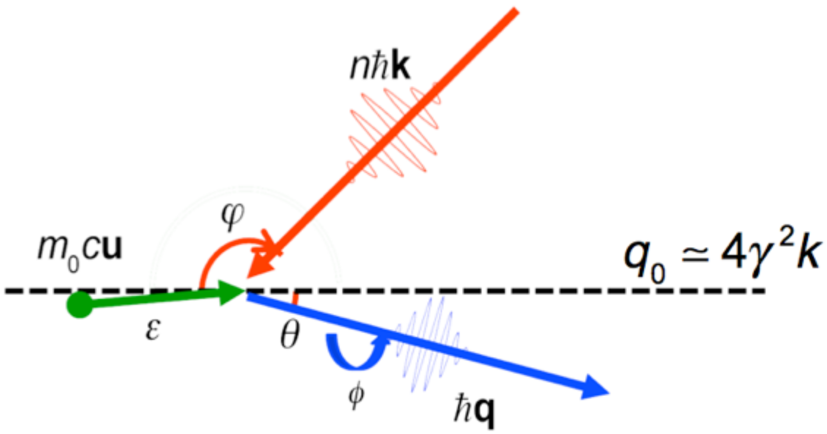

Energy-momentum conservation

$$q = k\frac{\gamma - u\cos(\varepsilon+\varphi)}{\gamma - u\cos\varepsilon + (1-\cos\varphi)\left\{\frac{A^2}{2\left[\gamma - u\cos(\varepsilon+\varphi)\right]} + \lambdabar k\right\}}$$

- Detection aperture $\quad \frac{\Delta q}{q} \simeq -\gamma^2\Delta\theta^2$
- Laser bandwidth $\quad \cancel{\frac{\Delta q}{q} \simeq \frac{\Delta k}{k}}$ O(10^{-4})
- Laser focal spot $\quad \cancel{\frac{\Delta q}{q} \simeq -\frac{1}{4}\Delta\varphi^2}$ O(10^{-4})
- Electron energy spread $\quad \frac{\Delta q}{q} \simeq 2\frac{\Delta\gamma}{\gamma}$
- Electron beam emittance $\quad \frac{\Delta q}{q} \simeq -\gamma^2\Delta\varepsilon^2$
- Nonlinear radiation pressure $\quad \cancel{\frac{\Delta q}{q} \simeq -\frac{\Delta A^2}{1+A^2}}$ $< 10^{-4}$

Modern, high gradient accelerators can create very small emittance & low energy spread at low charge

25 pC electron beam phase space

Electron bunch energy

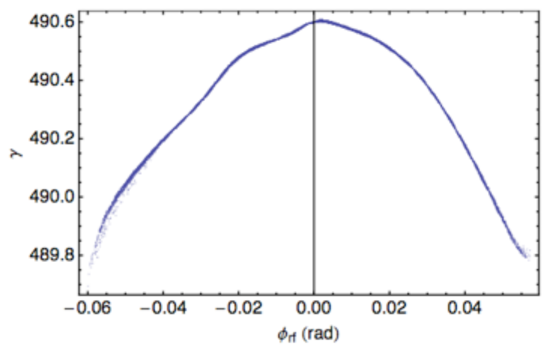

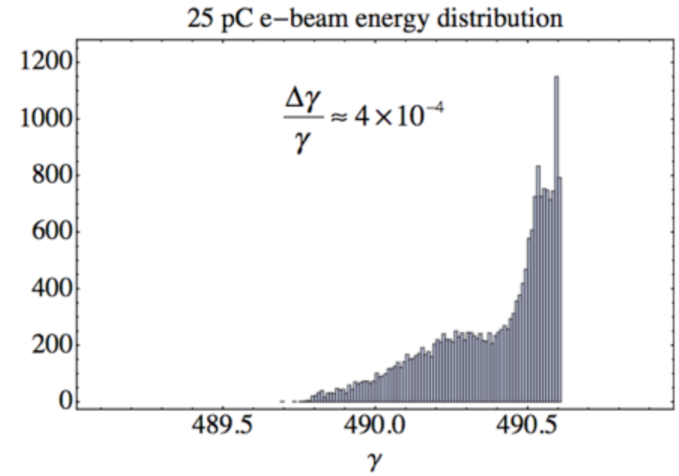

Focal spot $\varepsilon \approx 0.15$ mm mrad

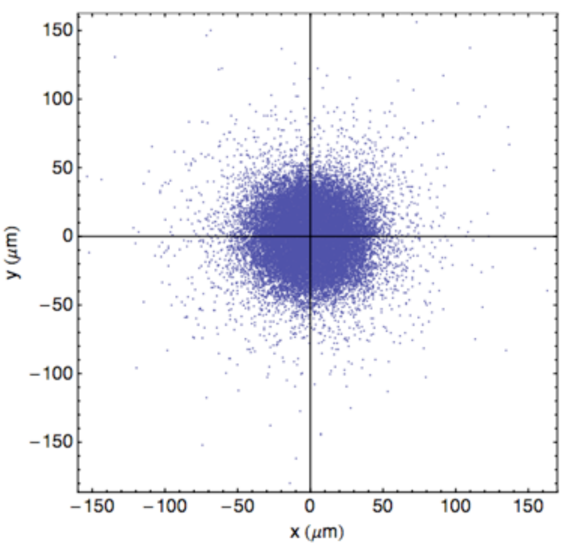

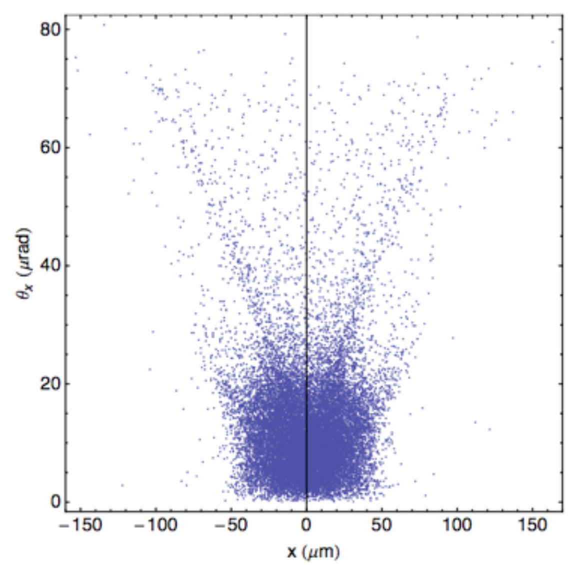

For low emittance e-beam and ps laser pulses, the dominant bandwidth factor is detection aperture

$$\Delta\Omega\ ;\ \pi\left(\frac{1}{\gamma}\right)^2$$

few mrad

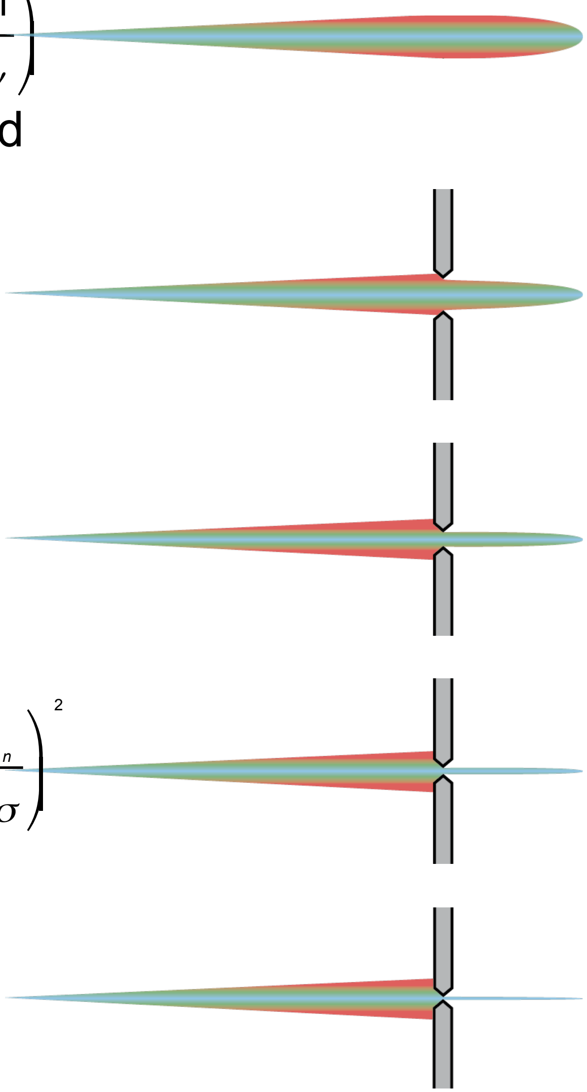

$$\Delta\Omega\ ;\ \pi\left(\frac{\varepsilon_n}{\gamma\sigma}\right)^2$$

few µrad

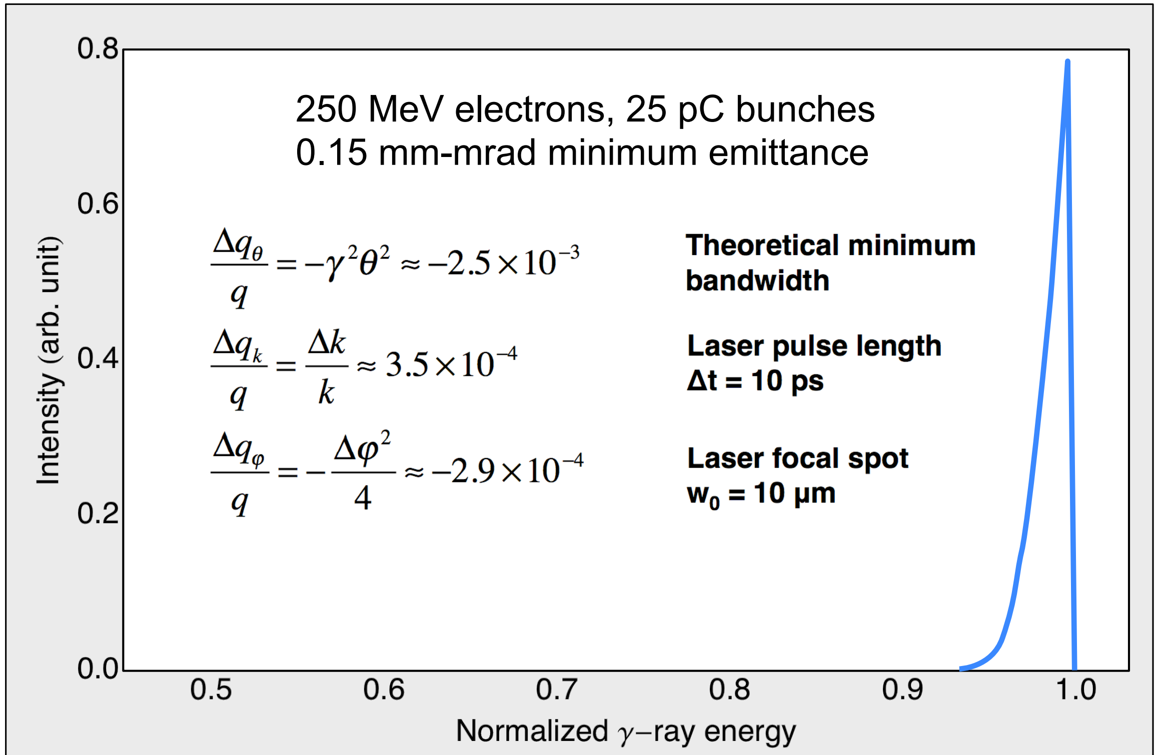

"Mono-Energetic Gamma-rays" - MEGa-rays

Optimally designed sources can have fractional bandwidths of ~10^{-3} FWHM

The characteristics of optimized MEGa-ray sources are unprecedented and enable “nuclear photonics”

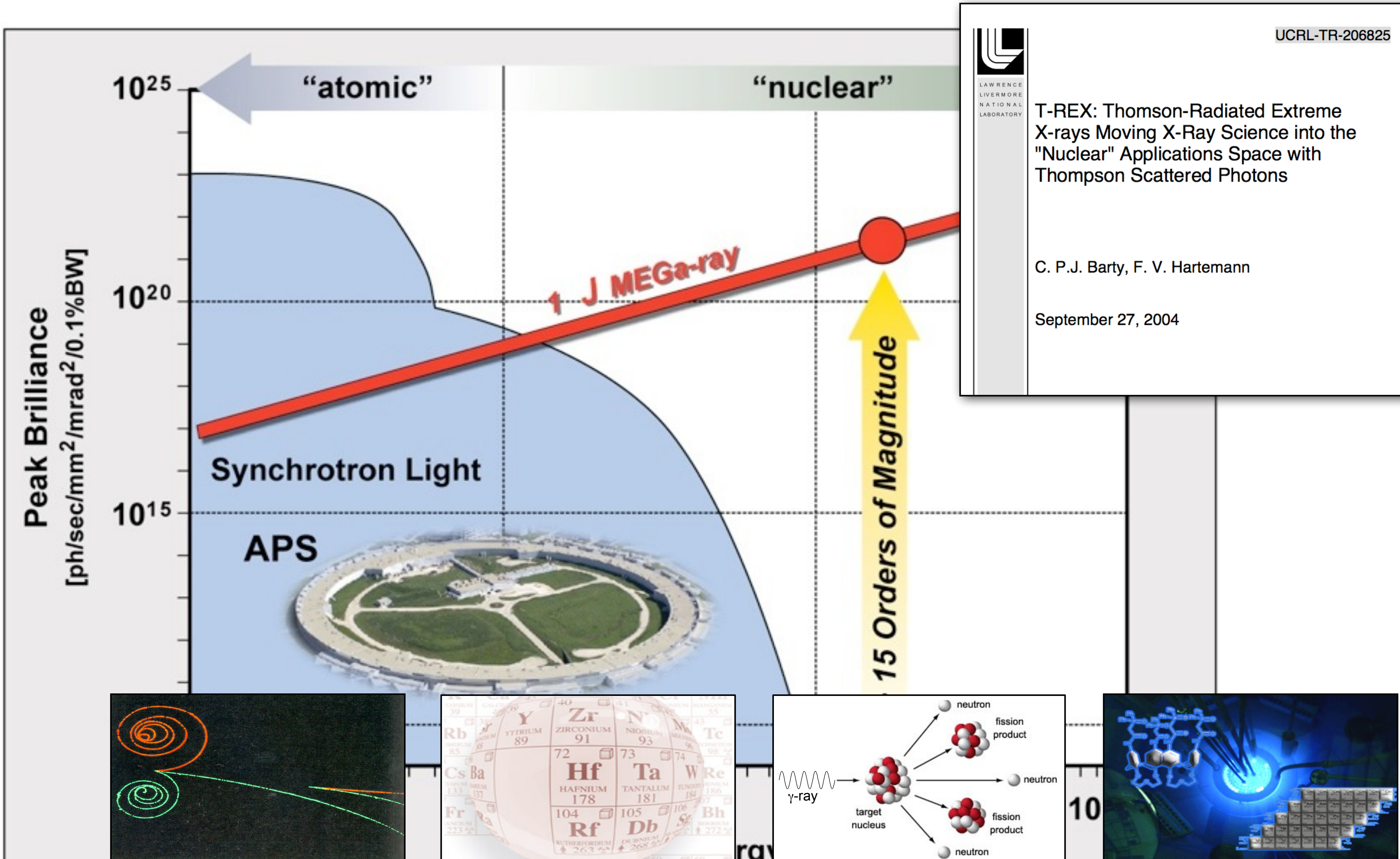

ps-duration, pulsed positron sources

isomer physics and spectroscopy

photo-fission and transmutation

micron-scale, ps-duration pulsed neutron sources

The T-REX (*Thomson-Radiated Extreme X-ray*) project created LLNL's first MEGa-ray source

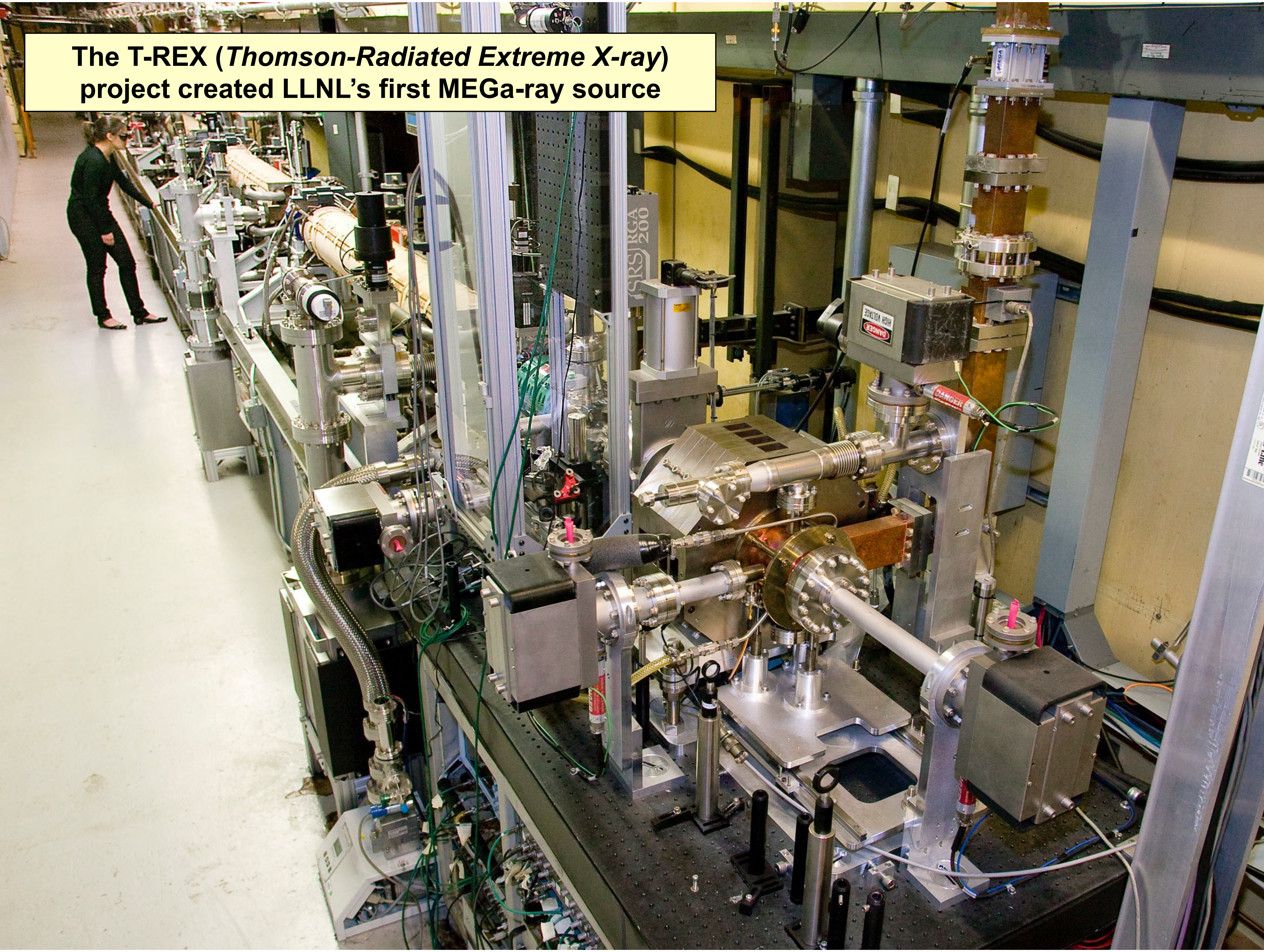

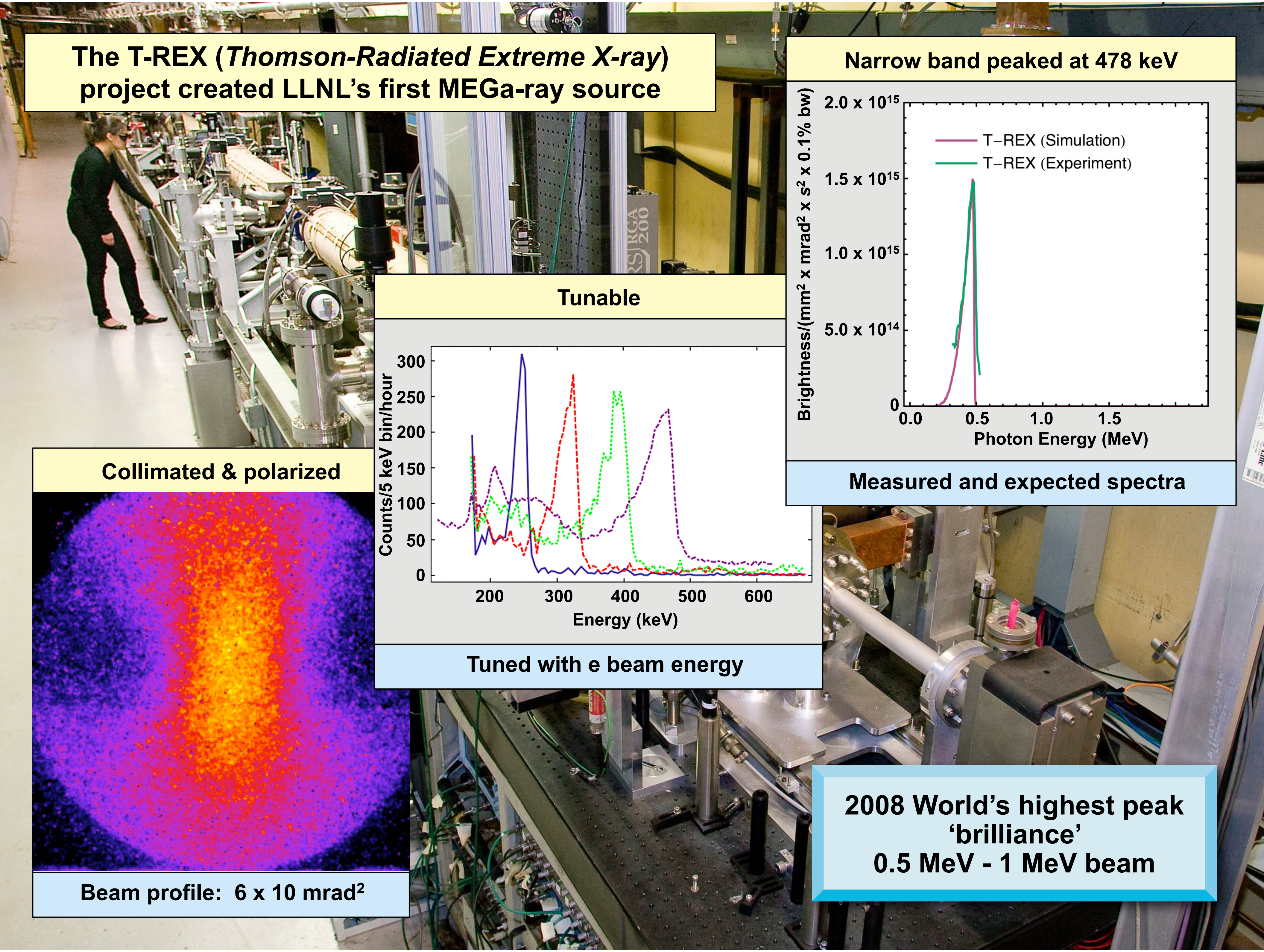
The T-REX (*Thomson-Radiated Extreme X-ray*)
project created LLNL's first MEGa-ray source
Narrow band peaked at 478 keV
Brightness/(mm² x mrad² x s² x 0.1% bw)
2.0 x 10¹⁵
1.5 x 10¹⁵
1.0 x 10¹⁵
5.0 x 10¹⁴
0
0.0
0.5
1.0
1.5
Photon Energy (MeV)
T−REX (Simulation)
T−REX (Experiment)
Measured and expected spectra
Tunable
Counts/5 keV bin/hour
300
250
200
150
100
50
0
200
300
400
500
600
Energy (keV)
Tuned with e beam energy
Collimated & polarized
Beam profile: 6 x 10 mrad²
2008 World's highest peak
'brilliance'
0.5 MeV - 1 MeV beam
RGA 200

The T-REX (*Thomson-Radiated Extreme X-ray*) project created LLNL's first MEGa-ray source

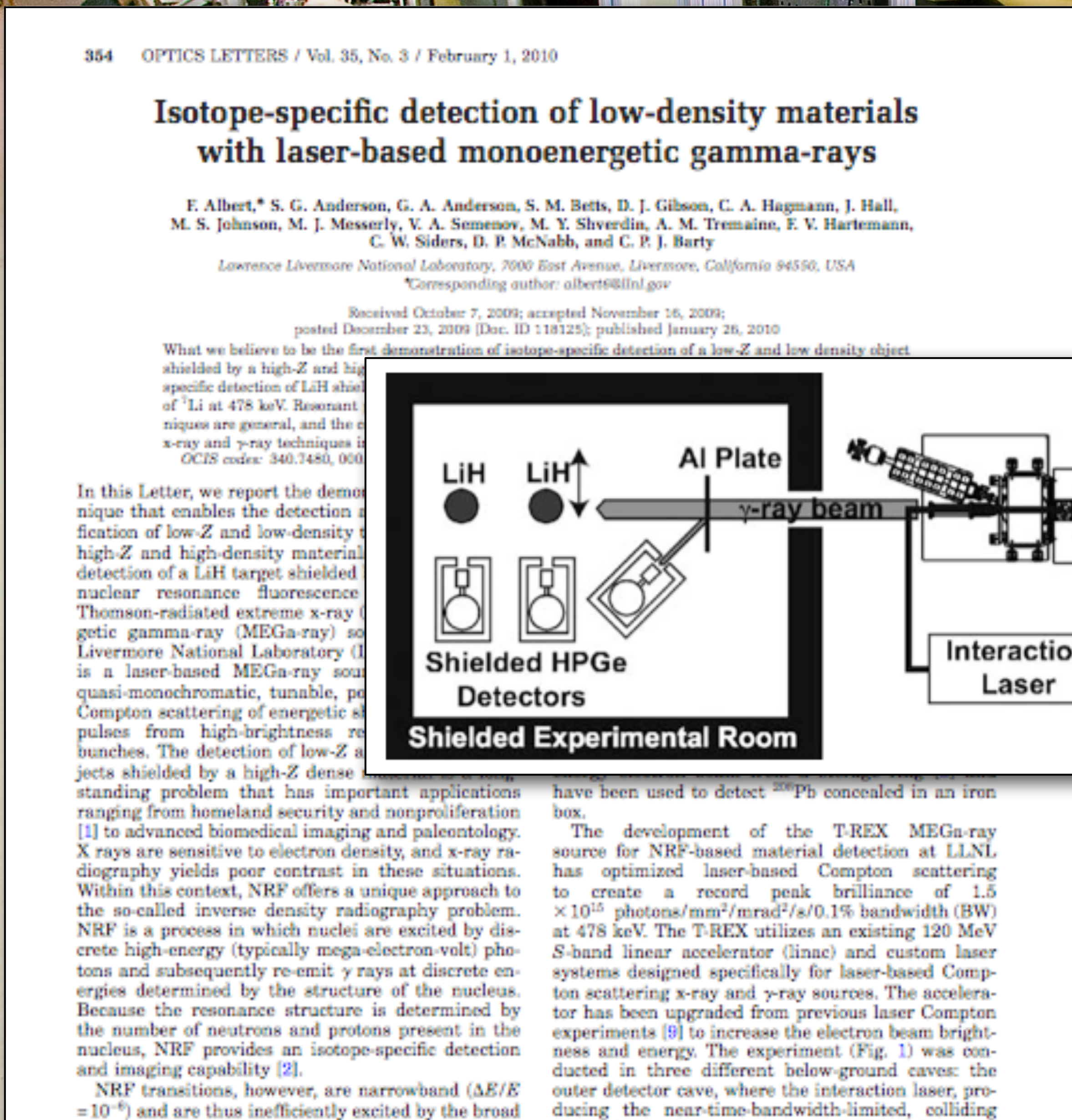

354 OPTICS LETTERS / Vol. 35, No. 3 / February 1, 2010

Isotope-specific detection of low-density materials with laser-based monoenergetic gamma-rays

F. Albert,* S. G. Anderson, G. A. Anderson, S. M. Betts, D. J. Gibson, C. A. Hagmann, J. Hall, M. S. Johnson, M. J. Messerly, V. A. Semenov, M. Y. Shverdin, A. M. Tremaine, F. V. Hartemann, C. W. Siders, D. P. McNabb, and C. P. J. Barty

Lawrence Livermore National Laboratory, 7000 East Avenue, Livermore, California 94550, USA

*Corresponding author: albert6@llnl.gov

Received October 7, 2009; accepted November 16, 2009; posted December 23, 2009 (Doc. ID 118125); published January 26, 2010

What we believe to be the first demonstration of isotope-specific detection of a low-Z and low density object shielded by a high-Z and hig… specific detection of LiH shiel… of ^{7}Li at 478 keV. Resonant… niques are general, and the c… x-ray and γ-ray techniques i… OCIS codes: 340.7480, 000…

In this Letter, we report the demo… nique that enables the detection … fication of low-Z and low-density … high-Z and high-density material… detection of a LiH target shielded … nuclear resonance fluorescence … Thomson-radiated extreme x-ray (… getic gamma-ray (MEGa-ray) so… Livermore National Laboratory (… is a laser-based MEGa-ray sour… quasi-monochromatic, tunable, p… Compton scattering of energetic … pulses from high-brightness re… bunches. The detection of low-Z a… jects shielded by a high-Z dense … standing problem that has important applications ranging from homeland security and nonproliferation [1] to advanced biomedical imaging and paleontology. X rays are sensitive to electron density, and x-ray radiography yields poor contrast in these situations. Within this context, NRF offers a unique approach to the so-called inverse density radiography problem. NRF is a process in which nuclei are excited by discrete high-energy (typically mega-electron-volt) photons and subsequently re-emit γ rays at discrete energies determined by the structure of the nucleus. Because the resonance structure is determined by the number of neutrons and protons present in the nucleus, NRF provides an isotope-specific detection and imaging capability [2].

NRF transitions, however, are narrowband ($\Delta E/E = 10^{-6}$) and are thus inefficiently excited by the broad …

… have been used to detect ^{208}Pb concealed in an iron box.

The development of the T-REX MEGa-ray source for NRF-based material detection at LLNL has optimized laser-based Compton scattering to create a record peak brilliance of 1.5×10^{15} photons/mm^2/mrad^2/s/0.1% bandwidth (BW) at 478 keV. The T-REX utilizes an existing 120 MeV S-band linear accelerator (linac) and custom laser systems designed specifically for laser-based Compton scattering x-ray and γ-ray sources. The accelerator has been upgraded from previous laser Compton experiments [9] to increase the electron beam brightness and energy. The experiment (Fig. 1) was conducted in three different below-ground caves: the outer detector cave, where the interaction laser, producing the near-time-bandwidth-limited, colliding …

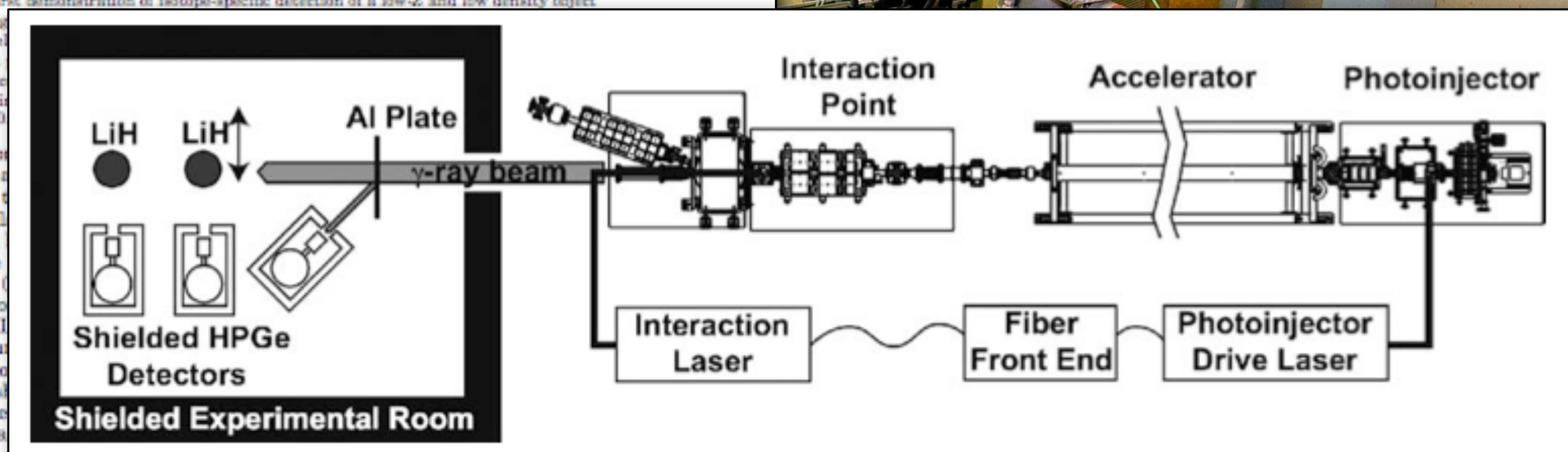

2008 World's highest peak 'brilliance'
0.5 MeV - 1 MeV beam

Transmission-based detection was used for our initial material detection experiments

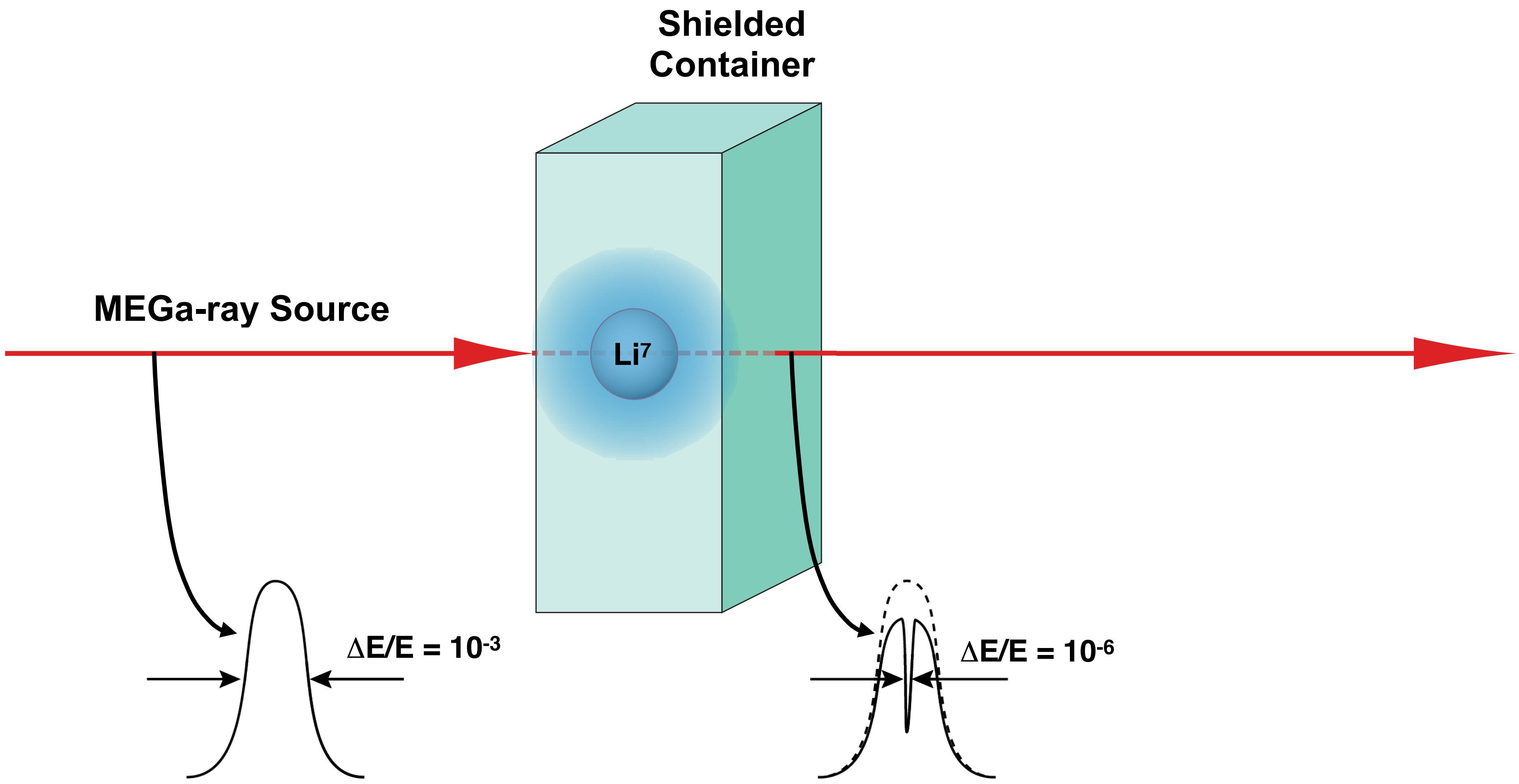

Transmission-based detection was used for our initial material detection experiments

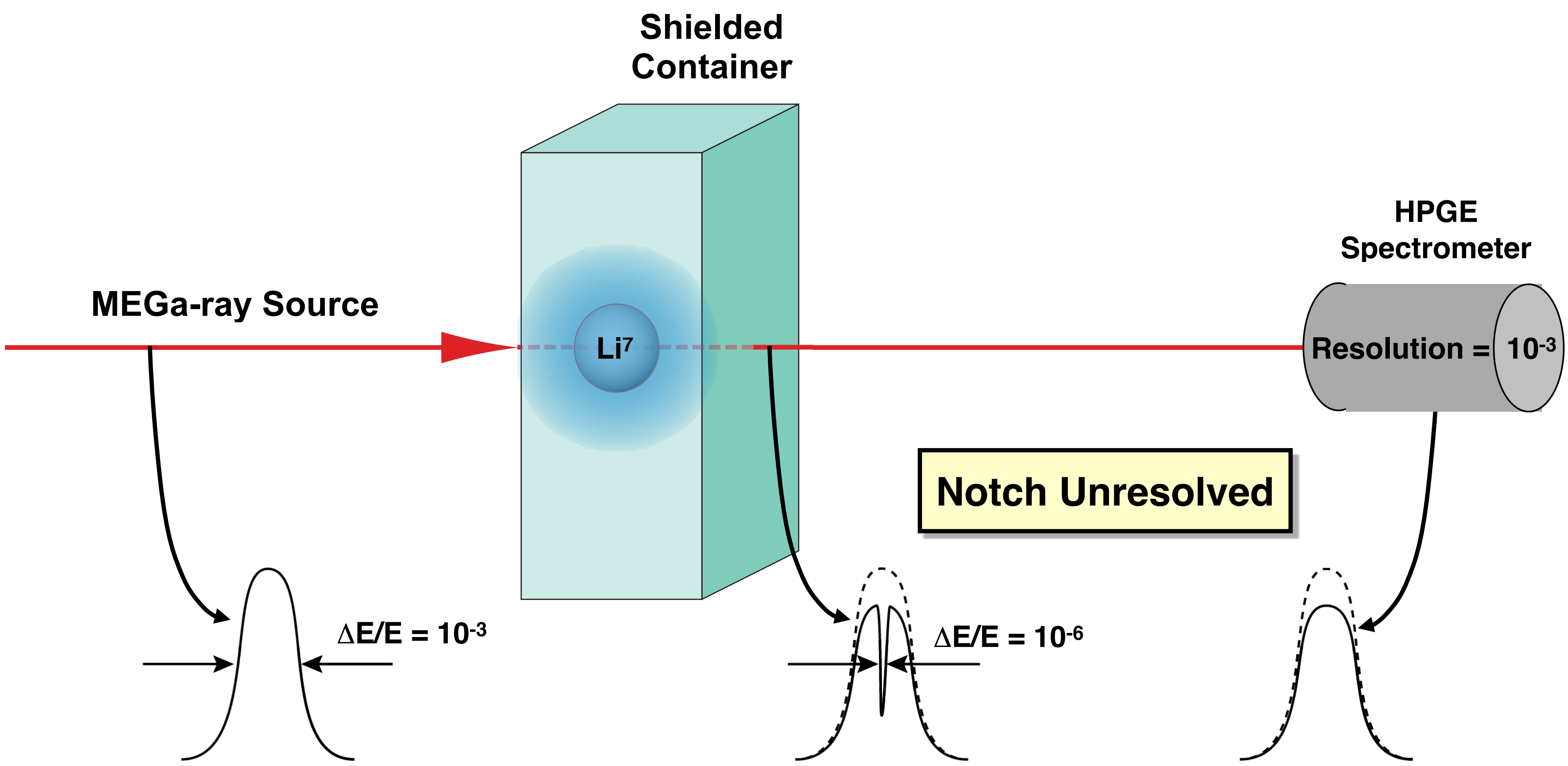

Transmission-based detection was used for our initial material detection experiments

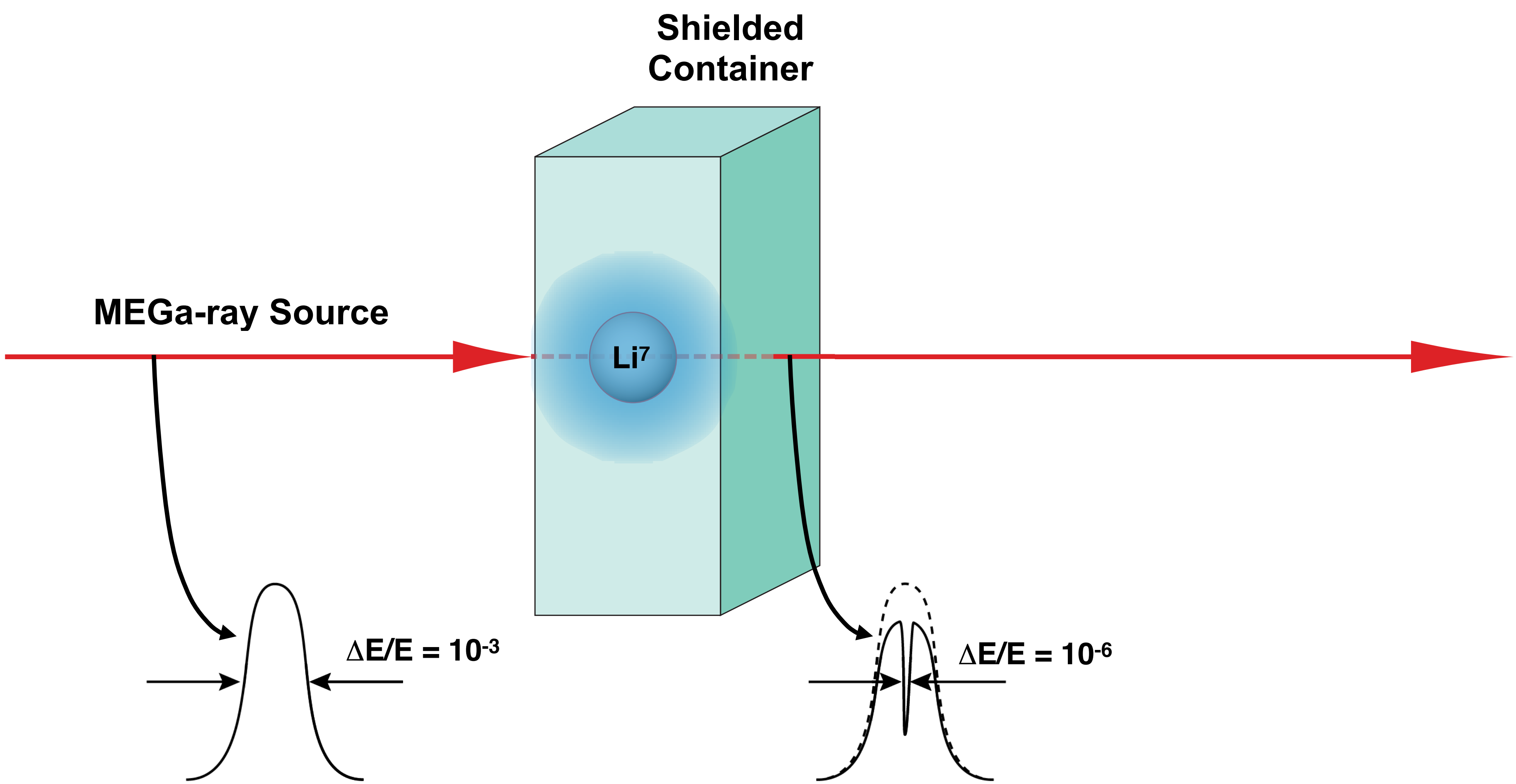

Transmission-based detection was used for our initial material detection experiments

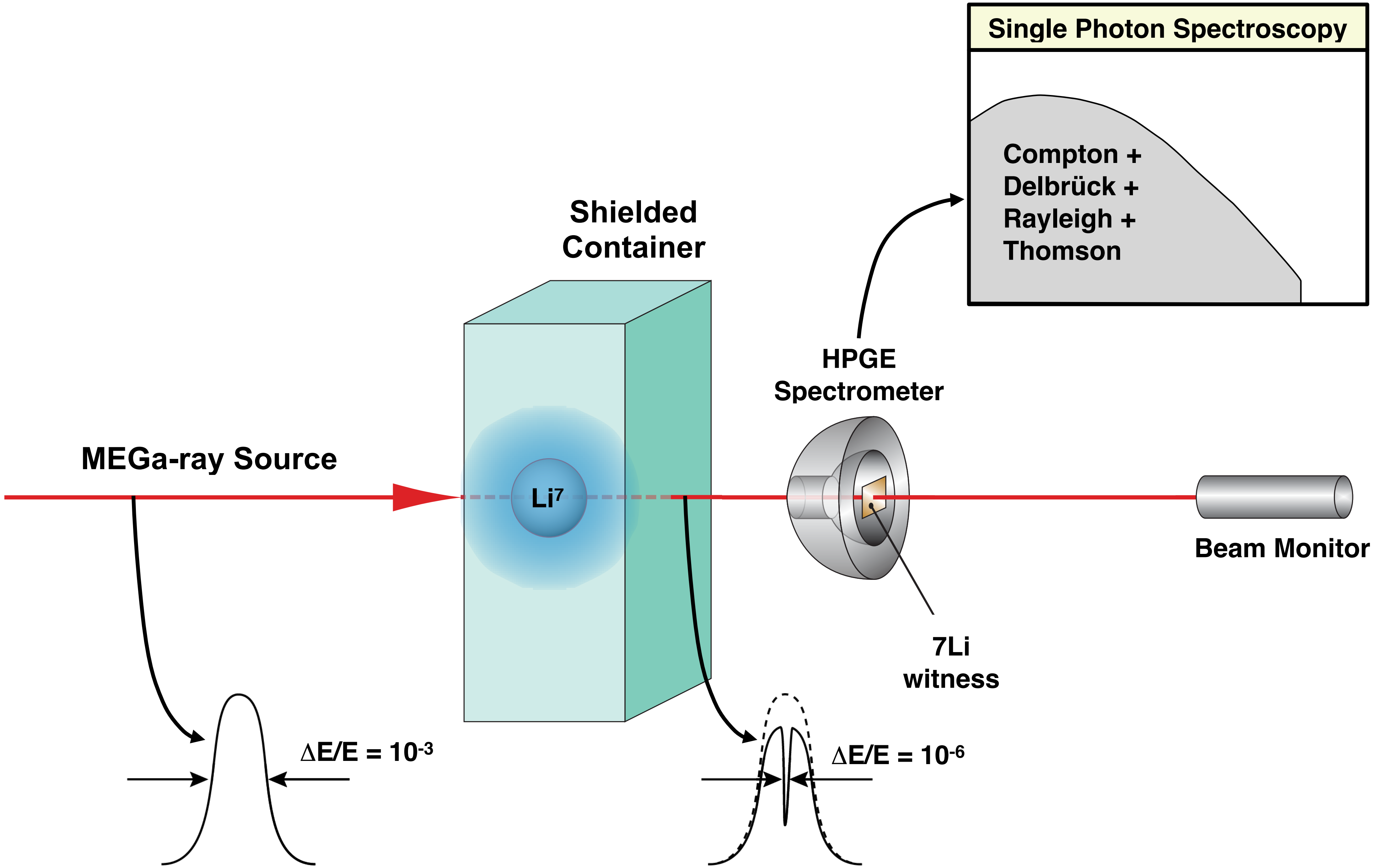

Transmission-based detection was used for our initial material detection experiments

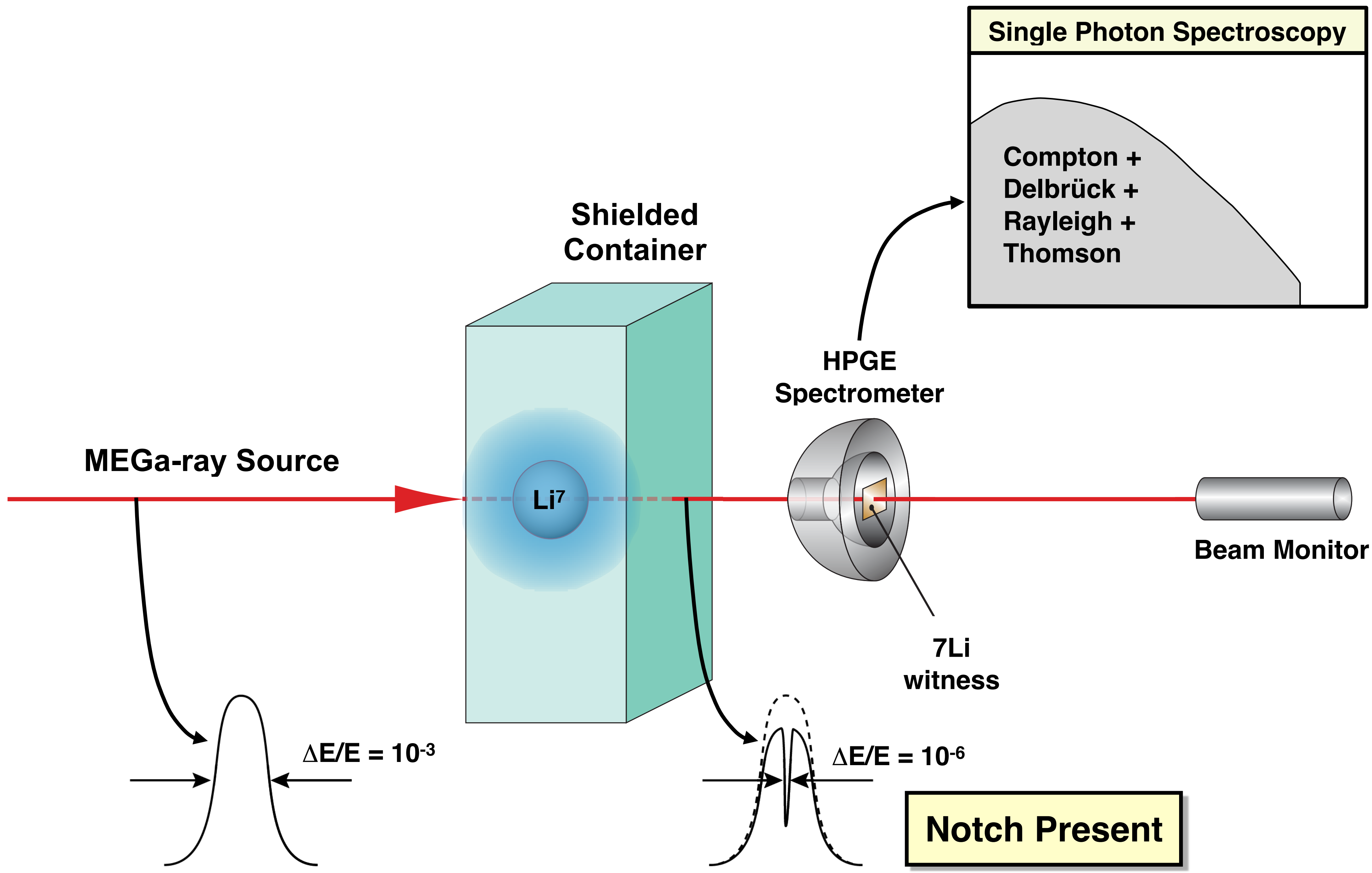

Transmission-based detection was used for our initial material detection experiments

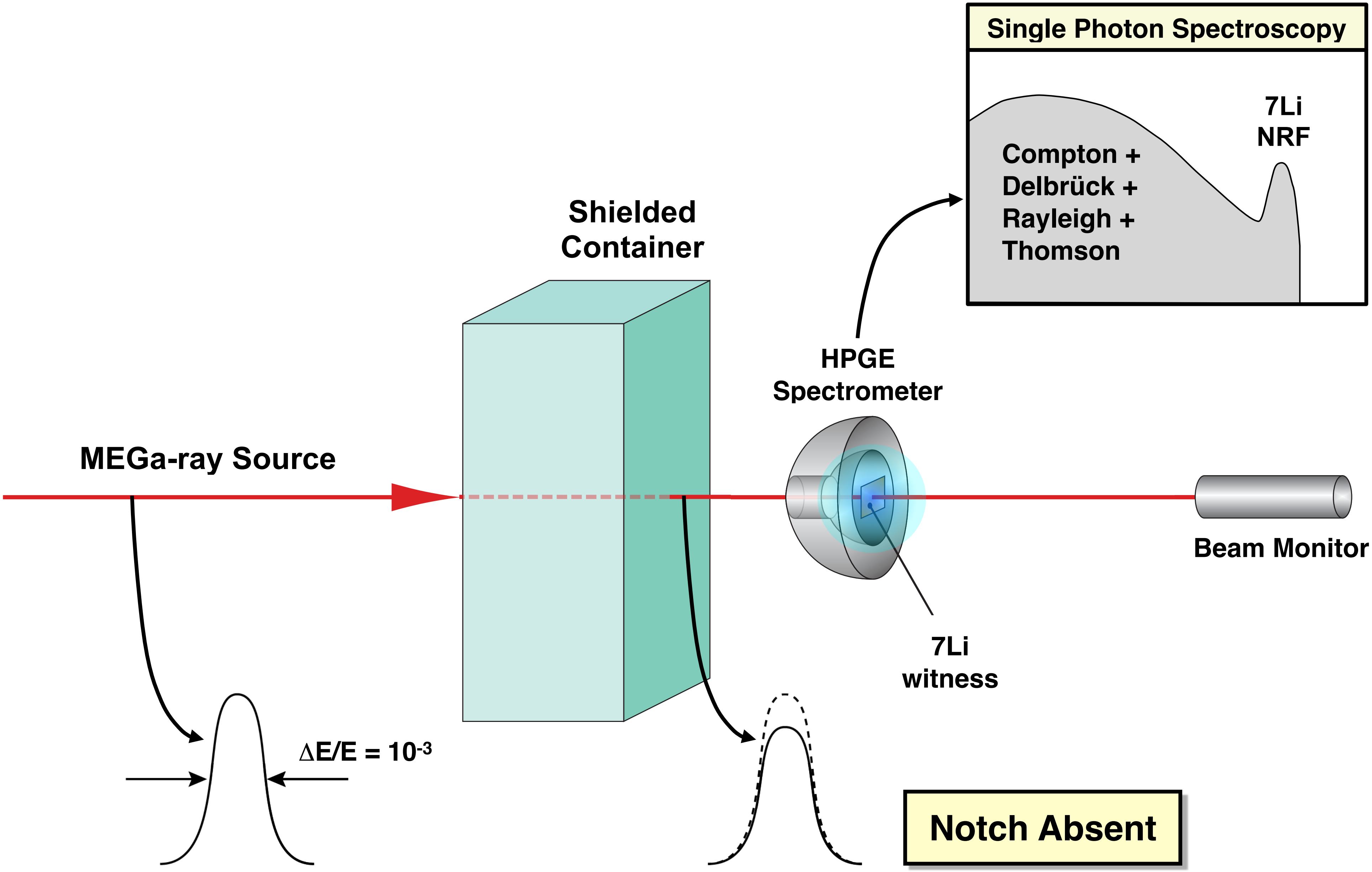

originally suggested by Prof. W. Bertozzi of MIT and Passport Systems

Transmission-based detection was used for our initial material detection experiments

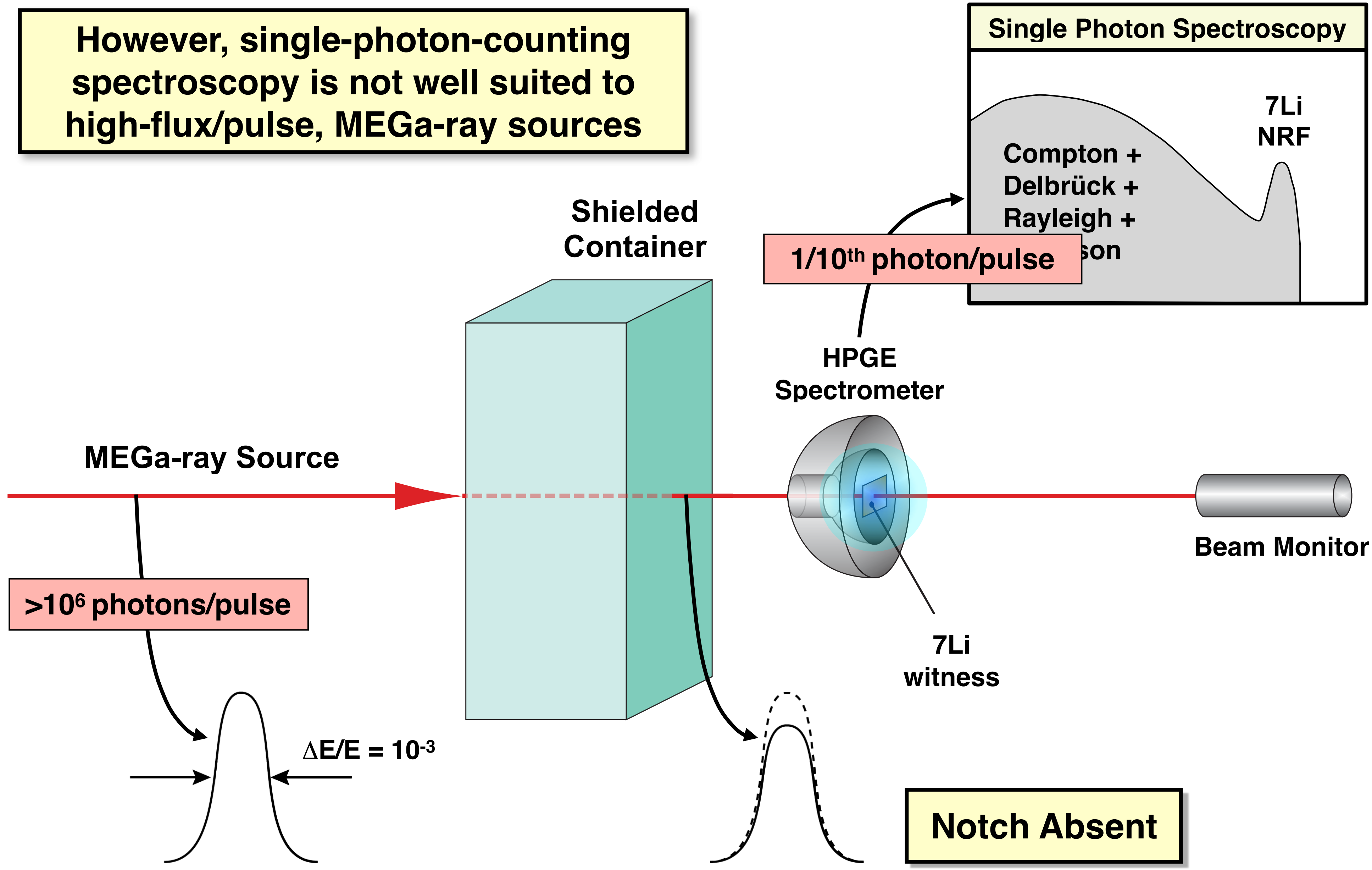

originally suggested by Prof. W. Bertozzi of MIT and Passport Systems

Transmission-based detection was used for our initial material detection experiments

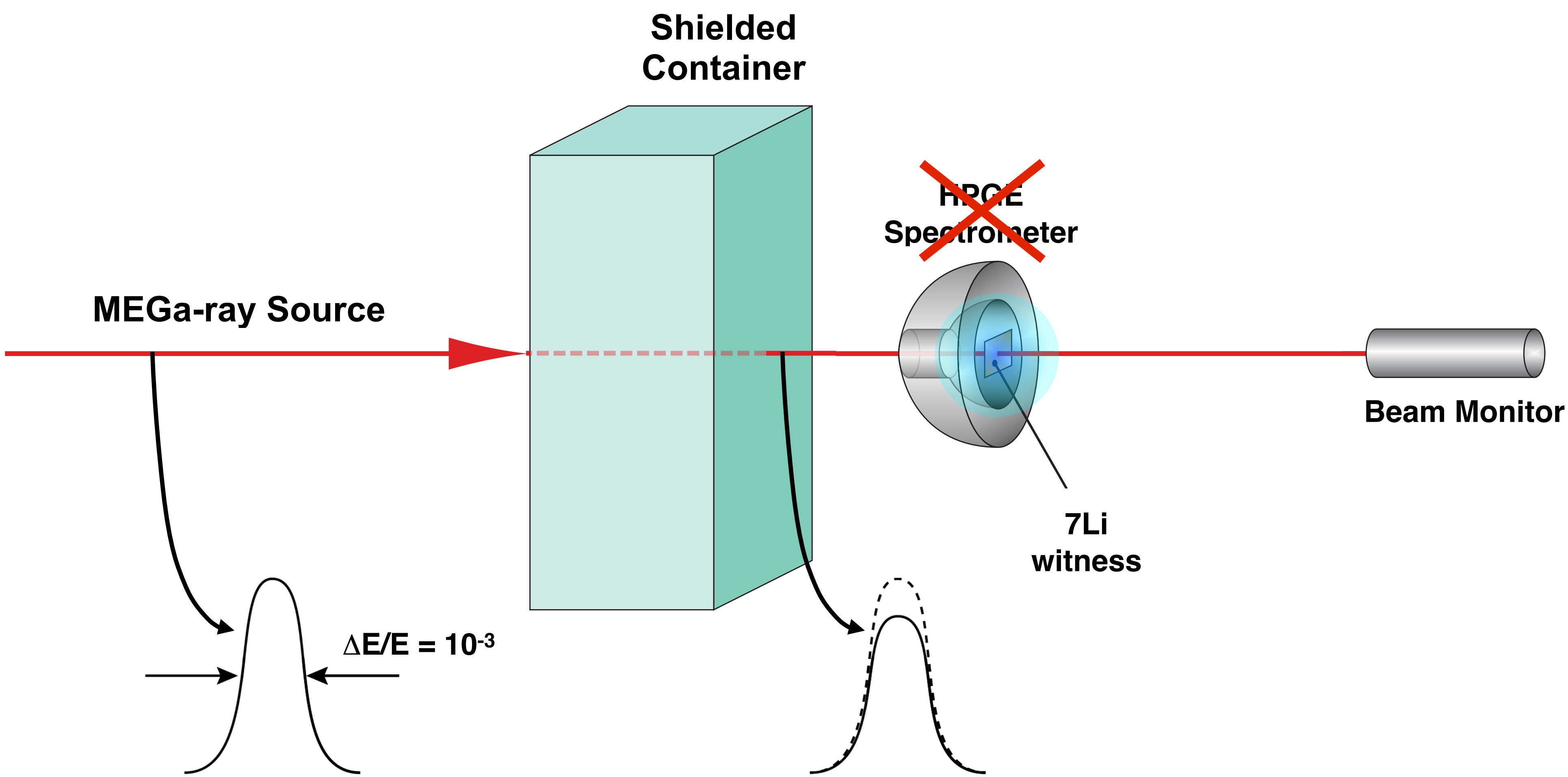

Dual Isotope Notch Observation (DINO) eliminates the need for high resolution spectroscopy

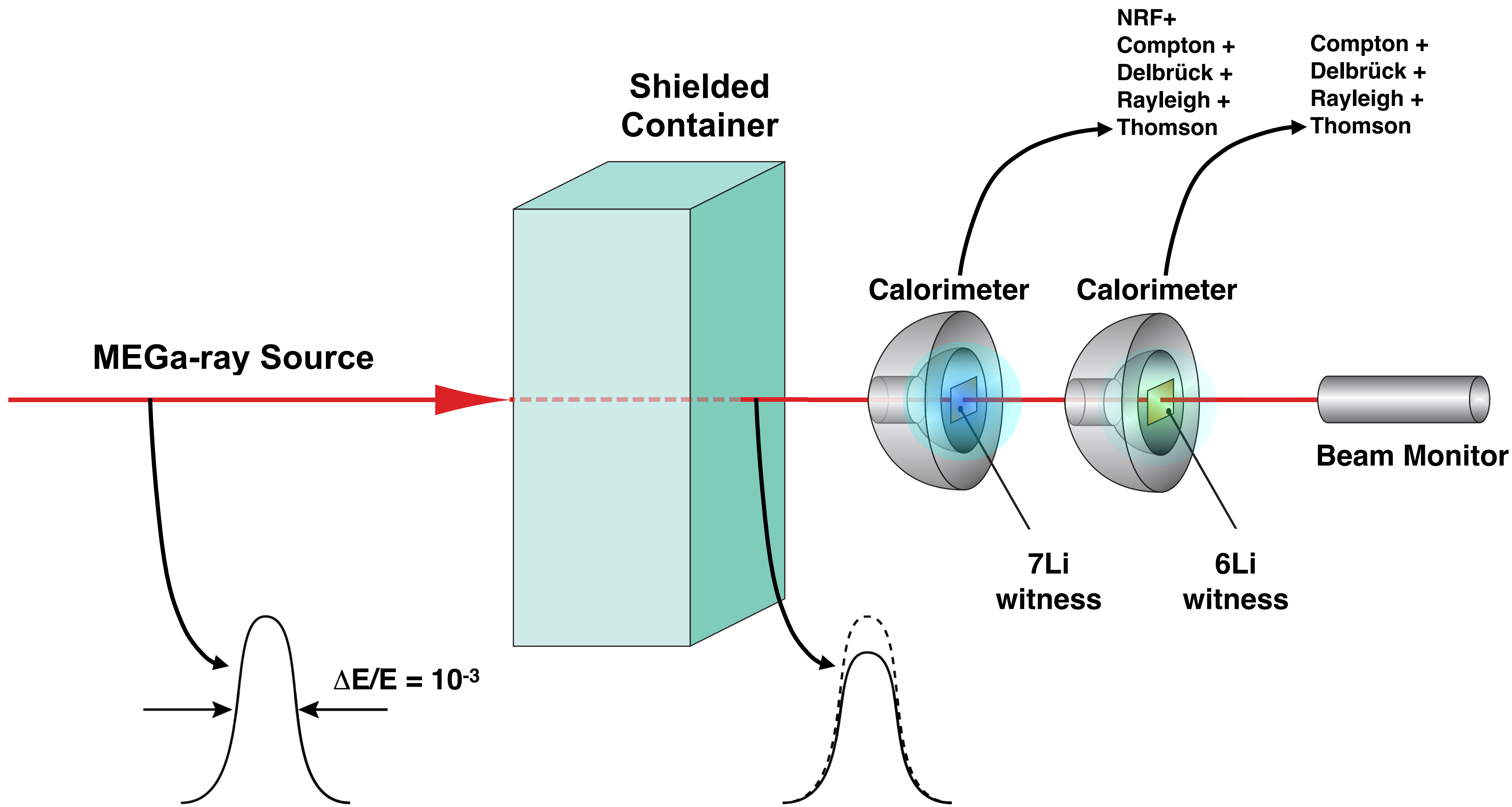

US patent #8,369,480 Dual isotope notch observer for material identification, assay and imaging

Dual Isotope Notch Observation (DINO) eliminates the need for high resolution spectroscopy

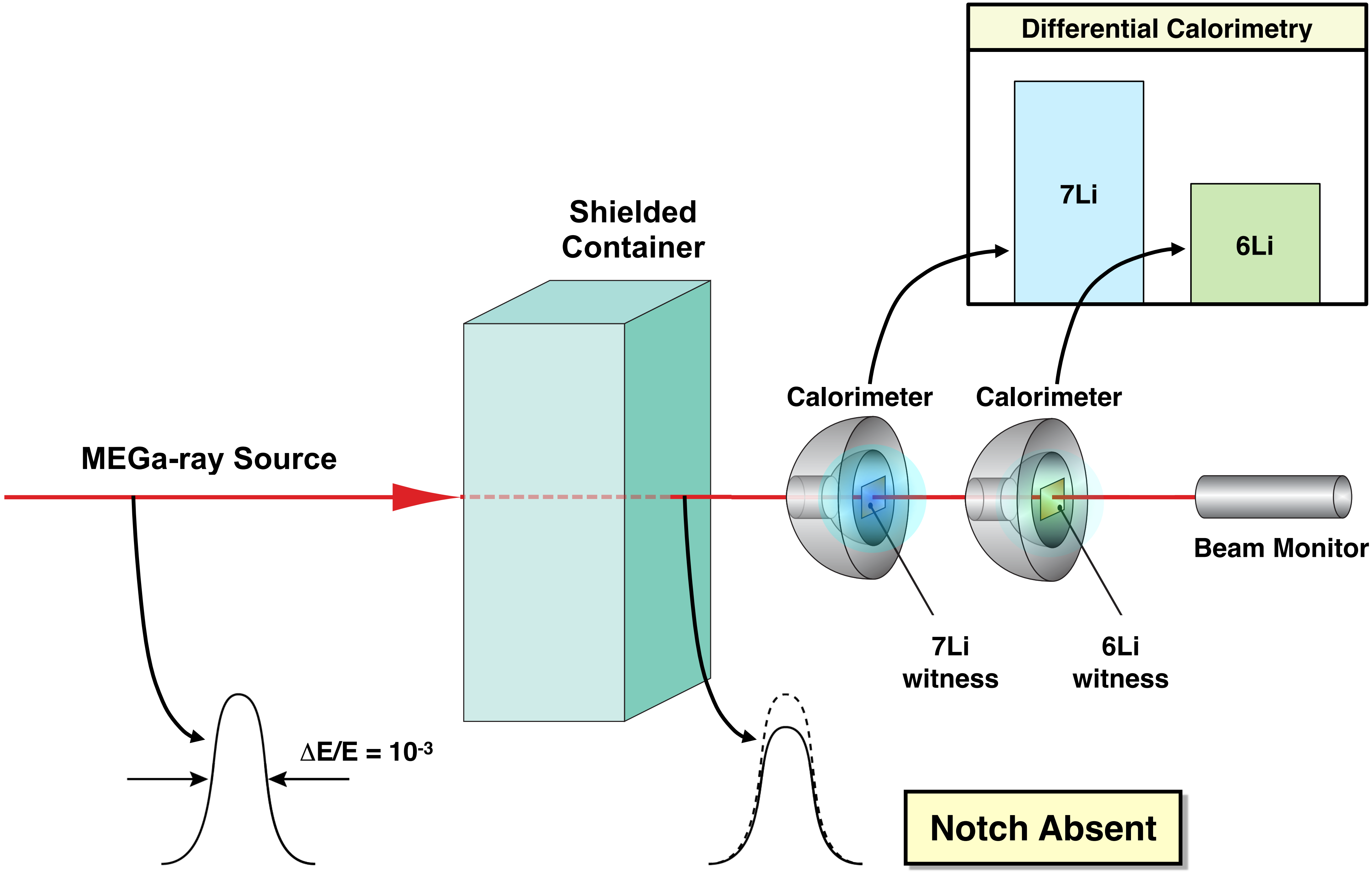

US patent #8,369,480 Dual isotope notch observer for material identification, assay and imaging

Dual Isotope Notch Observation (DINO) eliminates the need for high resolution spectroscopy

This technique not only avoids single photon spectroscopy but also enables precision ASSAY as well as detection

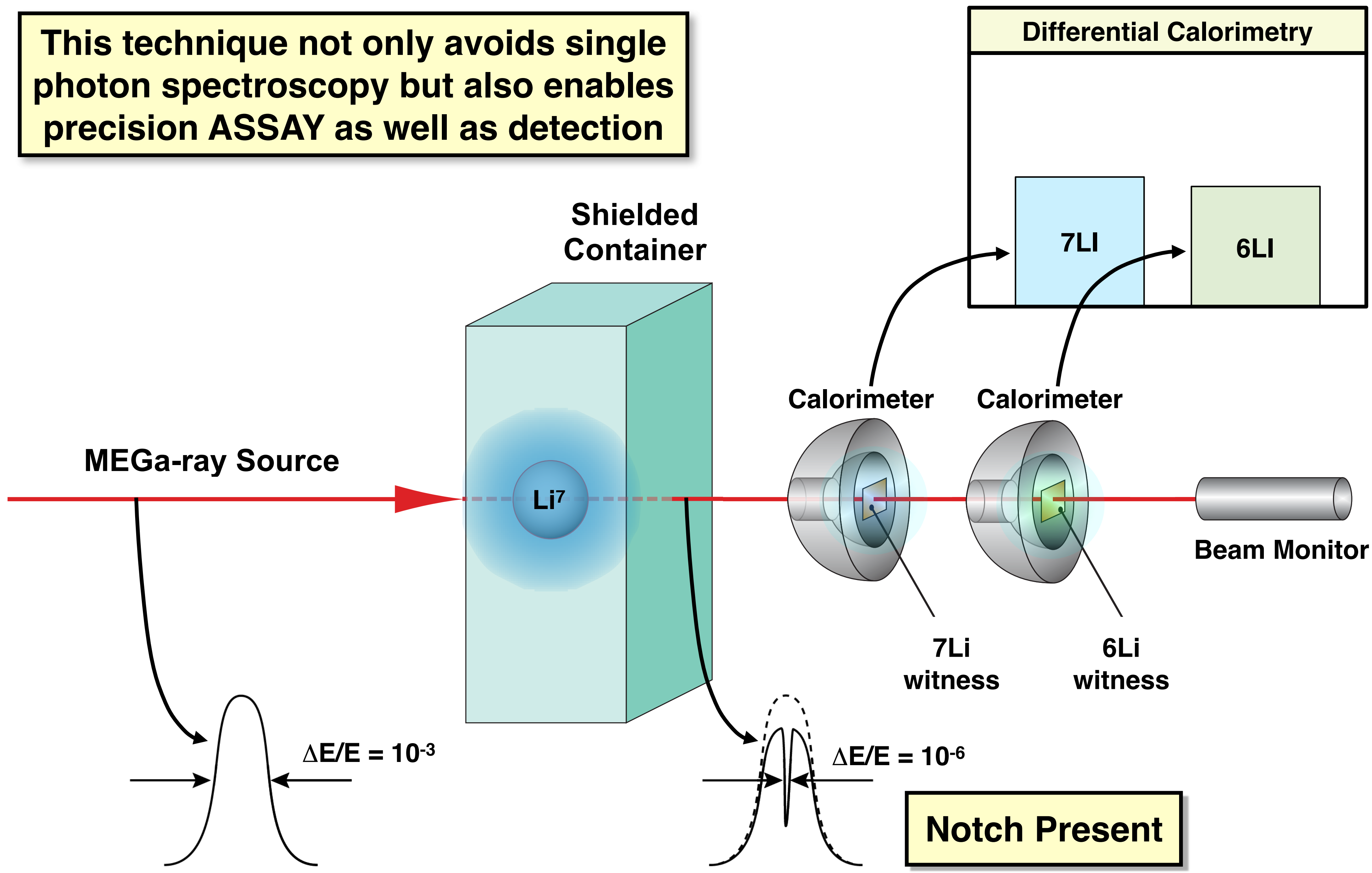

US patent #8,369,480 Dual isotope notch observer for material identification, assay and imaging

MEGa-ray sources and DINO detectors could transform our ability to assay nuclear fuels & monitor nuclear waste

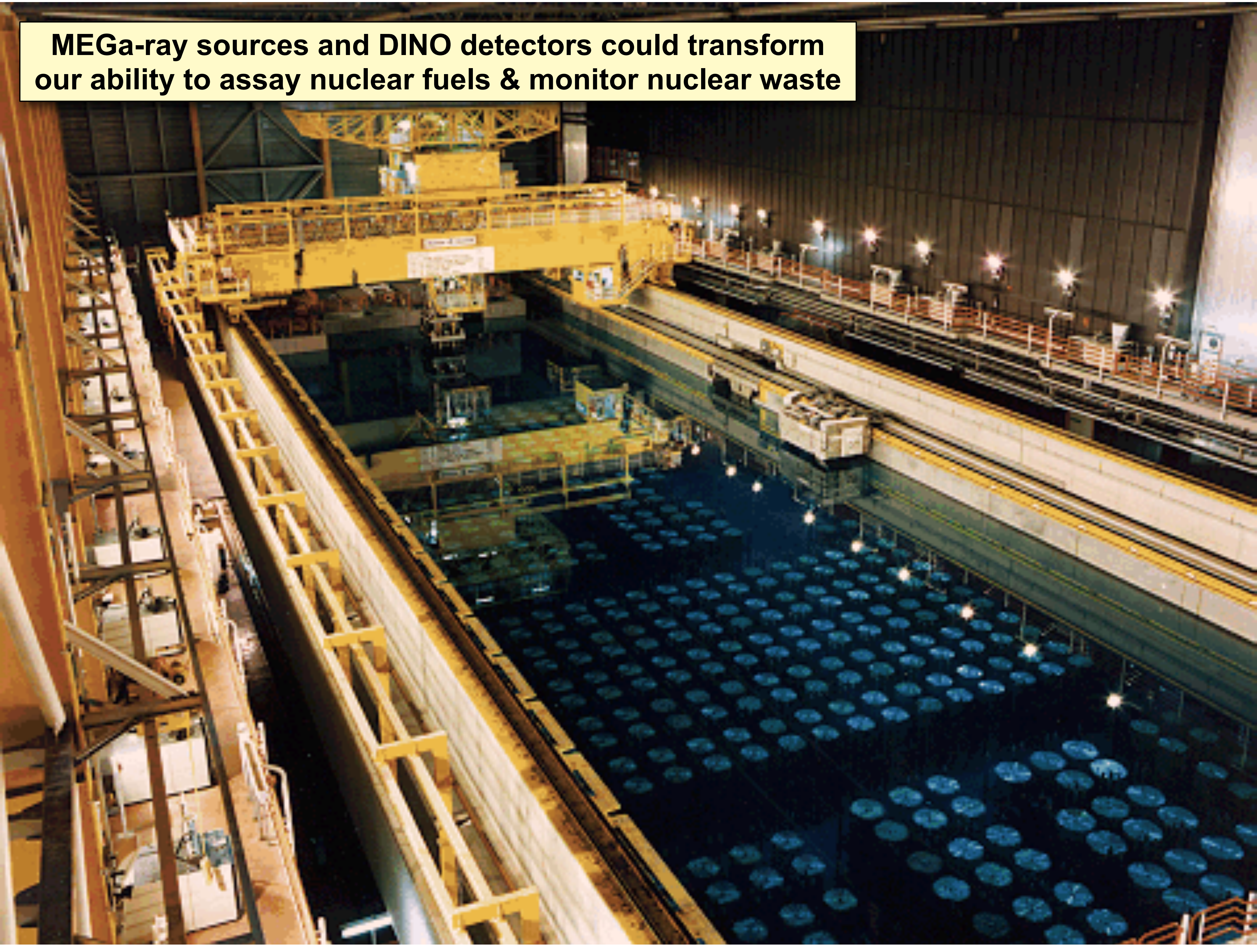

Improving the Scientific Basis for Managing DOE's Excess Nuclear Materials and Spent Nuclear Fuel
http://www.nap.edu/catalog/10684.html

IMPROVING THE SCIENTIFIC BASIS FOR MANAGING DOE'S EXCESS NUCLEAR MATERIALS AND SPENT NUCLEAR FUEL

Committee on Improving the Scientific Basis for Managing Nuclear Materials and Spent Nuclear Fuel through the Environmental Management Science Program

Board on Radioactive Waste Management

Division on Earth and Life Studies

NATIONAL RESEARCH COUNCIL
OF THE NATIONAL ACADEMIES

THE NATIONAL ACADEMIES PRESS
Washington, D.C.
www.nap.edu

Improving the Scientific Basis for Managing DOE's Excess Nuclear Materials and Spent Nuclear Fuel
http://www.nap.edu/catalog/10684.html

Spent DOE Nuclear Fuel

DOE manages an assortment of over 250 spent nuclear fuel (SNF) types that altogether comprise about 2,500 metric tons of heavy metal (MTHM).[5] DOE spent fuel was generated in military and civilian reactor development, research, and fuel testing programs. The inventory also includes irradiated fuel and target[6] assemblies that were placed in storage when DOE stopped reprocessing nuclear fuel for production purposes in 1992. DOE plans to dispose of its SNF along with commercial SNF and vitrified high-level waste in a repository at Yucca Mountain. Because DOE has only recently begun to prepare a license application for Yucca Mountain, uncertainty exists in the future waste acceptance criteria for the various types of DOE spent fuel.

Most types of DOE spent fuel have important characteristics that are different from commercial spent fuel, which will comprise most of the waste disposed in Yucca Mountain, if licensed and constructed. These are primarily differences in the chemical forms of the fuel and the cladding materials that encase it, and the isotopic composition of the fuel. The different characteristics affect the spent fuel's chemical stability and potential for gas generation, decay heat generation and potential for thermal damage under different storage and accident conditions, potential for inadvertent nuclear criticality, and attractiveness of the material for theft.

The EMSP should support research to help ensure safe and secure storage and disposal of DOE SNF. Research should emphasize materials characterization and stabilization, including developing a better understanding of corrosion, radiolytic effects, and accumulated stresses. This research should be directed toward determining a limited number of basic parameters that can be used to evaluate the long-term stability of each of the types of DOE SNF in realistic storage or repository environments.

The primary research challenge and opportunity in characterization is nondestructive assay of plutonium and other isotopes in the high-radiation environment that is typical of most spent fuels. Interim storage

[5] MTHM refers to the mass of uranium and/or plutonium used to fabricate the fuel. It does not include the mass of the fuel cladding or ancillary components.
[6] Most of DOE's nuclear materials were created in nuclear reactors through the capture of neutrons by various target isotopes, e.g., U-238 (see Appendix A).

The primary research challenge and opportunity in characterization is nondestructive assay of plutonium and other isotopes in the high-radiation environment that is typical of most spent fuels...

We are currently designing DINO detectors for Pu and U detection and assay applications

MC model of single-stage DINO detector system* (COG):

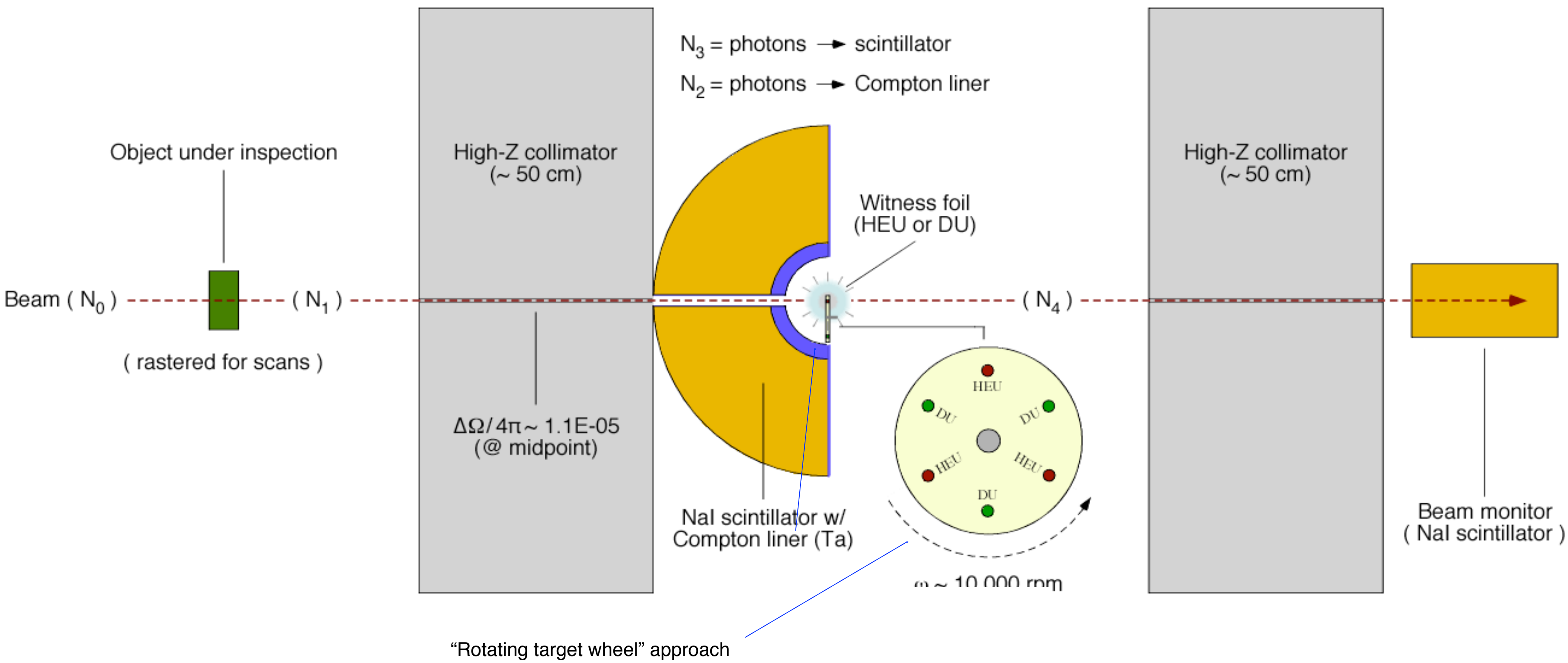

Design considerations include dimensions & configuration of the witness "pins", solid angle & composition of the calorimeter, thickness & composition of Compton liner, etc...

Proper design of the Compton liner can increase the ratio of NRF to background seen by the scintillator

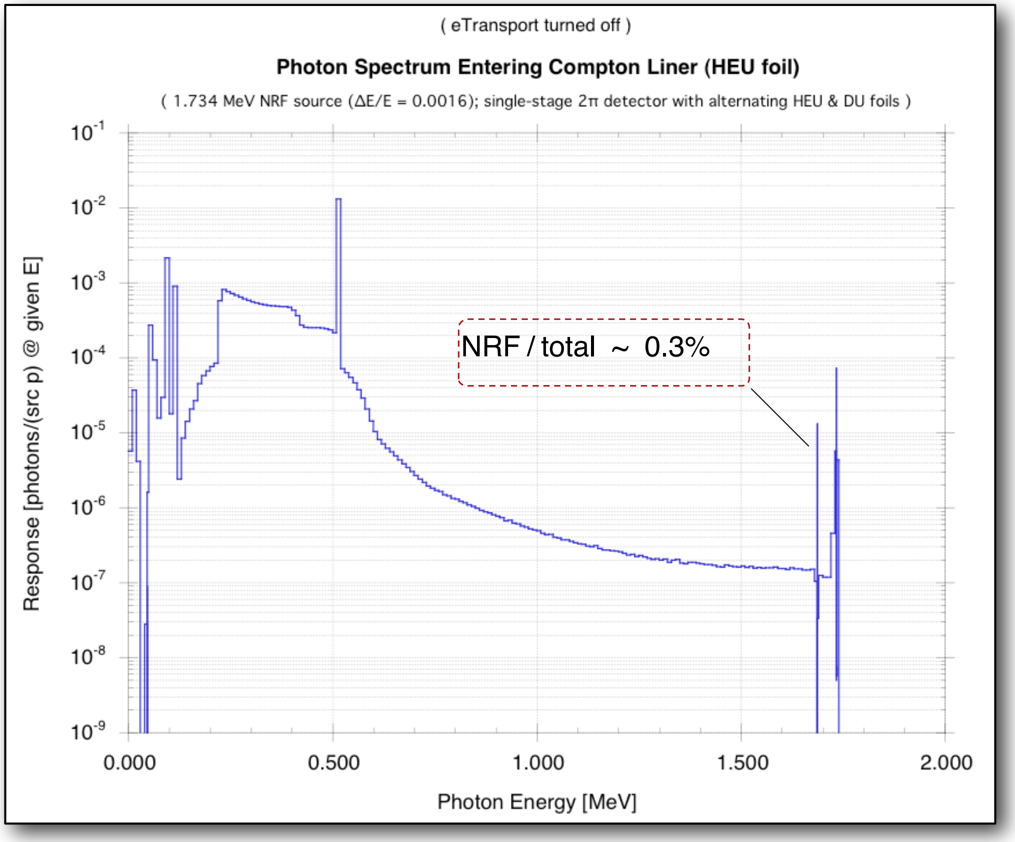

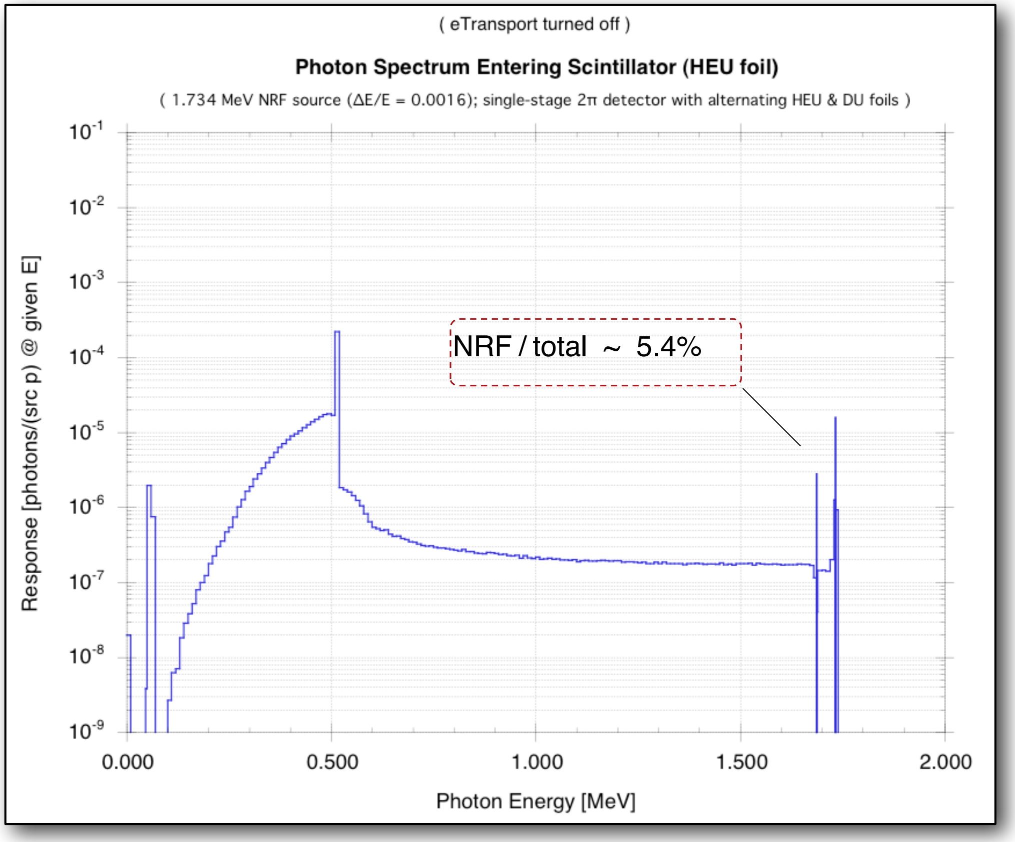

Monte Carlo simulations using COG

Precision assay and imaging of nuclear fuel is possible via resonant MEGa-ray absorption

Simulation Test Object	Conventional x-ray Image	1.73 MeV MEGa-ray Image
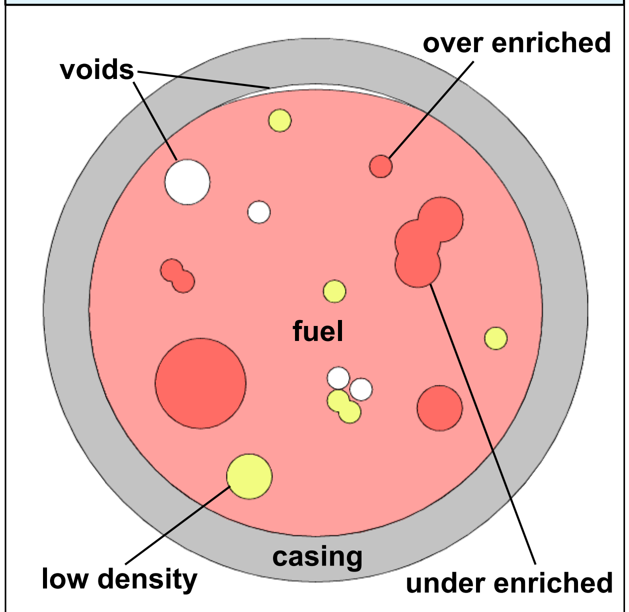	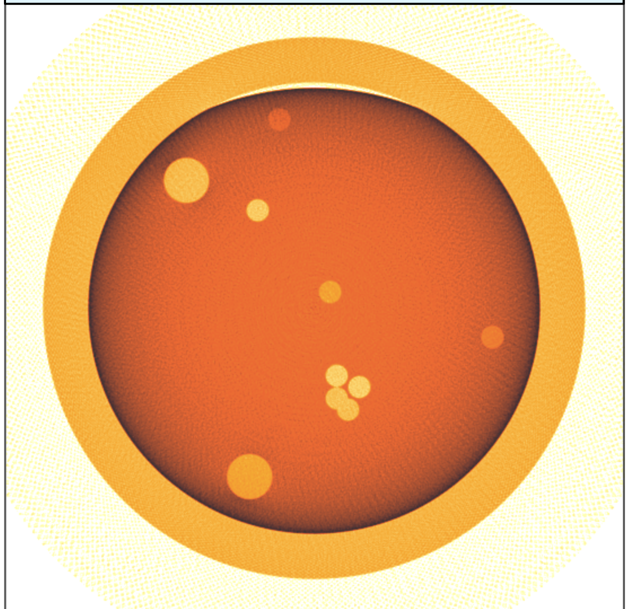	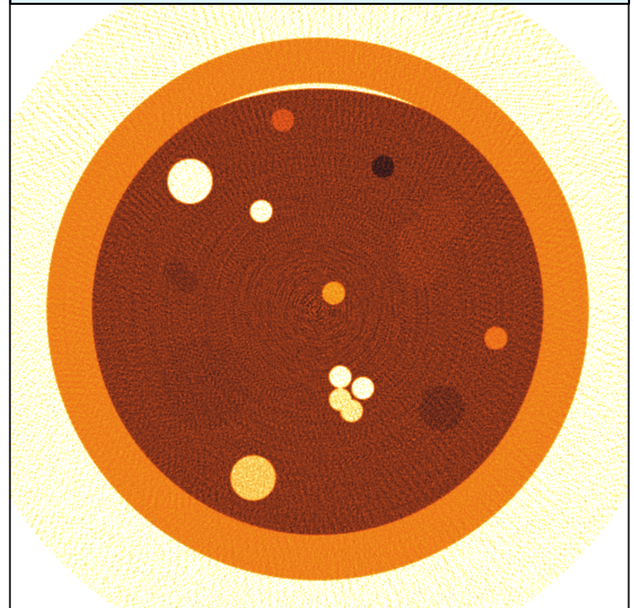
Fuel rod with density and enrichment defects	Can only identify the presence of density defects	Variations in enrichment can be seen & measured

Simulations indicate that the enrichment of fuel rods could be measured to ~3% accuracy in 5 to 6 minutes with future MEGa-ray sources and DINO detector arrangements

NRF-based materials evaluation will be much easier elsewhere in the periodic table

atomic number	isotope	oxide	natural isotopic abundance (%)	REE-Oxide weight % at Mountain Pass	REE Atomic % at Mountain Pass	REE Isotope % at Mountain Pass	cost per kg in 2009 (US$)	NRF gamma energy (keV)	NRF cross section (barns)	Background cross section (barns)	NRF to background cross section ratio
92	235U	UO_2	90.0	na	na	na	na	1733	26.0	20.0	1.3
39	89Y	Y_2O_3	100.0	0.130	0.0092	0.0092	$13.50	1507	24.5	6.9	3.6
40	90Zr	na	51.5	na	na	na	na	2186	5.5	6.1	0.9
57	138La	La_2O_3	0.1	33.784	2.5925	0.0023	$5.85	no data	no data	no data	no data
57	139La	La_2O_3	99.9	33.784	2.5925	2.5902	$5.85	1538	7.2	10.6	0.7
58	136Ce	Ce_2O_3	0.19	49.581	3.8096	0.0070	$4.15	552	5.4	23	0.2
58	138Ce	Ce_2O_3	0.25	49.581	3.8096	0.0096	$4.15	789	6.2	16	0.4
58	140Ce	Ce_2O_3	88.45	49.581	3.8096	3.3696	$4.15	1596	16.9	10.5	1.6
58	142Ce	Ce_2O_3	11.11	49.581	3.8096	0.4234	$4.15	2187	19.3	9.4	2.1
59	141Pr	Pr_2O_3	100.0	4.119	0.3168	0.3168	$15.15	no data	no data	no data	no data
60	142Nd	Nd_2O_3	27.2	11.158	0.8610	0.2342	$15.25	3424	46.8	9.1	5.1
60	143Nd	Nd_2O_3	12.2	11.158	0.8610	0.1050	$15.25	1407	10.8	12	0.9
60	144Nd	Nd_2O_3	23.8	11.158	0.8610	0.2049	$15.25	2186	17.4	9.8	1.8
60	145Nd	Nd_2O_3	8.3	[illegible]	[illegible]	[illegible]	[illegible]	[illegible]	1.8	15	0.1
60	146Nd	Nd_2O_3	17.2	[illegible]	[illegible]	[illegible]	[illegible]	[illegible]	14.9	19	0.8
60	148Nd	Nd_2O_3	5.7	[illegible]	[illegible]	[illegible]	[illegible]	[illegible]	5.4	9.1	0.6
60	150Nd	Nd_2O_3	5.6	[illegible]	[illegible]	[illegible]	[illegible]	[illegible]	1.8	14	0.1
62	144Sm	Sm_2O_3	3.1	[illegible]	[illegible]	[illegible]	[illegible]	[illegible]	55.2	9.5	5.8
62	144Sm	Sm_2O_3	3.1	[illegible]	[illegible]	[illegible]	[illegible]	[illegible]	16.6	11.5	1.4
62	147Sm	Sm_2O_3	15.0	[illegible]	[illegible]	[illegible]	[illegible]	[illegible]	2.2	20	0.1
62	148Sm	Sm_2O_3	11.2	[illegible]	[illegible]	[illegible]	[illegible]	[illegible]	8.4	12	0.7
62	149Sm	Sm_2O_3	13.8	[illegible]	[illegible]	[illegible]	[illegible]	[illegible]	2.2	23	0.1
62	150Sm	Sm_2O_3	7.4	[illegible]	[illegible]	[illegible]	[illegible]	[illegible]	23.1	13.6	1.7
62	152Sm	Sm_2O_3	26.8	[illegible]	[illegible]	[illegible]	[illegible]	[illegible]	18.0	9.7	1.9
62	152Sm	Sm_2O_3	26.8	[illegible]	[illegible]	[illegible]	[illegible]	[illegible]	70.5	15	4.7
62	154Sm	Sm_2O_3	22.8	0.850	0.0660	0.0150	$4.50	921	95.1	16	5.9
62	154Sm	Sm_2O_3	22.8	0.850	0.0660	0.0150	$4.50	1440	3.8	12.1	0.3
63	151Eu	Eu_2O_3	47.8	0.105	0.0082	0.0039	$465.00	808	16.7	60	0.3
63	153Eu	Eu_2O_3	52.2	0.105	0.0082	0.0043	$465.00	no data	no data	no data	no data
64	152Gd	Gd_2O_3	0.2	0.210	0.0164	0.0000	$6.50	344	5.0	50	0.1
64	154Gd	Gd_2O_3	2.2	0.210	0.0164	0.0004	$6.50	1241	735.3	13.8	53.3
64	155Gd	Gd_2O_3	14.8	0.210	0.0164	0.0024	$6.50	615	0.2	90	0.0
64	156Gd	Gd_2O_3	20.5	0.210	0.0164	0.0034	$6.50	1243	33.1	13.7	2.4
64	156Gd	Gd_2O_3	20.5	0.210	0.0164	0.0034	$6.50	1367	32.4	13	2.5
64	156Gd	Gd_2O_3	20.5	0.210	0.0164	0.0034	$6.50	2745	16.1	10.2	1.6
64	156Gd	Gd_2O_3	20.5	0.210	0.0164	0.0034	$6.50	3071	41.2	10	4.1
64	157Gd	Gd_2O_3	15.7	0.210	0.0164	0.0026	$6.50	131	2.8	500	0.0
64	158Gd	Gd_2O_3	24.8	0.210	0.0164	0.0041	$6.50	1264	60.9	13.7	4.4
64	158Gd	Gd_2O_3	24.8	0.210	0.0164	0.0041	$6.50	3201	25.0	9.9	2.5
64	160Gd	Gd_2O_3	21.9	0.210	0.0164	0.0036	$6.50	1224	56.5	13.7	4.1
65	159Tb	Tb_2O_3	100.0	0.016	0.0013	0.0013	$350.00	58	192.7	3800	0.1
65	159Tb	Tb_2O_3	100.0	0.016	0.0013	0.0013	$350.00	581	4.4	28	0.2

The ratio of the NRF to background cross section for many materials is significantly greater than that for the actinides

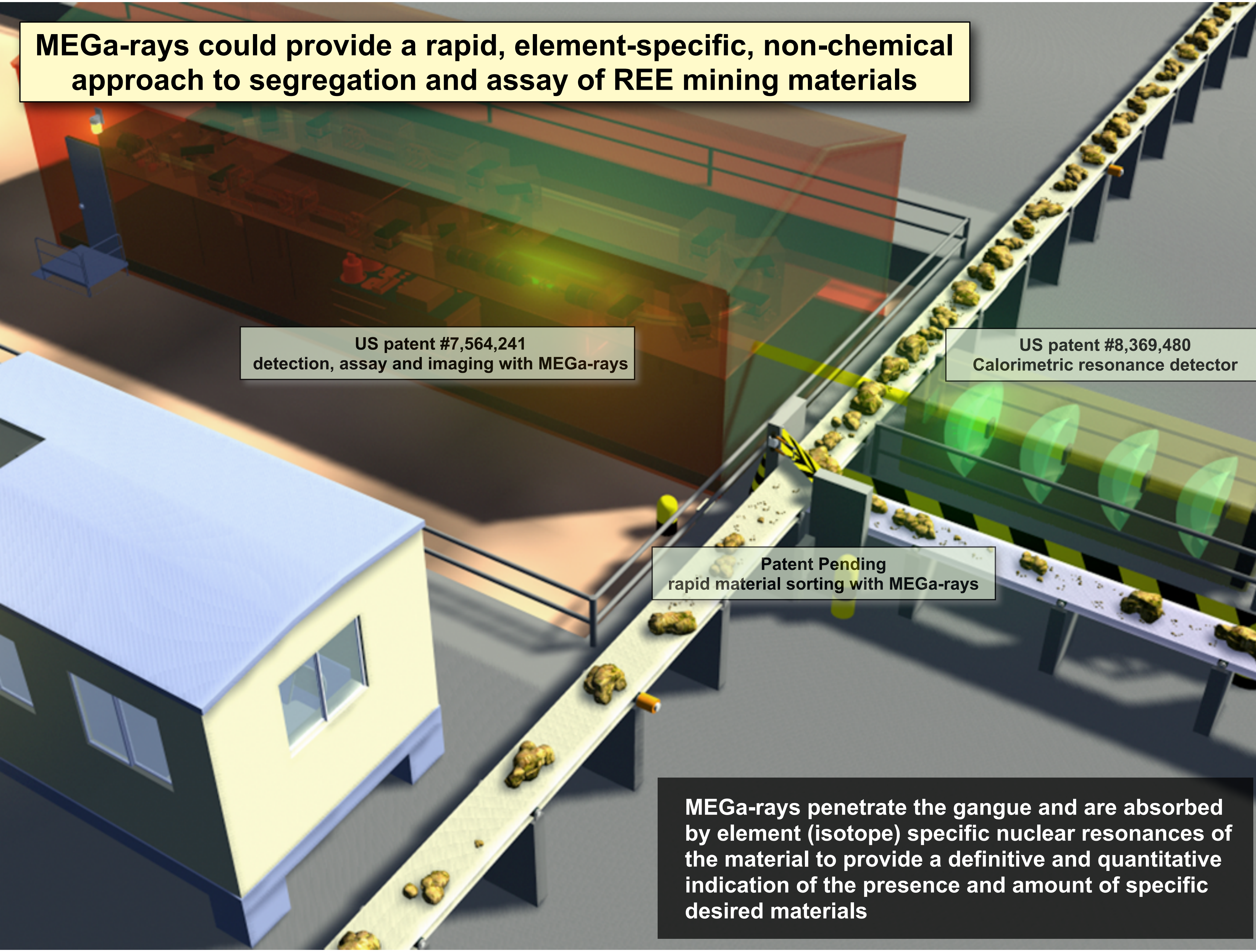
MEGa-rays could provide a rapid, element-specific, non-chemical approach to segregation and assay of REE mining materials
US patent #7,564,241
detection, assay and imaging with MEGa-rays
US patent #8,369,480
Calorimetric resonance detector
Patent Pending
rapid material sorting with MEGa-rays
MEGa-rays penetrate the gangue and are absorbed by element (isotope) specific nuclear resonances of the material to provide a definitive and quantitative indication of the presence and amount of specific desired materials

The Potential NRF-based Applications of MEGa-rays and DINO are Numerous

HEU Grand Challenge
detection of shielded material

Nuclear Fuel Assay
100 parts per million per isotope

Waste Imaging & Assay
non-invasive content certification

Industrial NDE
micron-scale & isotope specific

Medical Imaging
low density & isotope specific

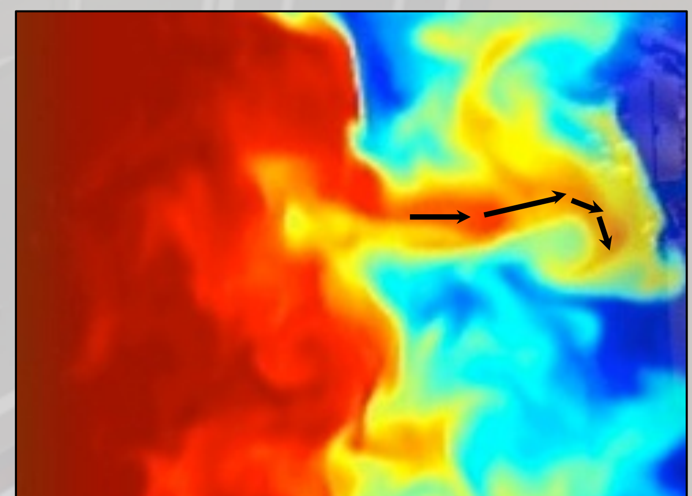

Dense Plasma Science
isotope mass, position & velocity

Compact, mobile or relocatable MEGa-ray sources are desired in many applications

Desired MEGa-rays:
1.73 MeV photons
(250 MeV electrons)
10^6 ph/s/eV flux
0.1% bandwidth
Truck size or smaller

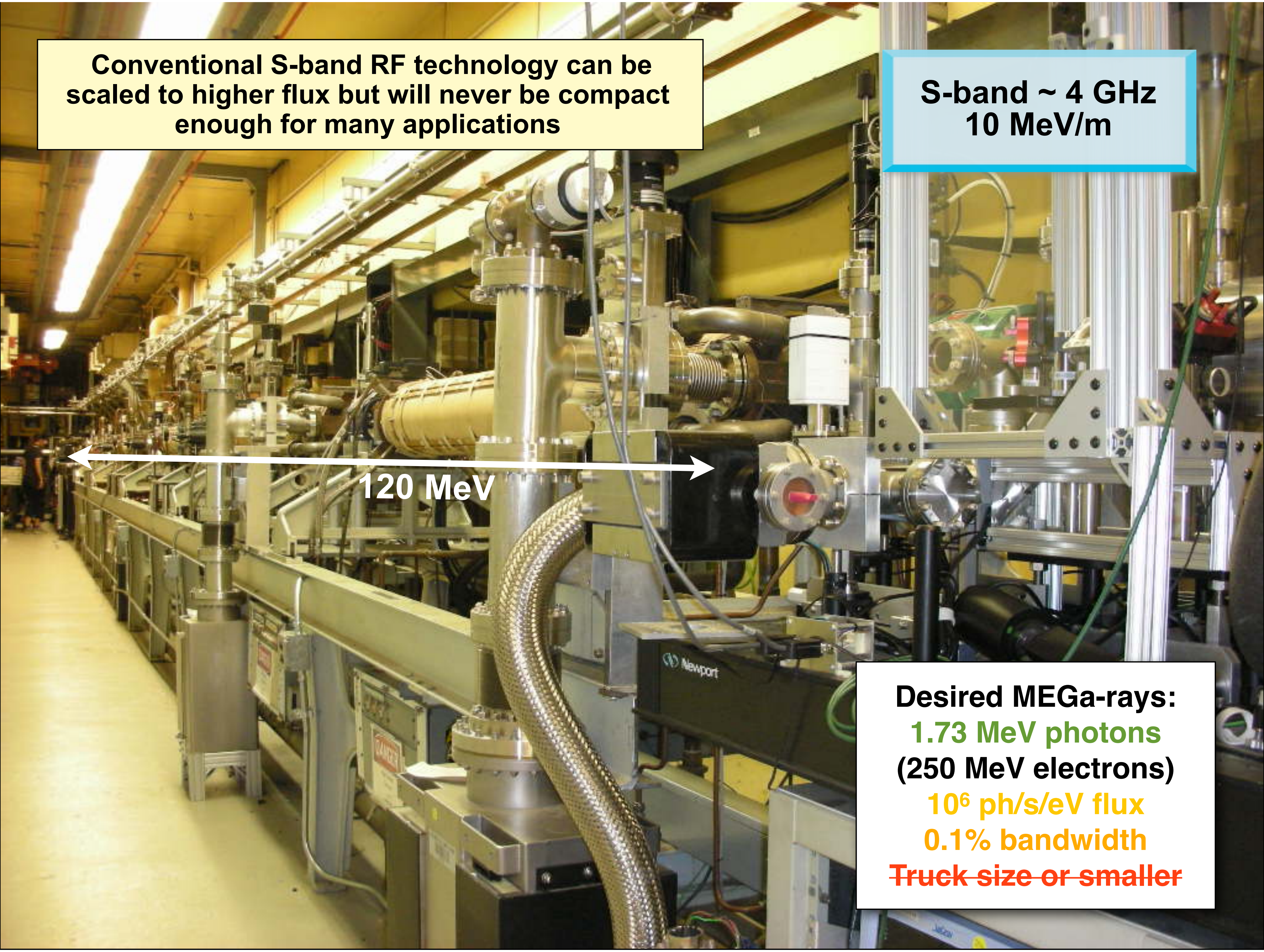
Conventional S-band RF technology can be scaled to higher flux but will never be compact enough for many applications
S-band ~ 4 GHz
10 MeV/m
120 MeV
Newport
Desired MEGa-rays:
1.73 MeV photons
(250 MeV electrons)
10^6 ph/s/eV flux
0.1% bandwidth
~~Truck size or smaller~~

Laser wakefield "accelerators" can be extremely small but have large energy spreads and will require very large, complicated lasers to scale

Laser Wakefield
10,000 MeV/m!

Desired MEGa-rays:
1.73 MeV photons
(250 MeV electrons)
625 ~~10^6 ph/s/eV flux~~
60% ~~0.1% bandwidth~~
~~Truck size or smaller~~


High gradient x-band technology developed at DOE's SLAC National Accelerator Lab enables compact, high flux MEGa-ray machines
X-Band ~ 12 GHz
Grad > 100 MeV/m
> 120 MeV?
Desired MEGa-rays:
1.73 MeV photons
(250 MeV electrons)
10⁶ ph/s/eV flux
0.1% bandwidth
Truck size or smaller

The key metric for isotopic applications is "Specific Spectral Density"

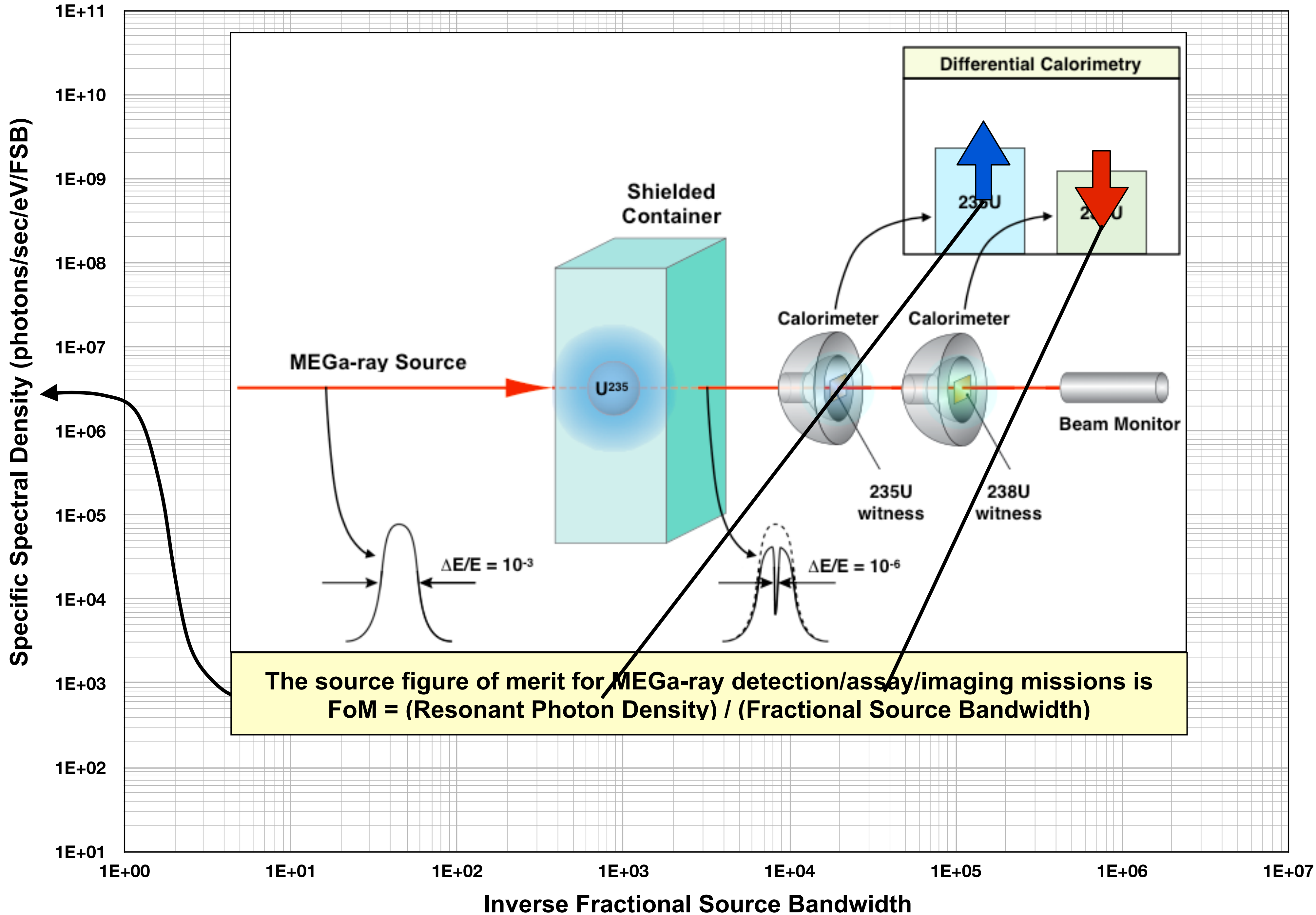

The key metric for isotopic applications is “Specific Spectral Density”

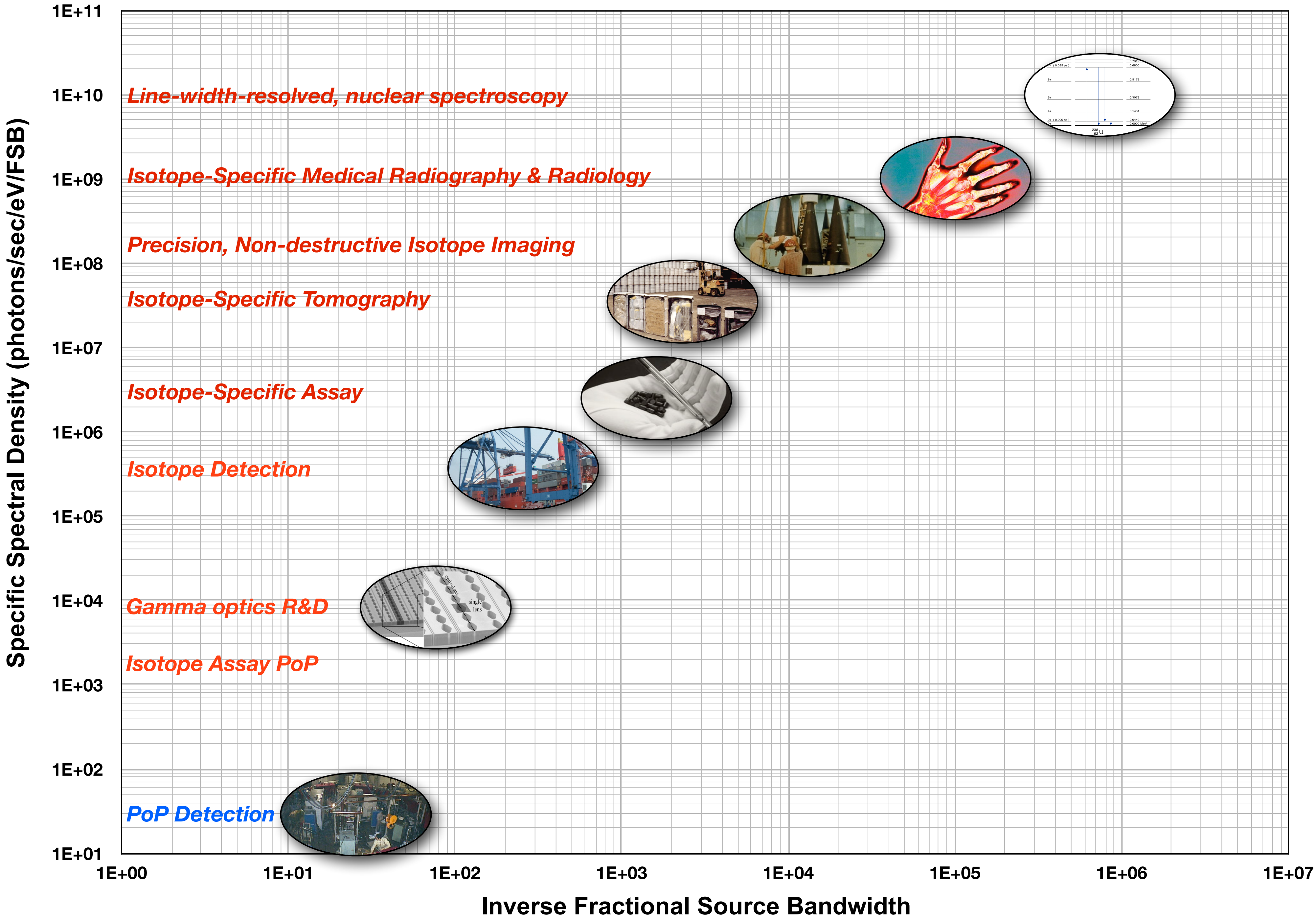

2013 “Picket Fence” multi-GHz, laser-Compton source concept

potential bandwidth = 0.1%
effective repetition rate = 240 kHz
FOM > 1,000,000x that of T-REX

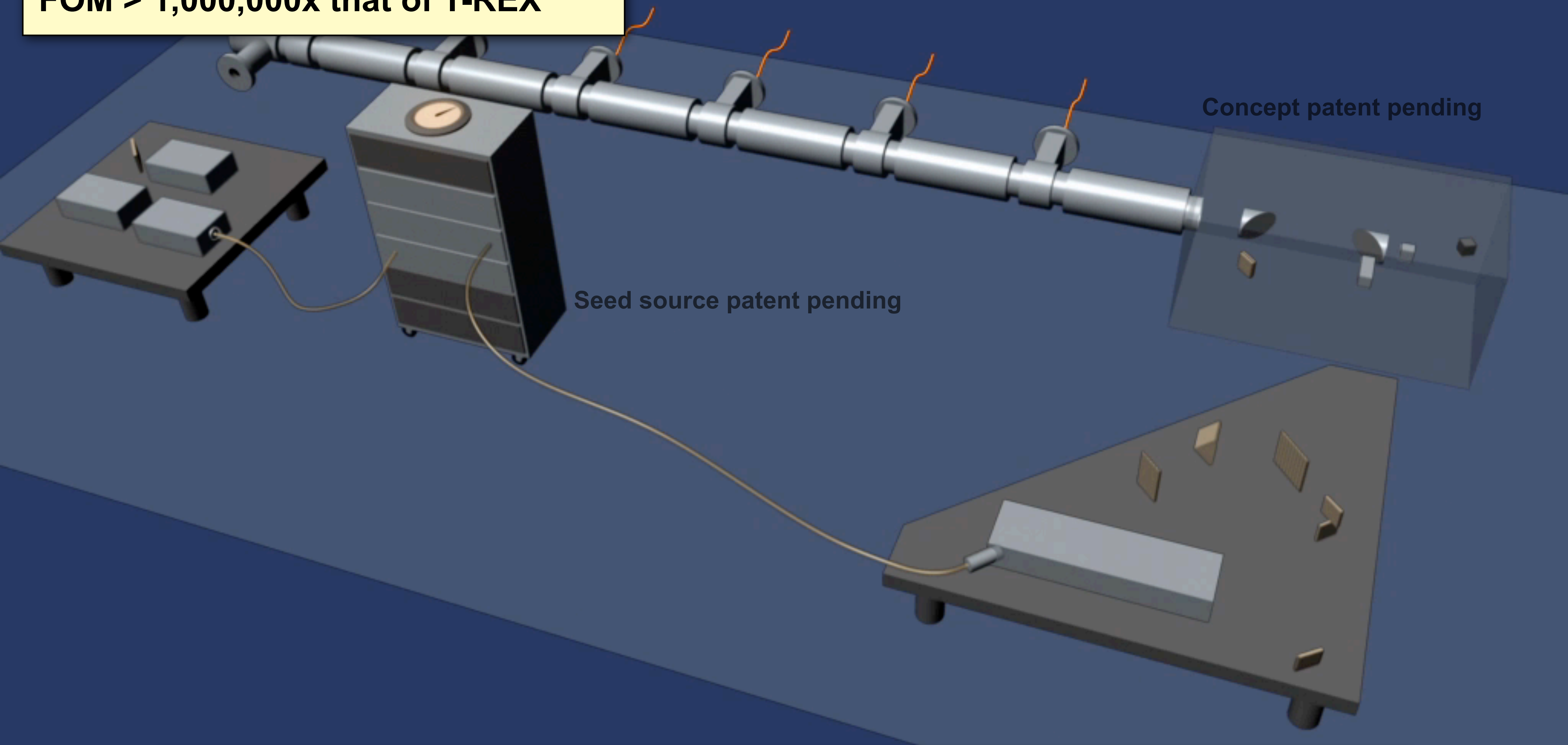

This configuration enables near “unity” efficiency, operates with high beam current, minimizes bandwidth and is intrinsically synchronized to RF clock

"CW" method for generation of 11.424 GHz, synchronized train of picosecond IR pulses

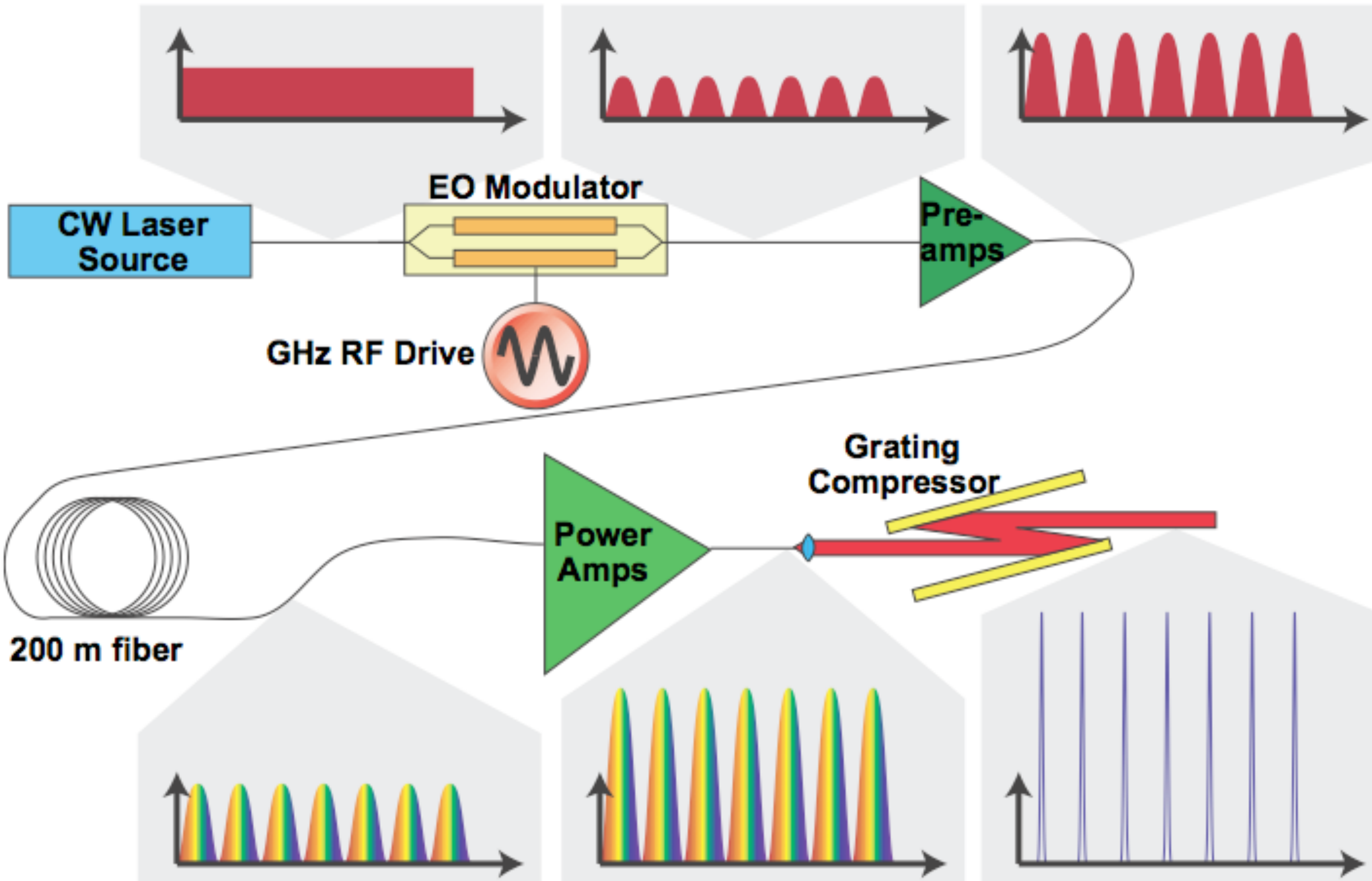

“CW” method for generation of 11.424 GHz, synchronized train of picosecond IR pulses

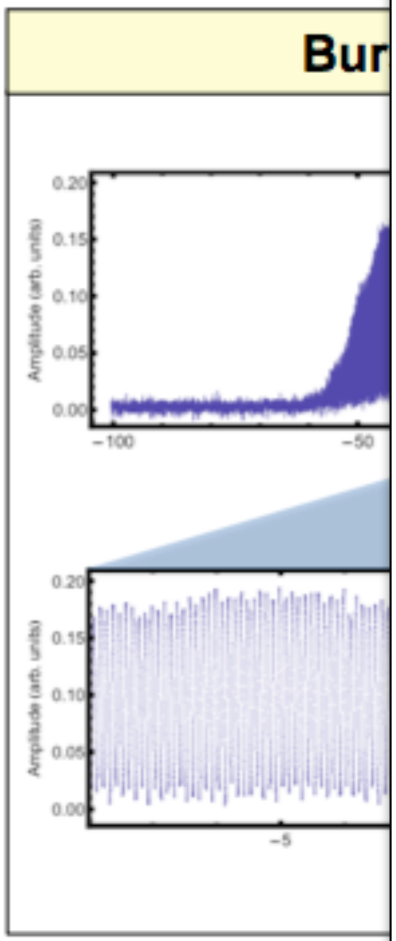

Widely tunable 11 GHz femtosecond fiber laser based on a non-modelocked source

Matthew A. Prantil,[1*] Eric Cormier,[2] Jay W. Dawson,[1] David J. Gibson,[1] Michael J. Messerly,[1] Christopher P. J. Barty,[1]

[1]*Lawrence Livermore National Laboratory, Livermore, California 94550*
[2]*University of Bordeaux, France*
**Corresponding author: prantil2@llnl.gov*

Received Month X, XXXX; revised Month X, XXXX; accepted Month X, XXXX; posted Month X, XXXX (Doc. ID XXXXX); published Month X, XXXX

An 11 GHz fiber laser built on a modulated CW platform is described and characterized. This compact, vibration-insensitive, fiber based system can be operated at wavelengths compatible with high energy fiber technology, is driven by an RF signal directly, and is tunable over a wide range of drive frequencies. The demonstration system when operated at 1040 nm is capable of 50 ns bursts of 575 micro-pulses produced at a macro-pulse rate of 83 kHz where the macro-pulse and micro-pulse energies are 1.8 μJ and 3.2 nJ respectively. Its micro-pulses are compressed to a duration of 850 fs.

OCIS Codes: 060.3510, 140.7090

Very-short-pulse laser sources (in the range of picoseconds to femtoseconds) with high repetition rates (100 MHz to tens of GHz) are needed to drive short-wavelength high-energy photon sources via higher-order nonlinear optical parametric interactions, and as photo-cathode illuminators to create photo-electrons in high frequency particle accelerators. Other applications of these ultrafast pulse laser systems include materials processing, 3-D lithography, high-data-rate laser communication, and remote sensing systems. The system architecture described here is wavelength compatible with high energy fiber technology, is driven directly by an RF source (and thus sidesteps synchronization issues), and allows for amplification to materials-processing pulse energies. Moreover, the ability to modify electronically the temporal pulse shape, in amplitude and phase [1, 2], offers the possibility of controlling various complex photochemical processes and quantum control of interactions on molecular time scales.

We generate a laser pulse train by modulating a continuous-wave (cw) laser with an RF source. Several groups [2, 3] have converted cw lasers to sub-ps, high frequency pulse trains; however, these groups have relied on “time-lens” techniques [4] to generate ps-level bandwidths, then used soliton compression at 1550 nm in specially optimized fibers to generate further bandwidth while simultaneously compressing the pulse. At the 1030-1070 nm wavelengths where we wish to work, the soliton compression scheme is not feasible because the dispersion in standard fibers has the opposite sign from dispersion at 1550 nm. In the demonstration of this cw-modulation concept reported here, we rely on self-phase modulation (SPM) [5] to generate 3.2 nm of bandwidth and compress the pulse with a grating-pair compressor. To reduce allow high pulse energies at modest average laser power, we

the groups (macro-pulses) occur at mult-kHz rates while the individual pulses (micro-pulses) are at multi-GHz rates. Alternatively, the micro-pulses might be directly amplified to modest energies for a clock-distribution scheme, or driven to micro-joule energies to create tens of kilowatts of power for machining or supercontinuum sources.

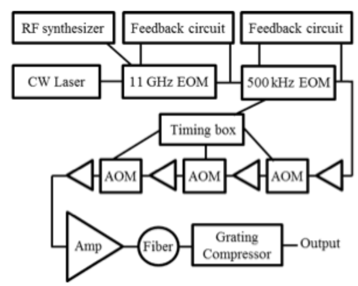

Figure 1 Schematic diagram of the experiment.

The architecture, shown in Figure 1, begins with a cw laser: a New Focus Velocity laser set to provide a 1040 nm beam. The beam is sent through an EOSPACE-brand, Z-cut, 20 GHz, dual drive Mach-Zehnder electro-optic modulator (EOM) monitored by a control circuit (YY Labs, Inc.) to keep the modulator null-biased – that is, biased to block light when the RF drive is off.. This modulator is driven with 20.1 dBm of 5.7 GHz RF power. Because of the null bias, the RF creates an 11.4 GHz laser pulse train with 44 ps pulse length and no cw component as shown in Figure 2; the latter prevents stimulated Brillouin scattering from damaging subsequent fiber amplifiers. A second EOM temporally slices macro-pulses at a 500 kHz rate with 50 ns duration; thus each macro-pulse contains approximately

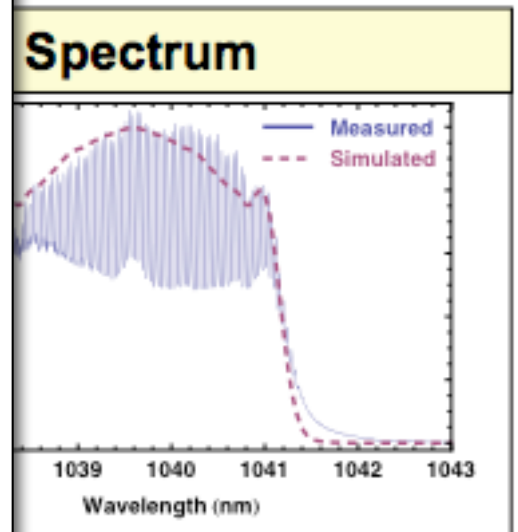

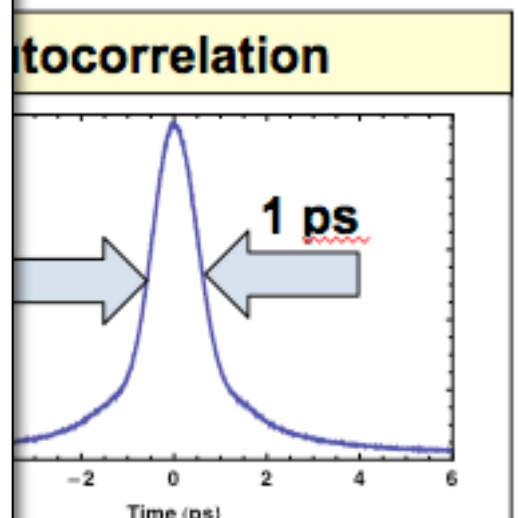

B194 X-Band Test Station

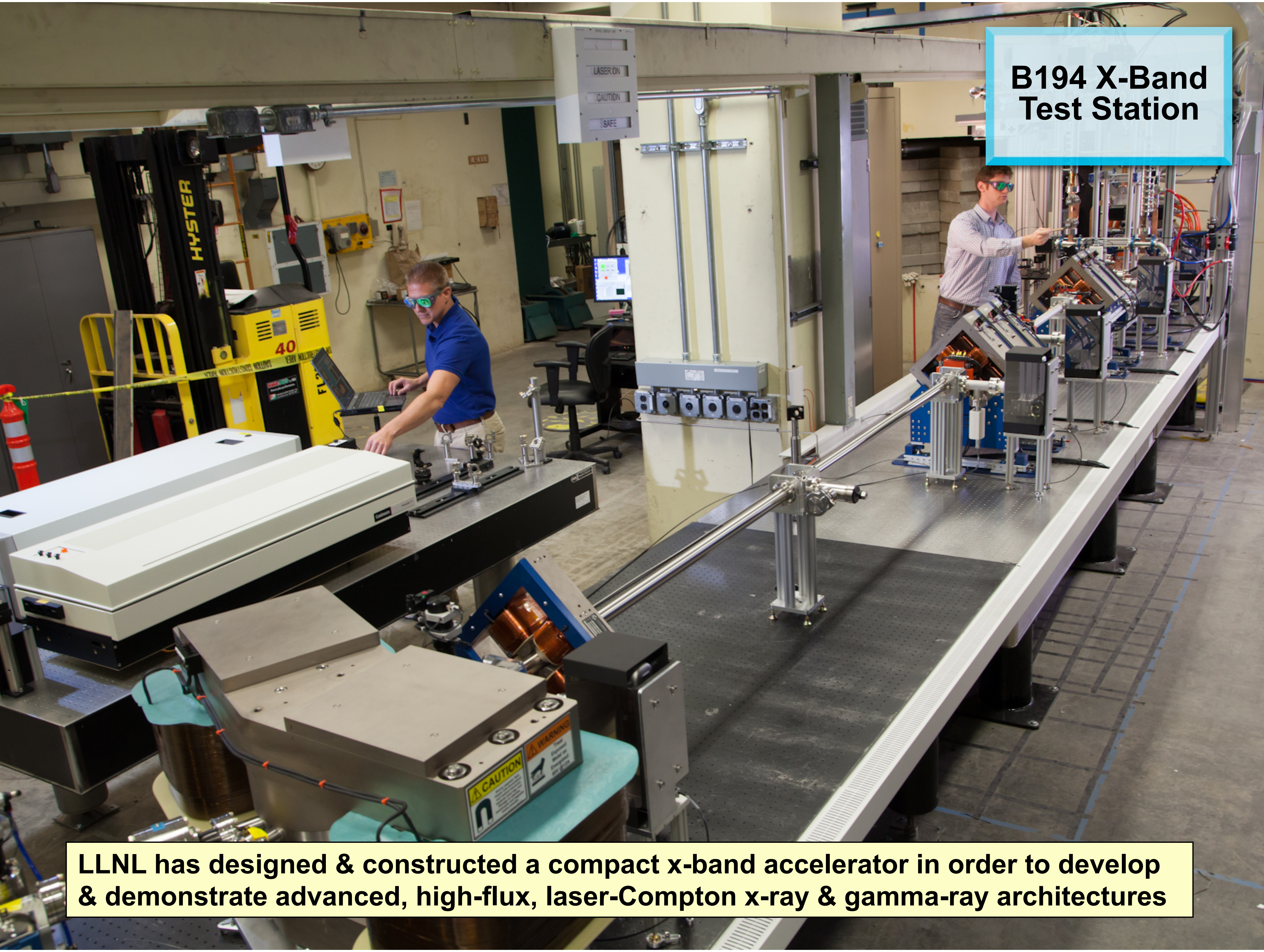

LLNL has designed & constructed a compact x-band accelerator in order to develop & demonstrate advanced, high-flux, laser-Compton x-ray & gamma-ray architectures

B194 X-Band Test Station

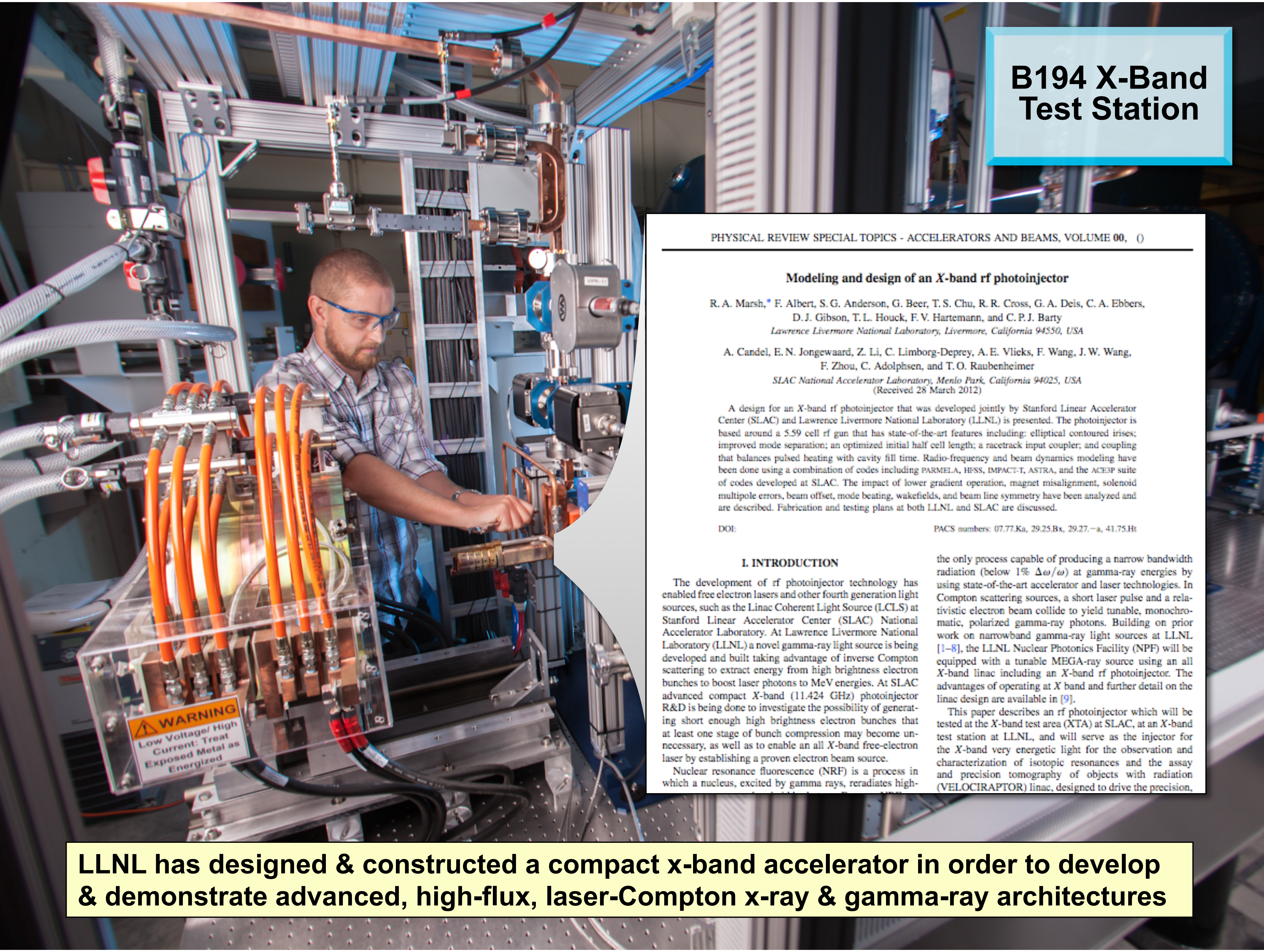

PHYSICAL REVIEW SPECIAL TOPICS - ACCELERATORS AND BEAMS, VOLUME **00**, ()

Modeling and design of an *X*-band rf photoinjector

R. A. Marsh,* F. Albert, S. G. Anderson, G. Beer, T. S. Chu, R. R. Cross, G. A. Deis, C. A. Ebbers, D. J. Gibson, T. L. Houck, F. V. Hartemann, and C. P. J. Barty
Lawrence Livermore National Laboratory, Livermore, California 94550, USA

A. Candel, E. N. Jongewaard, Z. Li, C. Limborg-Deprey, A. E. Vlieks, F. Wang, J. W. Wang, F. Zhou, C. Adolphsen, and T. O. Raubenheimer
SLAC National Accelerator Laboratory, Menlo Park, California 94025, USA
(Received 28 March 2012)

A design for an *X*-band rf photoinjector that was developed jointly by Stanford Linear Accelerator Center (SLAC) and Lawrence Livermore National Laboratory (LLNL) is presented. The photoinjector is based around a 5.59 cell rf gun that has state-of-the-art features including: elliptical contoured irises; improved mode separation; an optimized initial half cell length; a racetrack input coupler; and coupling that balances pulsed heating with cavity fill time. Radio-frequency and beam dynamics modeling have been done using a combination of codes including PARMELA, HFSS, IMPACT-T, ASTRA, and the ACE3P suite of codes developed at SLAC. The impact of lower gradient operation, magnet misalignment, solenoid multipole errors, beam offset, mode beating, wakefields, and beam line symmetry have been analyzed and are described. Fabrication and testing plans at both LLNL and SLAC are discussed.

DOI: PACS numbers: 07.77.Ka, 29.25.Bx, 29.27.−a, 41.75.Ht

I. INTRODUCTION

The development of rf photoinjector technology has enabled free electron lasers and other fourth generation light sources, such as the Linac Coherent Light Source (LCLS) at Stanford Linear Accelerator Center (SLAC) National Accelerator Laboratory. At Lawrence Livermore National Laboratory (LLNL) a novel gamma-ray light source is being developed and built taking advantage of inverse Compton scattering to extract energy from high brightness electron bunches to boost laser photons to MeV energies. At SLAC advanced compact *X*-band (11.424 GHz) photoinjector R&D is being done to investigate the possibility of generating short enough high brightness electron bunches that at least one stage of bunch compression may become unnecessary, as well as to enable an all *X*-band free-electron laser by establishing a proven electron beam source.

Nuclear resonance fluorescence (NRF) is a process in which a nucleus, excited by gamma rays, reradiates high- the only process capable of producing a narrow bandwidth radiation (below 1% $\Delta\omega/\omega$) at gamma-ray energies by using state-of-the-art accelerator and laser technologies. In Compton scattering sources, a short laser pulse and a relativistic electron beam collide to yield tunable, monochromatic, polarized gamma-ray photons. Building on prior work on narrowband gamma-ray light sources at LLNL [1–8], the LLNL Nuclear Photonics Facility (NPF) will be equipped with a tunable MEGA-ray source using an all *X*-band linac including an *X*-band rf photoinjector. The advantages of operating at *X* band and further detail on the linac design are available in [9].

This paper describes an rf photoinjector which will be tested at the *X*-band test area (XTA) at SLAC, at an *X*-band test station at LLNL, and will serve as the injector for the *X*-band very energetic light for the observation and characterization of isotopic resonances and the assay and precision tomography of objects with radiation (VELOCIRAPTOR) linac, designed to drive the precision,

LLNL has designed & constructed a compact x-band accelerator in order to develop & demonstrate advanced, high-flux, laser-Compton x-ray & gamma-ray architectures

X-band accelerator and diode-pumped laser technology will enable compact and relocatable MEGa-ray sources

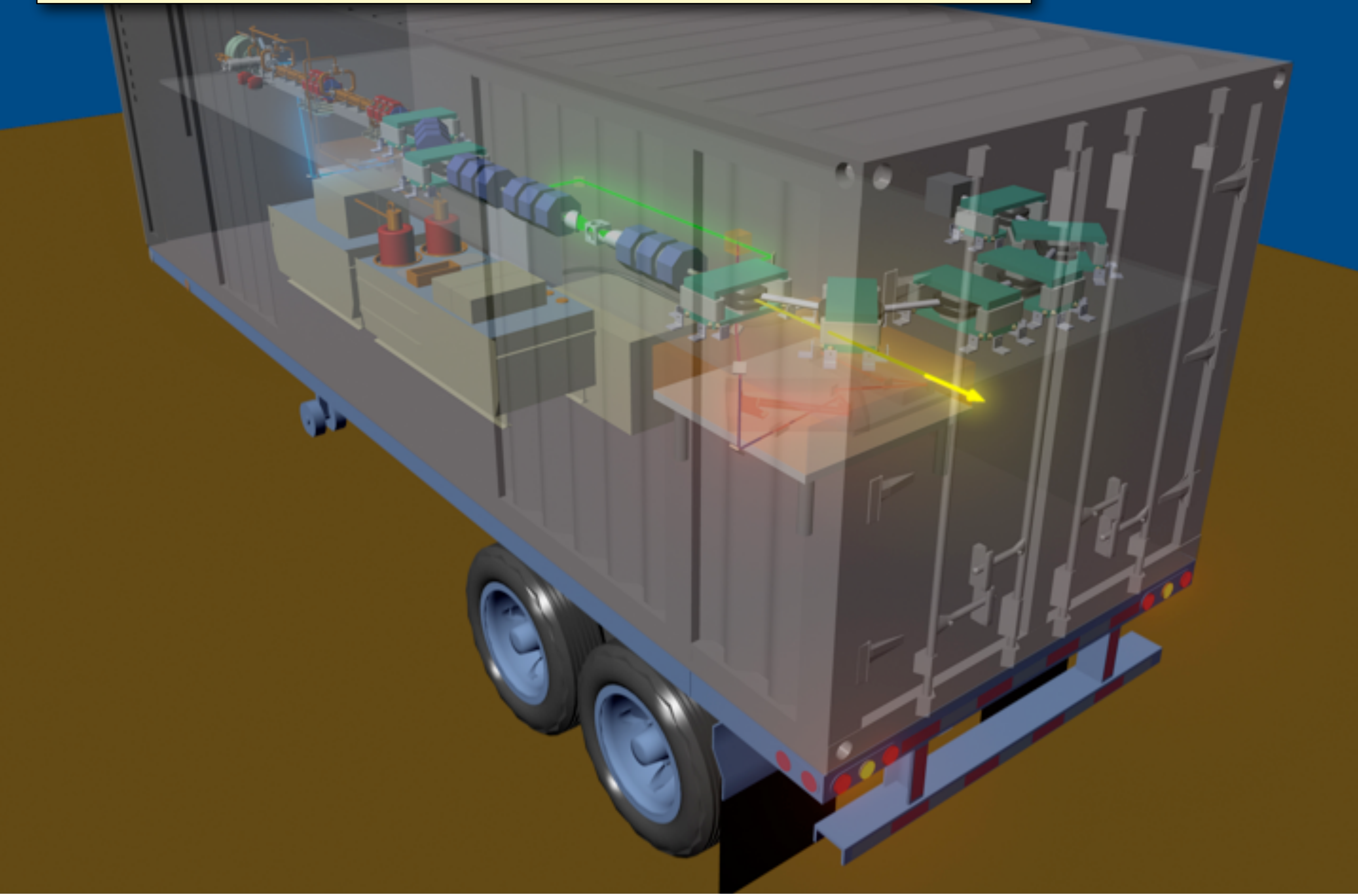

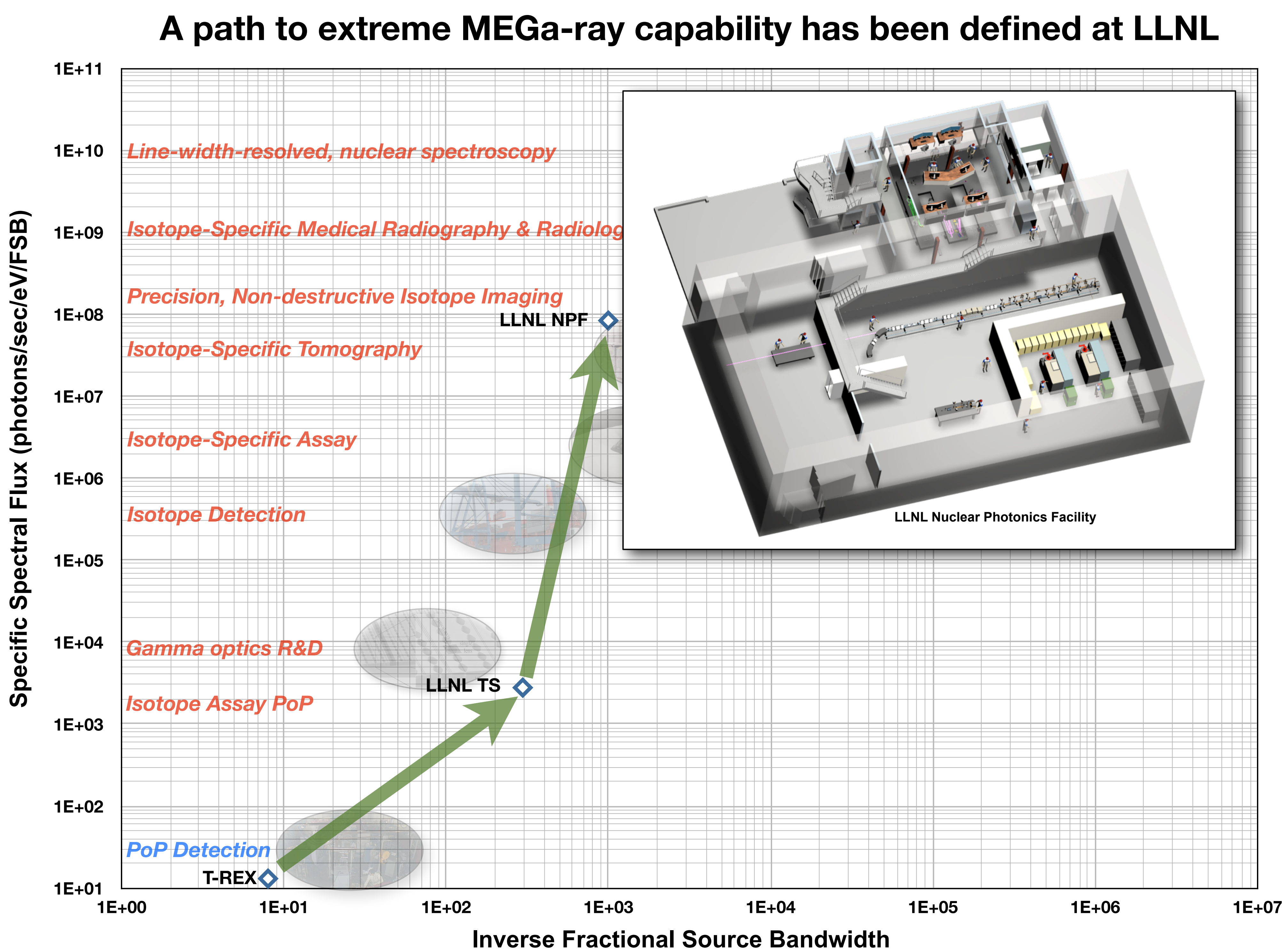
A path to extreme MEGa-ray capability has been defined at LLNL
Specific Spectral Flux (photons/sec/eV/FSB)
Inverse Fractional Source Bandwidth
1E+11
1E+10
1E+09
1E+08
1E+07
1E+06
1E+05
1E+04
1E+03
1E+02
1E+01
1E+00
1E+01
1E+02
1E+03
1E+04
1E+05
1E+06
1E+07
Line-width-resolved, nuclear spectroscopy
Isotope-Specific Medical Radiography & Radiolog
Precision, Non-destructive Isotope Imaging
Isotope-Specific Tomography
Isotope-Specific Assay
Isotope Detection
Gamma optics R&D
Isotope Assay PoP
PoP Detection
T-REX
LLNL TS
LLNL NPF
LLNL Nuclear Photonics Facility

LLNL's planned Nuclear Photonics Facility (NPF) would house the world's first "purpose built" MEGa-ray capability and will develop compact and rapid, isotope-specific material detection, assay and imaging technologies

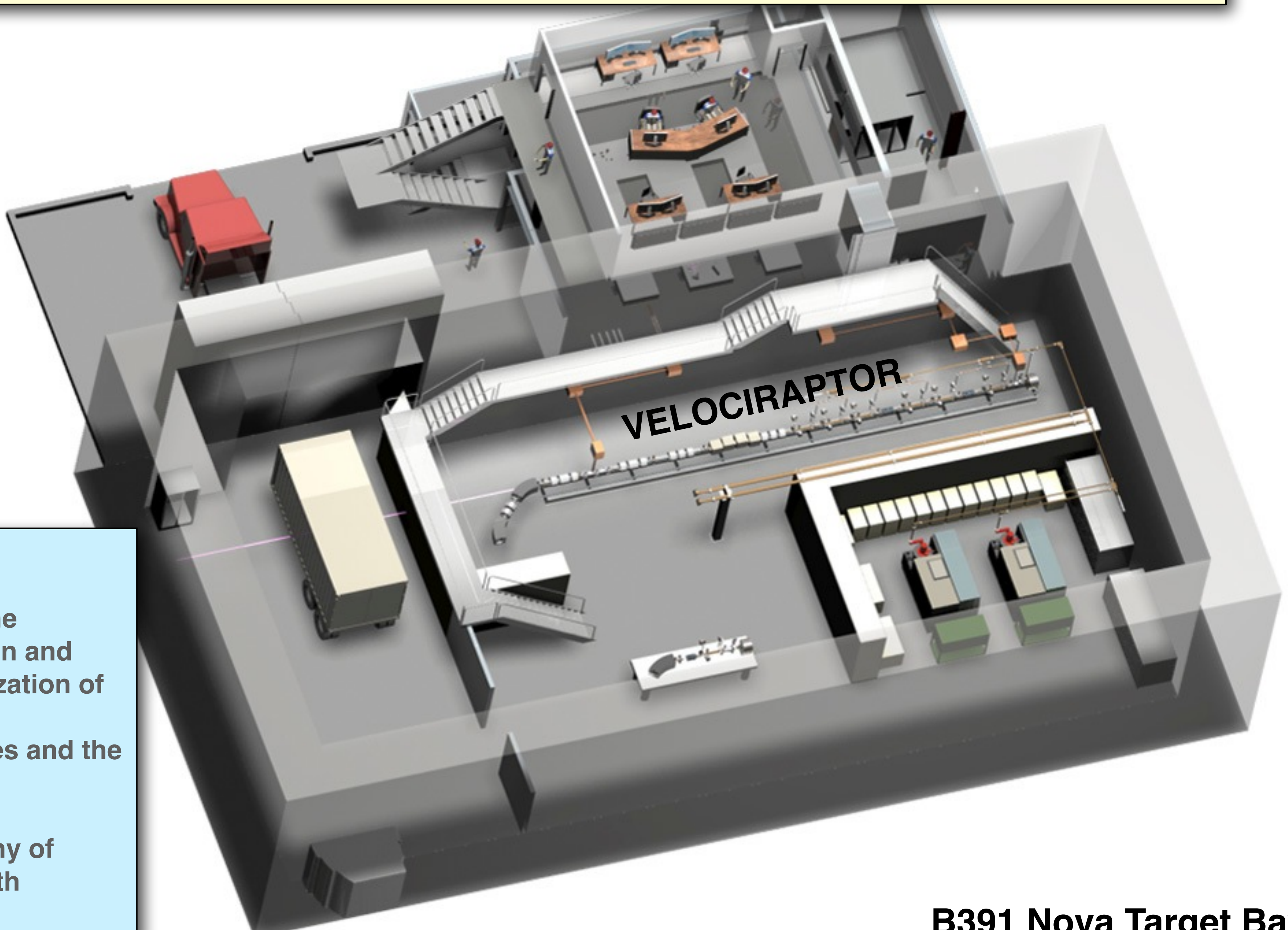

Very
Energetic
Light for the
Observation and
Characterization of
Isotopic
Resonances and the
Assay and
Precision
Tomography of
Objects with
Radiation

B391 Nova Target Bay

LLNL’s planned Nuclear Photonics Facility (NPF) would house the world’s first “purpose built” MEGa-ray capability and will develop compact and rapid, isotope-specific material detection, assay and imaging technologies

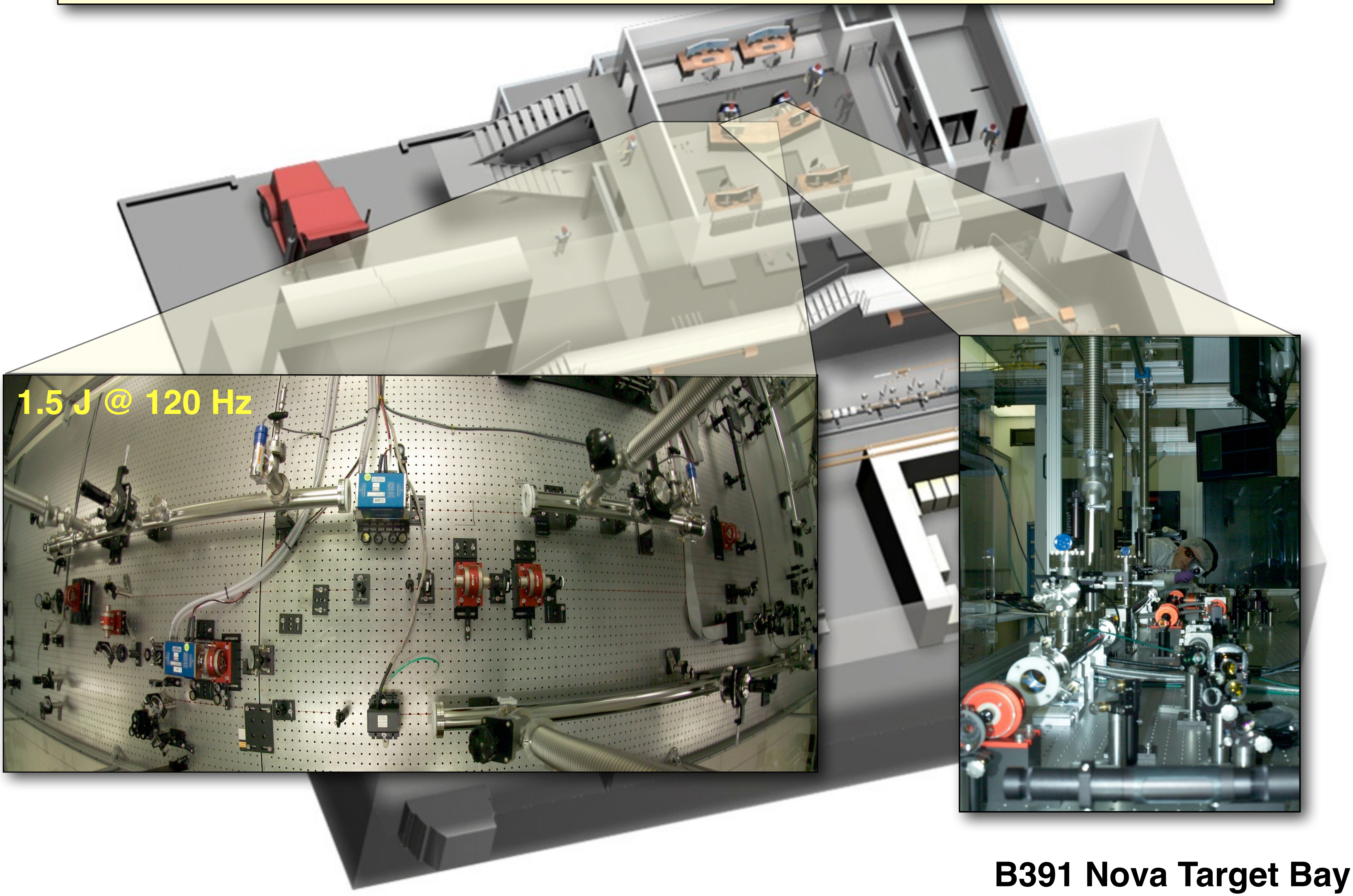

A path to extreme MEGa-ray capability has been defined at LLNL

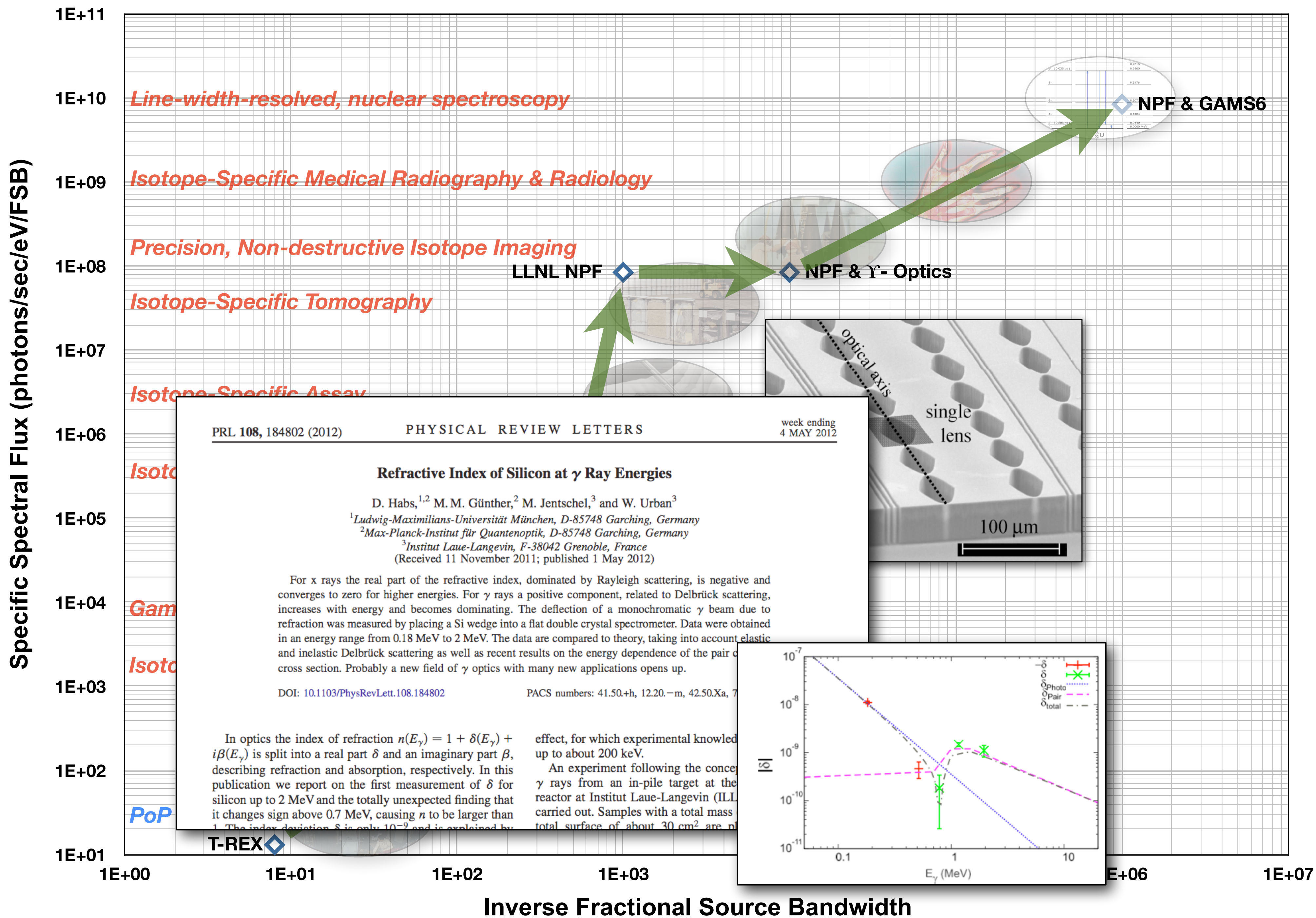

A path to extreme MEGa-ray capability has been defined at LLNL

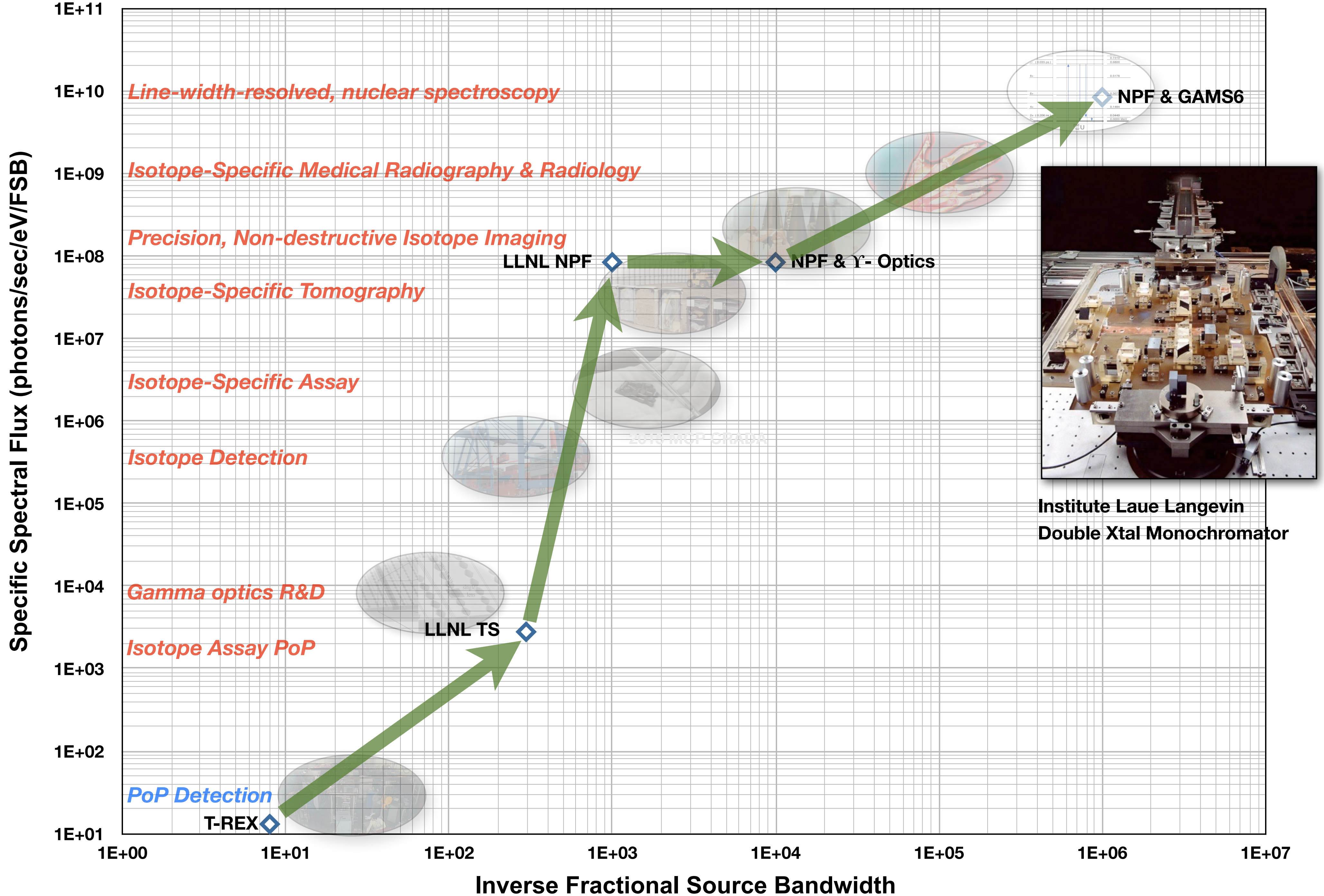

Next generation MEGa-ray projects are now emerging to pursue isotope science & applications

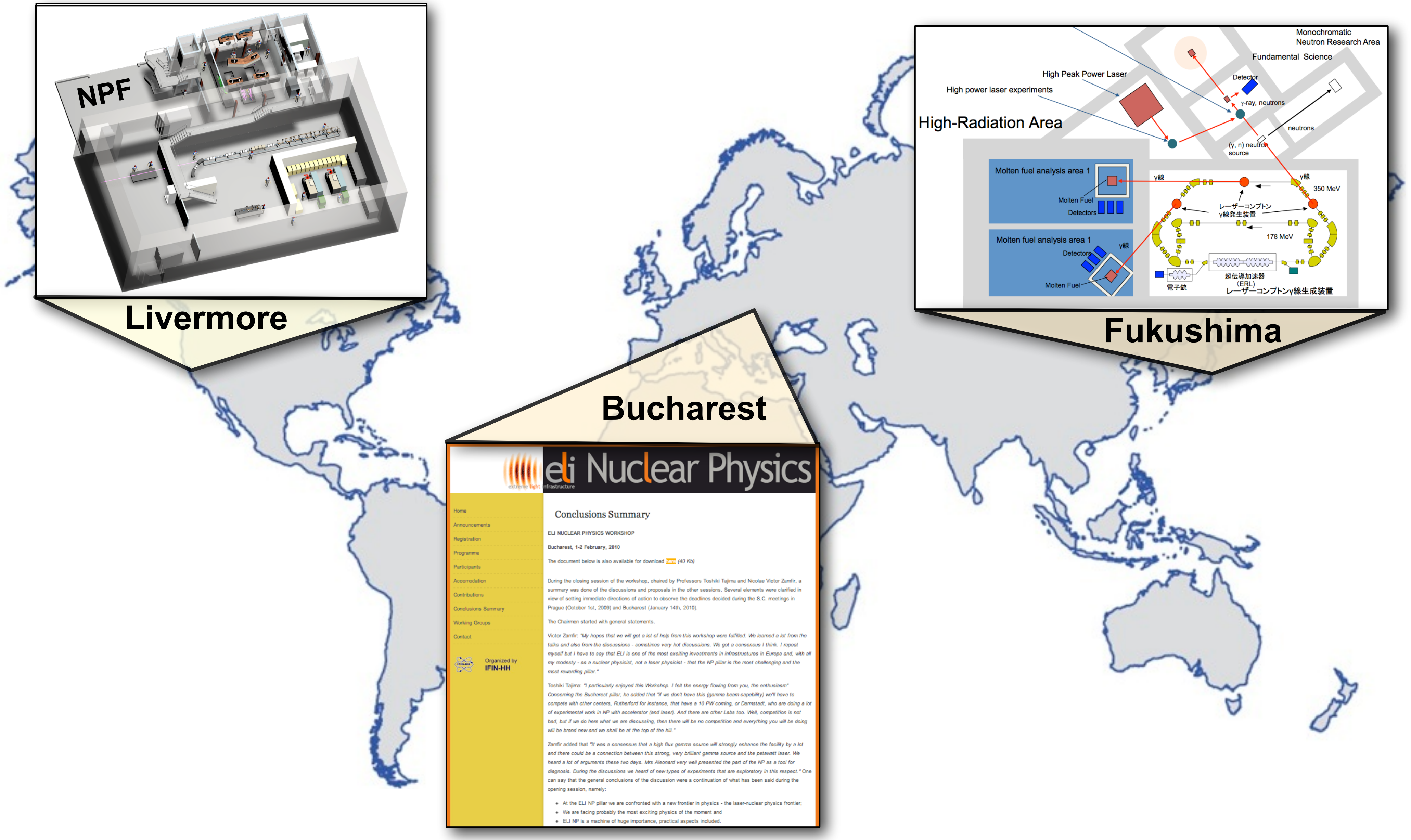

ELI NP - ELI Nuclear Physics
Bucharest, Romania
293M euro project will include a
1MeV-20MeV MEGa-ray beam line

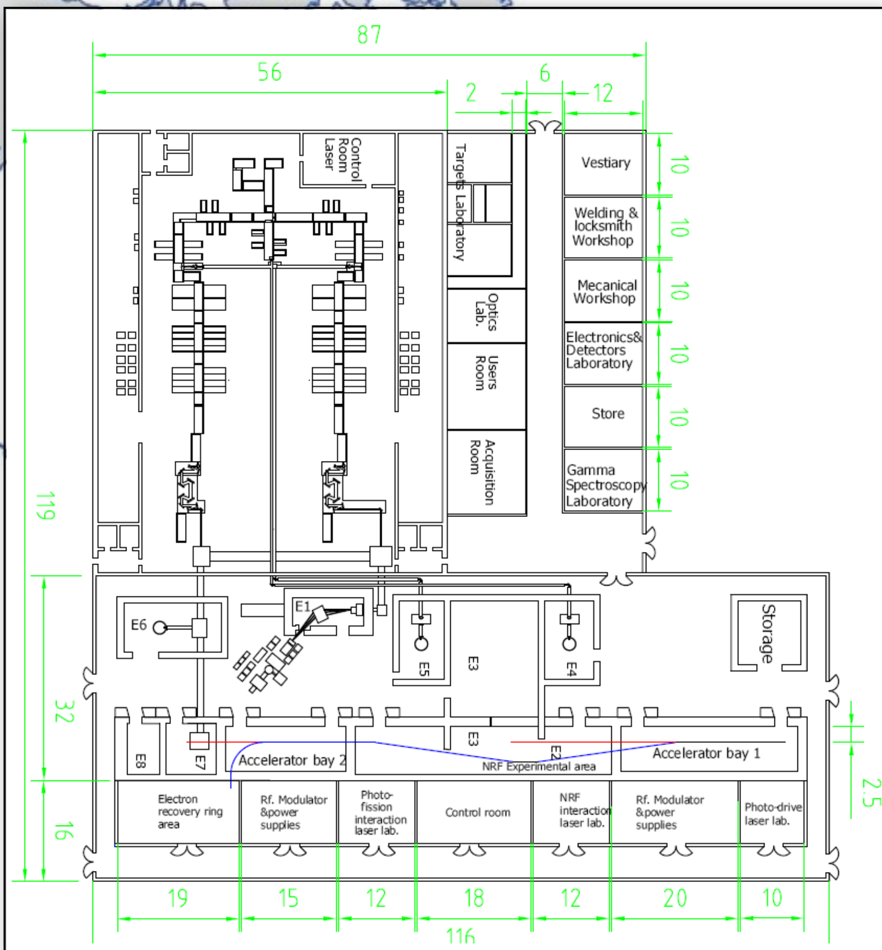

ELI-NP

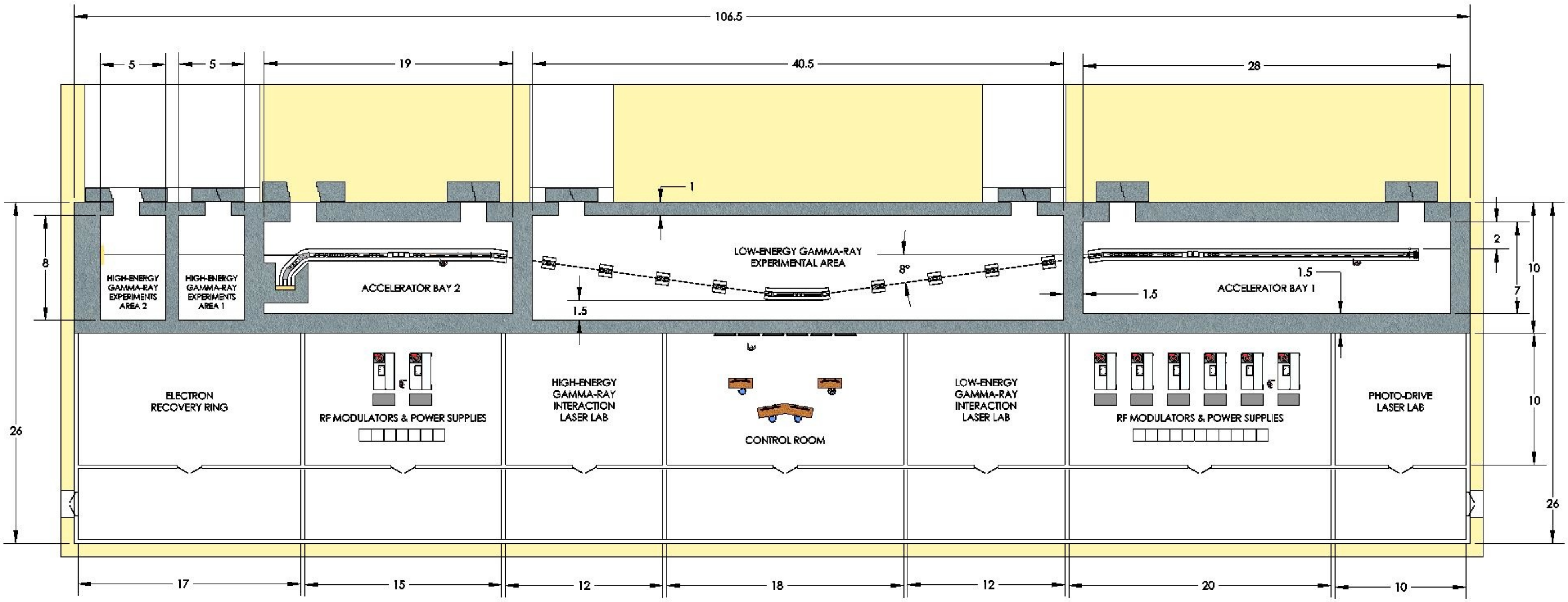

Fig. 14b

Fig. 14a and 14b: Overall view of the proposed ELI-NP γ source

The age of “Nuclear Photonics” is upon us

- **Laser-Compton gamma-ray sources are becoming for the “isotope” what the laser was for the “atom”**

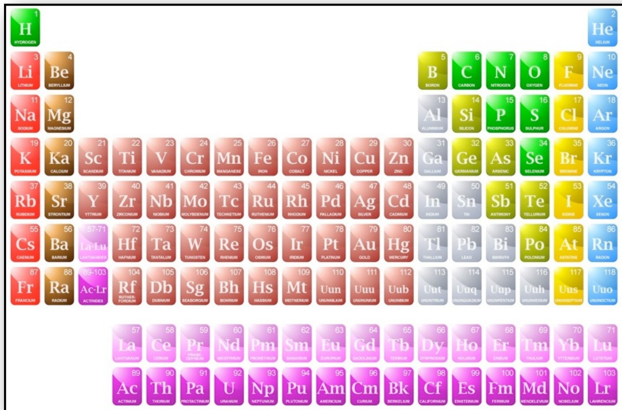

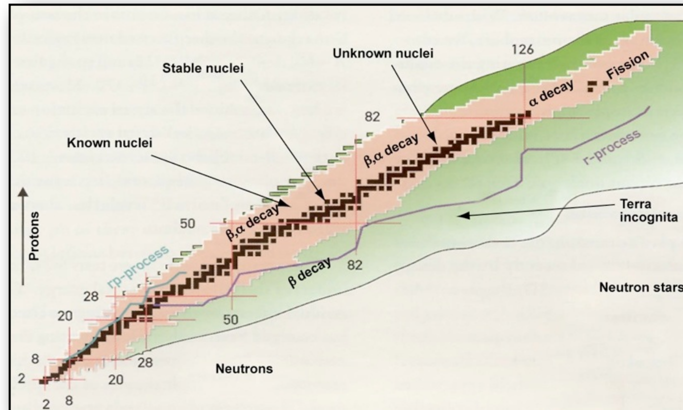

- **Mono-energetic gamma-rays enable novel, isotope-specific material detection, assay & imaging capabilities for a wide range of applications**

- **New nuclear science and nuclear engineering opportunities are emerging**

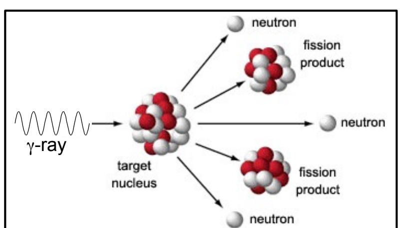

photo-fission and transmutation

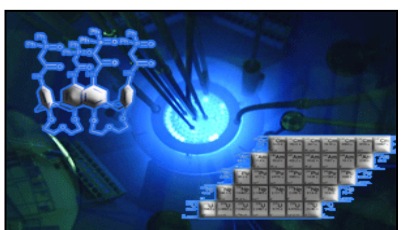

micron-scale, ps-duration pulsed neutron sources

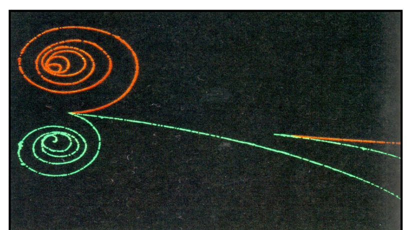

ps-duration, pulsed positron sources

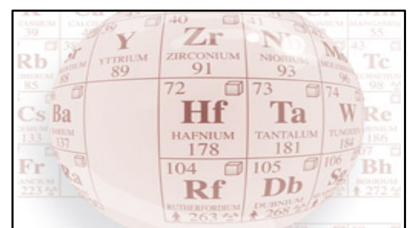

isomer physics and spectroscopy